DISSECTION OF THE MECHANISMS CONTROLLING H3K9ME3 AND DNA METHYLATION IN *NEUROSPORA CRASSA*

by

JORDAN DAVID GESSAMAN

A DISSERTATION

Presented to the Department of Biology
and the Graduate School of the University of Oregon
in partial fulfillment of the requirements
for the degree of
Doctor of Philosophy

September 2017

DISSERTATION APPROVAL PAGE

Student: Jordan David Gessaman

Title: Dissection of the Mechanisms Controlling H3K9me3 and DNA Methylation in *Neurospora crassa*

This dissertation has been accepted and approved in partial fulfillment of the requirements for the Doctor of Philosophy degree in the Department of Biology by:

Dr. Kryn Stankunas	Chairperson
Dr. Eric Selker	Advisor
Dr. Bruce Bowerman	Core Member
Dr. Eric Johnson	Core Member
Dr. Diane Hawley	Institutional Representative

and

Sara D. Hodges	Interim Vice Provost and Dean of the Graduate School

Original approval signatures are on file with the University of Oregon Graduate School.

Degree awarded September 2017

DISSERTATION ABSTRACT

Jordan David Gessaman

Doctor of Philosophy

Department of Biology

September 2017

Title: Dissection of the Mechanisms Controlling H3K9me3 and DNA Methylation in *Neurospora crassa*

Trimethylation of histone H3 lysine 9 (H3K9me3) and DNA methylation mark heterochromatin, contributing to gene silencing and normal cellular functions. My research investigated the control of H3K9me3 and DNA methylation in the fungus *Neurospora crassa*. The H3K9 methyltransferase complex, DCDC, consists of DIM-5, DIM-7, DIM-9, DDB1, and CUL4. Each component of DCDC is required for H3K9me3. The DIM-9/DDB1/CUL4 subunits are reminiscent of known cullin E3 ubiquitin ligases. I showed that aspects of CUL4-based E3 ubiquitin ligases are not required for H3K9me3 and DNA methylation in Neurospora.

H3K9me3 is bound by heterochromatin protein 1 (HP1) to recruit the DIM-2 DNA methyltransferase and the HCHC histone deacetylase complex. HCHC consists of HP1, CDP-2, HDA-1, and CHAP. Both HP1 and CDP-2 harbor chromodomains that bind H3K9me3, and CHAP contains two putative AT-hook domains that bind A:T-rich DNA. To test the contributions of these domains to HCHC function, I deleted the chromodomains of HP1 and CDP-2. Deletion of the HP1 chromodomain resulted in a reduction of DNA methylation, which was not exacerbated by deletion of the CDP-2 chromodomain. A strain with deletions of *chap* and the HP1 chromodomain showed a

DNA methylation phenotype comparable to the loss of the HDA-1 catalytic subunit. These findings support a model in which recognition of H3K9me3 and A:T-rich DNA by HP1 and CHAP, respectively, are required for proper HCHC function.

To examine the relationships between H3K9me3, DNA methylation, and histone acetylation, I utilized *in vivo* protein tethering of core heterochromatin components. The requirement of DIM-7 for native heterochromatin, previously implicated in localizing the H3K9 methyltransferase DIM-5, was not bypassed by DIM-5 tethering, indicating that DIM-7 has additional roles within the DCDC. Artificial localization of the HCHC histone deacetylase, by tethering HP1 or HDA-1, resulted in induction of H3K9me3, DNA methylation, and gene silencing, but silencing did not require H3K9me3 or DNA methylation. HCHC-mediated establishment of H3K9me3 was not required for *de novo* heterochromatin formation at native heterochromatic loci suggesting a role in heterochromatin spreading. Together, this work implicates HDA-1 activity as a key driver of heterochromatin spreading and silencing.

This dissertation includes previously published and unpublished co-authored material.

CURRICULUM VITAE

NAME OF AUTHOR: Jordan David Gessaman

GRADUATE AND UNDERGRADUATE SCHOOLS ATTENDED:

University of Oregon, Eugene, Oregon
University of Washington, Seattle, Washington

DEGREES AWARDED:

Doctor of Philosophy, Biology, 2017, University of Oregon
Bachelor of Science, Biochemistry, 2011, University of Washington

AREAS OF SPECIAL INTEREST:

Epigenetics
Genetics
Chromatin

PROFESSIONAL EXPERIENCE:

Graduate Student, Eric Selker, University of Oregon, 2011-2017

Teaching Assistant, Department of Biology, University of Oregon, 2011-2012

GRANTS, AWARDS, AND HONORS:

Pete von Hippel Graduate Scholar Award, Department of Biology, 2016

Genetics Training Grant, National Institutes of Health, 2012-2015

PUBLICATIONS:

Gessaman, J. D. & Selker, E. U. Induction of H3K9me3 and DNA methylation by tethered heterochromatin factors in *Neurospora crassa*. *In preparation*

Honda, S.*, Bicocca, V. T. *, Gessaman, J. D. *, Rountree, M. R. *, Yokoyama, A., Yu, E. Y., et al. (2016). Dual chromatin recognition by the histone deacetylase complex HCHC is required for proper DNA methylation in *Neurospora crassa*. Proceedings of the National Academy of Sciences, 113(41), E6135–E6144. http://doi.org/10.1073/pnas.1614279113

Adhvaryu, K. K. *, Gessaman, J. D. *, Honda, S., Lewis, Z. A., Grisafi, P. L., & Selker, E. U. (2014). The Cullin-4 complex DCDC does not require E3 ubiquitin ligase elements to control heterochromatin in Neurospora. Eukaryotic Cell, EC.00212–14. http://doi.org/10.1128/EC.00212-14

* These authors contributed equally to this work.

ACKNOWLEDGMENTS

I wish to sincerely thank Dr. Eric Selker for years of thoughtful discussions and guidance throughout my graduate career. Additionally, I thank my former mentors Drs. Michael Rountree and Andrew Klocko for their invaluable help and advice during the beginning of my projects as well as the ongoing support and feedback from the entire Selker Laboratory. I also appreciate the advice, feedback, and encouragement from my dissertation advisory committee: Drs. Kryn Stankunas, Bruce Bowerman, Eric Johnson, Diane Hawley, and Andrew Berglund. I am also grateful for the support of my family and friends over the course of my graduate school career. Finally, my most heartfelt appreciation goes to my inspiring wife, Kylie Gessaman, who chose to join me on this journey six years ago and without whom I would not be the person or scientist I am today.

TABLE OF CONTENTS

Chapter Page

Chapter Page

Chapter Page

LIST OF FIGURES

Figure Page

Figure Page

LIST OF TABLES

Table Page

CHAPTER I

INTRODUCTION

The chromatin state designated heterochromatin was first defined based on its cytological appearance (Heitz, 1928). Relative to active chromatin, referred to as euchromatin, this densely staining fraction of the genome is regarded as a more "closed" form of chromatin, which serves as an impediment to cellular processes like recombination and transcription (Grewal & Jia, 2007). Recently, heterochromatin has come to the forefront of biomedical research, in part because of its connection to human diseases, including cancer (Sharma, Kelly, & Jones, 2010). In addition, heterochromatin has been implicated in facilitating normal cellular processes, including chromosome segregation, which depends on proper centromere function, suppression of illegitimate recombination between repetitive elements, and silencing of invasive transposable elements (Grewal & Jia, 2007; Peng & Karpen, 2008; Rountree & Selker, 2009). Heterochromatic regions typically contain repetitive DNA and are characterized by a relative paucity of genes, trimethylation of lysine 9 on histone H3 (H3K9me3), methylation of cytosines in DNA (DNA methylation), and hypo-acetylated histones H3 and H4 (Bühler & Gasser, 2009; Grewal & Jia, 2007; Henikoff, 2000; Lewis et al., 2009). Despite advances in the understanding of the mechanisms underlying the formation and maintenance of heterochromatin, our grasp of the interplay between these aspects and the contributions of individual components of the heterochromatin machinery remains incomplete.

The filamentous fungus *Neurospora crassa* has emerged as a well-suited, though not broadly studied, model system to dissect the control of heterochromatin formation and maintenance. *N. crassa* has a compact genome of roughly ten thousand genes, generally without redundant copies, spread across approximately 40 megabase pairs. Unlike the case in higher eukaryotes (Dodge, Kang, Beppu, Lei, & Li, 2004; Okano, Bell, Haber, & Li, 1999; Peters et al., 2001; Ronemus, Galbiati, Ticknor, Chen, & Dellaporta, 1996; Tachibana et al., 2002), H3K9me3 and DNA methylation are not required for viability in Neurospora (Tamaru et al., 2003). Moreover, other classical model systems, such as the yeast *Schizosaccharomyces pombe* and the insect *Drosophila melanogaster*, lack the DNA methylation found in both higher eukaryotes and *N. crassa* (Elgin & Reuter, 2013; Grewal & Jia, 2007; Rountree & Selker, 2010; Saksouk et al., 2014).

In Neurospora, H3K9me3 and DNA methylation are commonly associated with relics of a genome defense system, RIP (repeat-induced point mutation) (Lewis et al., 2009; Selker, 1990). The RIP machinery detects duplicated sequences and generates polarized transition mutations (G:C to A:T) (Cambareri, Jensen, Schabtach, & Selker, 1989). The A:T-rich sequences then serve as signals to promote the establishment of H3K9me3 and DNA methylation (Lewis et al., 2009; Miao, Freitag, & Selker, 2000; Tamaru & Selker, 2003). While the precise mechanism is unclear, previous genetic studies revealed that the histone methyltransferase (HMTase) DIM-5 (named for defective in DNA methylation) is recruited to these A:T-rich regions and is solely responsible for all H3K9me3 found in the genome (Tamaru & Selker, 2001). DIM-5 activity depends on all members of the five-protein complex, DCDC (DIM-5/-7/-9, CUL4, DDB1 Complex) (Lewis, Adhvaryu, Honda, Shiver, Knip, Sack, et al., 2010b) but

DIM-7 alone appears necessary to target DIM-5 to incipient heterochromatic regions (Lewis, Adhvaryu, Honda, Shiver, & Selker, 2010a). H3K9me3 is recognized and bound by heterochromatin protein 1 (HP1) through a conserved chromodomain (Freitag, Hickey, Khlafallah, Read, & Selker, 2004a). The C-terminus of HP1, harboring a conserved chromoshadow domain, facilitates the dimerization of HP1 molecules and is required for interactions with cofactors (Honda & Selker, 2008; Honda et al., 2016). These cofactors include the DNA methyltransferase (DIM-2), a putative histone demethylase (DMM) complex, a nucleosome remodeler (MI-2), and a histone deacetylase complex (HCHC) (Honda & Selker, 2008; Honda et al., 2010; 2012).

DIM-2 catalyzes all DNA methylation in Neurospora (Kouzminova & Selker, 2001). Expansion of H3K9me3 and DNA methylation into euchromatin is prevented by the DMM (DNA methylation modulator) complex, which consists of a putative JmjC domain demethylase (DMM-1) and a DNA-binding protein (DMM-2) (Honda et al., 2010).

The HCHC complex is comprised of HP1, the chromodomain protein CDP-2, the histone deacetylase HDA-1, and the AT-hook protein CHAP (Honda et al., 2012). Disruption of the histone deacetylase activity of HDA-1 selectively modulates H3K9me3 and DNA methylation levels resulting in hyper-methylation at centromeres and highly A:T-rich regions but hypomethylation at less A:T-rich regions (Honda et al., 2012; 2016).

The work described in this dissertation contains published, co-authored material and unpublished material. Chapter II was published with co-authors Keyur Adhvaryu, Shinji Honda, Zachary Lewis, Paula Grisafi, and Eric Selker. Chapter II describes work

to explore the possibility that the DIM-9, DDB1, and CUL4 subunits of the DCDC H3K9 methyltransferase complex functions as a cullin E3 ubiquitin ligase. This work demonstrated that core features of cullin E3 ubiquitin ligases are not required for the establishment of DNA methylation. Chapter III was published with co-authors Shinji Honda, Vincent Bicocca, Michael Rountree, Ayumi Yokoyama, Eun Yu, Jeanne Selker, and Eric Selker. This work dissected the role of the HCHC histone deacetylase complex in heterochromatin establishment, maps interactions between subunits, and evaluates subunit contributions to HCHC function. Chapter IV discusses unpublished work that used *in vivo* protein tethering of heterochromatin machinery to clarify the relationships between heterochromatic features and explored the role of HCHC-mediated histone deacetylation in heterochromatin spreading and gene silencing.

CHAPTER II

THE CULLIN-4 COMPLEX DCDC DOES NOT REQUIRE E3 UBIQUITIN LIGASE ELEMENTS TO CONTROL HETEROCHROMATIN IN *NEUROSPORA CRASSA*

This work was published in volume 14 of the journal *Eukaryotic Cell* in January 2015. I generated CUL4 constructs harboring a deletion of the C-terminus and assayed the ability of these constructs to rescue a *cul4*-null strain with respect to DNA methylation, H3K9me3, and methyl methanesulfonate (MMS) sensitivity. Additionally, I created a deletion of *rbx1* and characterized its effect on DNA methylation and MMS sensitivity. Keyur Adharyvu performed mutational analysis of CUL4 lysine 863 and similarly assessed the ability of these constructs to rescue DNA methylation and MMS sensitivity. Additionally, he was responsible for testing the requirement of the COP9 signalosome, $H2A^{K122}$, and components of the DNA repair machinery for DNA methylation. Shinji Honda conducted the protein purification and sample preparation for mass spectrometry. Zachary Lewis reproduced the CUL4 lysine 863 observations by reintroducing mutated *cul4* into in a strain with a complete deletion of the native *cul4* gene. Paula Grisafi analyzed the levels of H2A ubiquitination in wild-type and *cul4*-null backgrounds. Eric Selker was the principle investigator for this work.

Introduction

Ubiquitination, the addition of ubiquitin moieties to proteins, is a multistep process that regulates the intracellular stability, localization, and function of numerous

proteins (Hershko & Ciechanover, 1998; Komander & Rape, 2012). Ubiquitin is activated by an E1 enzyme and then transferred to a substrate by an E2 ubiquitin-conjugating enzyme under the direction of multisubunit cullin-RING E3 ubiquitin ligases (CRLs) (Petroski & Deshaies, 2005; Pickart, 2001). Cullins form the scaffold of CRLs by bridging substrate adaptor proteins that interact with their N termini and catalytic proteins that interact with their C termini (Petroski & Deshaies, 2005).

Cullin-4 (CUL4) complexes control cell cycle progression, DNA repair, and signal transduction (Jackson & Xiong, 2009; Lewis, Adhvaryu, Honda, Shiver, Knip, Sack, et al., 2010b). The *Neurospora crassa* DCDC (DIM-5/-7/-9/CUL4/DDB1 complex) is essential for methylation of lysine 9 of histone H3 (H3K9) and DNA methylation (Lewis, Adhvaryu, Honda, Shiver, Knip, Sack, et al., 2010b). The DCDC resembles established CRLs, in which the substrate specificity adaptor protein DDB1/DIM-8 (DNA-damage-binding protein 1) serves as a bridge between CUL4 and the DCAF (DDB1 and CUL4-associated factor) DIM-9. These members of the DCDC, in turn, associate with the histone methyltransferase DIM-5 and its partner, DIM-7 (Lewis, Adhvaryu, Honda, Shiver, Knip, Sack, et al., 2010b). In addition, as in validated CRLs, CUL4 is modified by attachment of the ubiquitin-like protein NEDD8 in DCDC (Lewis, Adhvaryu, Honda, Shiver, Knip, Sack, et al., 2010b). Similarly, the *Schizosaccharomyces pombe* fission yeast CUL4 complex CLRC directs H3K9 methylation, although the potentially ubiquitinated substrate for this complex remains elusive (Horn, Bastie, & Peterson, 2005; Jia, Kobayashi, & Grewal, 2005; K. Zhang, Mosch, Fischle, & Grewal, 2008), as with DCDC.

Fruitless efforts to find putative substrates for ubiquitination by DCDC led us to explore the possibility that this complex has an ubiquitination-independent function. The C terminus of cullins, which is essential for the catalytic activity of CRLs, directly interacts with the E2 ligase and RBX1/ROC1, a small RING domain catalytic protein that facilitates the attachment of ubiquitin moieties onto substrates (Zimmerman, Schulman, & Zheng, 2010). The flexible backbone of cullins undergoes conformational changes to bring RBX1 and the E2 ligase in close proximity to the substrates, which are recruited by the adaptor protein bound to the N terminus (J. Liu & Nussinov, 2011). Covalent attachment of NEDD8 to an invariant lysine in the C terminus regulates the stability and activity of cullins (Boh, Smith, & Hagen, 2011; Duda et al., 2008; Hotton & Callis, 2008; Merlet, Burger, Gomes, & Pintard, 2009). To explore the contribution of neddylation in the regulation of *N. crassa* CUL4 functions, we mutated the CUL4 NEDD8 attachment site and found, surprisingly, that the neddylation-site mutants have normal histone H3K9 methylation and DNA methylation, although CUL4-mediated DNA repair is compromised. We also report that a deletion of the C terminus of CUL4, including the neddylation site and a region mediating the interaction with the E2 ligase and RBX1, does not affect DNA methylation or heterochromatin formation; again, only DNA repair is compromised. Furthermore, a deletion of the gene coding for RBX1 does not affect DNA methylation, although DNA repair is disrupted. Taken together, our findings imply that *N. crassa* DCDC directs H3K9 and DNA methylation through an ubiquitination-independent mechanism.

Results and Discussion

To test the possible role of CUL4 neddylation in DNA methylation and DNA repair, we replaced the predicted neddylated lysine (K863) with non-neddylatable residues and introduced the constructs, with or without a FLAG tag, at the his-3 locus of a *cul4*^{RIP1} null mutant (Fig. 1A; see also Fig. 2). The control strain, bearing FLAG-tagged wild-type *cul4*, exhibited a protein doublet (Fig. 1B), presumably reflecting the neddylated and unneddylated forms of CUL4 (Lewis, Adhvaryu, Honda, Shiver, Knip, Sack, et al., 2010b; Xu et al., 2010). Mutation of the predicted neddylation site eliminated the slower-migrating band (Fig. 1B). We tested DNA methylation in strains expressing mutant or wild-type forms of *cul4*. Strikingly, the DNA methylation defect of the *cul4*^{RIP1} null mutant was fully rescued by all of the constructs bearing mutations of K863 (Fig. 1C; see also Fig. 3). Neddylation-deficient mutants were also able to rescue the DNA methylation defect of a *cul4* deletion mutant (Fig. 4). Complementation of the DNA methylation defect implies that H3K9 trimethylation (H3K9me3) was also restored, as H3K9 methylation is required for DNA methylation in *N. crassa* (Tamaru et al., 2003; Tamaru & Selker, 2001). After we obtained some of the findings reported here, Zhao and colleagues reported a neddylation site mutation of *N. crassa* CUL4 and claimed that it interfered with H3K9 trimethylation (Zhao et al., 2010). We do not consider the reported chromatin immunoprecipitation assay results to be robust, however, and it appears that neither DNA methylation nor global H3K9 methylation was examined.

CUL4 and DDB1, each of which is encoded by a single gene in *N. crassa* (Galagan et al., 2003), interact with multiple substrate adaptors known as DCAFs (DDB1

and CUL4-associated factors) to carry out various functions (J. Lee & Zhou, 2007). DIM-9/DCAF26 is required for the establishment of H3K9me3 by the DCDC (Lewis, Adhvaryu, Honda, Shiver, Knip, Sack, et al., 2010b; Xu et al., 2010). To address the possibility that neddylation of *N. crassa* CUL4 might be required for another function, such as DNA repair, we tested the sensitivity of wild-type and K863 mutants to the alkylating agent methyl methanesulfonate (MMS) and the topoisomerase inhibitor camptothecin (CPT). The neddylation mutants, like the $cul4^{RIP1}$ null mutant, were highly sensitive to both drugs (Fig. 1D), suggesting that neddylation of CUL4 is required for resistance to these drugs, presumably through DNA repair pathways. Interestingly, the neddylation-defective mutants showed less sensitivity to the microtubule inhibitor thiabendazole (TBZ) (Lewis, Adhvaryu, Honda, Shiver, Knip, Sack, et al., 2010b), consistent with heterochromatin formation being independent of CUL4 neddylation. To test if the absence of neddylation affects the integrity of DCDC, we performed a proteomic analysis of proteins immunoprecipitated with DIM-8-FLAG from the neddylation-site mutant (a *cul4* mutant with K-to-A mutation at residue 863 [$cul4^{K863A}$]). The recovery of all DCDC components implies that the neddylation of CUL4 is not required for DCDC formation.

The C-termini of cullins are critical for their ubiquitin ligase activities (Hotton & Callis, 2008; Petroski & Deshaies, 2005) and mediate interactions with the E2 ligases, a RING domain protein (ROC1/RBX1), CAND1, and the signalosome (Hotton & Callis, 2008; Petroski & Deshaies, 2005) (Fig. 1A). Biochemical studies suggest that neddylation of cullins promotes polyubiquitination by increasing the affinity of cullins for the E2 ligase and RBX1 (Merlet et al., 2009). The COP9 signalosome complex (CSN)

removes NEDD8 from cullins to permit interaction of the cullin C terminus with CAND1 (Hotton & Callis, 2008; Merlet et al., 2009; J.-T. Wu, Chan, & Chien, 2006; S. Wu et al., 2013), limiting ubiquitination and promoting the exchange of substrate receptors (Pierce et al., 2013; S. Wu et al., 2013). The absence of the COP9 signalosome causes the degradation of cullins by uncontrolled autoubiquitination (Qun He, Cheng, He, & Liu, 2005). Interestingly, we found that DNA methylation is unaffected by the absence of an active signalosome (see Supplemental Information and Fig. 5).

Recently, it was speculated that ubiquitination of histone H2A lysine 122 (H2AK122ub) by CRL4B may direct DNA methylation (Yang et al., 2015). We failed to detect ubiquitination of the corresponding lysine on *N. crassa* H2A (H2AK119) (see Supplemental Information), consistent with observations in *Saccharomyces cerevisiae* (Swerdlow, Schuster, & Finley, 1990), suggesting that H2A ubiquitination is absent, and we found that replacement of K119 with alanine, a non-modifiable residue, does not affect DNA methylation (Fig. 6). Clearly, DCDC does not operate by ubiquitination of H2AK119.

Our observation that neddylation of CUL4 is not required for DNA methylation raised the possibility that *N. crassa* DCDC is not acting as a ubiquitin ligase for heterochromatin formation. To further explore this possibility, we generated and tested a deletion mutant that lacks the CUL4 C terminus (residues 824 to 923; Fig. 1A), including both the neddylation site and regions of interaction with CAND1 and RBX1. The deletion did not affect DNA methylation or H3K9me3 (Fig. 7A and B), suggesting that CUL4 is not involved in catalyzing ubiquitination in this context. In contrast, like the neddylation site mutant, the deletion mutant was sensitive to chemicals that cause DNA damage (Fig.

7C), consistent with a requirement for the ubiquitin ligase activity of a CUL4 complex for DNA repair.

An expectation based on our findings is that the *N. crassa* RBX1 homolog is required for DNA repair but not DNA methylation. We found that the *N. crassa rbx1* homologue is essential for the viability of the organism, but we were able to build a heterokaryotic strain in which the major nuclear component has a deletion of the gene, presumably resulting in a strong reduction of the protein (see Supplemental Information and Fig. 8). DNA repair was compromised in the heterokaryon, but DNA methylation was normal (Fig. 9A and B). Altogether, our findings render it highly unlikely that CUL4 is operating as an ubiquitin ligase for heterochromatin formation and DNA methylation. Perhaps CUL4 simply serves as a scaffold for assembly of the H3K9 methylation machinery.

It is interesting to consider the possible generality of our findings. CUL4 is essential in *Schizosaccharomyces pombe*, complicating studies of its role in heterochromatin formation. Mutation of the *S. pombe* CUL4 neddylation site perturbs heterochromatic silencing (Horn et al., 2005; Jia et al., 2005), consistent with the possibility that CLRC, the fission yeast counterpart of DCDC, is operating as a true E3 ubiquitin ligase, despite fruitless efforts to find a likely ubiquitination substrate for this apparent CRL (Horn et al., 2005; Jia et al., 2005; K. Zhang et al., 2008). It is noteworthy, however, that *S. pombe*, unlike *N. crassa*, requires two CUL4-dependent complexes for heterochromatin formation: CLRC, which sports a DDB1-related protein (Rik1) in place of DDB1, methylates H3K9, whereas CUL4/DDB1^{CDT2} directs polyubiquitination and the subsequent degradation of the antisilencing protein Epe1. Defects in

CUL4/DDB1^{CDT2} lead to the loss of gene silencing (Braun et al., 2011). Thus, it is possible that neddylation is required for the degradation of Epe1 by the CUL4/DDB1^{CDT2} complex but not for H3K9me3 by CLRC. There are other indications that cullin complexes do not always conform to accepted models. Inhibition of the NEDD8-activating enzyme (NAE) by MLN4924 causes rapid deneddylation of cullins without perturbing the global CRL network, and mutation of the neddylation site on CUL1 (CUL1^{K780R}) does not prevent the assembly of CUL1 with SKP1 and the substrate adaptor F-box proteins (Bennett, Rush, Gygi, & Harper, 2010). Knockdown experiments in HeLa cells have implicated CUL4 and DDB1 in histone methylation (Higa et al., 2006), raising the possibility that E3-like complexes similar to DCDC carry out ubiquitination-independent functions in a variety of organisms. Our finding that DCDC is not a true CRL raises the question of why and how H3K9 methylation requires such intricate multicomponent protein complexes.

Materials and Methods

Neurospora Strains and Methods

N. crassa strains were maintained, grown, and crossed using previously described procedures (Davis, 2000a). All strains and primers used in this study are listed in Appendices C and D, respectively. *N. crassa* transformation (Margolin, Freitag, & Selker, 1997), DNA isolation (C. E. Oakley, Weil, Kretz, & Oakley, 1987), Southern blotting (Selker & Stevens, 1987), and protein isolation and Western blotting (Honda & Selker, 2008) were performed as previously described. For drug sensitivity assays, serial

dilutions of conidia were spot tested on medium with or without methyl methanesulfonate (MMS; 0.015%), camptothecin (CPT; 0.3 μg/ml), or thiabendazole (TBZ; 0.5 μg/ml), obtained from Sigma-Aldrich (Lewis, Adhvaryu, Honda, Shiver, Knip, Sack, et al., 2010b).

cul4 Constructs

We constructed plasmids to complement the *cul4* mutant with the wildtype *cul4+* gene (with its native promoter and downstream regions; plasmid pKA67) or *flag-cul4+* (pKA122; this and similar constructs include Met-FLAG-5XGly-HAT-5XGly-3XFLAG-5XGly-CUL4, abbreviated as FLAG-CUL4 for simplicity) (Lewis, Adhvaryu, Honda, Shiver, Knip, Sack, et al., 2010b). To generate *the flag-cul4*^{K863A} construct we used pKA122 as template with primers 2286 and 2287 in the PCR-based QuickChangeTM Site-Directed Mutagenesis protocol (Stratagene) to generate plasmid pKA124 (*flag-cul4*^{K863A}). PCR-driven overlap extension was used to generate pKA287 (*cul4*^{K863A}) and pKA288 (*cul4*^{K863R}) (Heckman & Pease, 2007). Briefly, genomic DNA from wildtype strain (N150) was used as template in PCR reactions with the following primers: *cul4*^{K863A} (primers 2193, 2194, 2286 and 2287) and *cul4*^{K863R} (primers 2193, 2194, 3417 and 3418). The PCR products were sequenced to confirm the presence of mutations and then cloned into the ApaI and SpeI site of pBM61(Margolin et al., 1997), to generate pKA287 and pKA288. To construct pKA294 (*flag-cul4*^{K863R}), pKA288 (*cul4*^{K863R}) was digested with NotI and NruI to isolate a 581 bp fragment containing the mutation and this fragment was used to replace the corresponding region of *cul4* gene in pKA124. Plasmid pKA294 was digested with DraI and plasmids pKA124, pKA287, pKA288 were digested

with NdeI and targeted to the *his-3* locus of strain N3892 by electroporation (Margolin et al., 1997). *His+* transformants were selected for each construct. Primers 1664 and 2201 were used to amplify a part of the *cul4* gene from the *his-3* locus of these *his+* strains and the PCR products were sequenced to reconfirm the presence of desired mutations.

We also introduced the neddylation-site mutant alleles into a *cul4* deletion mutant. Primers 2193 and 2194 were used in PCR reaction with plasmids pKA67 (13) ($cul4^{+}$), pKA287 ($cul4^{K863A}$) or pKA288 ($cul4^{K863R}$) as template to amplify wild-type or mutant alleles. The gene coding for the positive selectable marker bar was obtained by PCR using plasmid pBARKS1 (Pall, 1993) as template with primers 1652 and 1653. The PCR products for wildtype or neddylation-site mutant allele and bar were co-transformed into the *cul4* deletion mutant (N3169) by electroporation (Margolin et al., 1997). Multiple bar^{+} transformants were selected for each of the *cul4* alleles and their DNA methylation was analyzed by Southern blotting (Fig. 4).

To generate *flag-*$cul4^{1-823}$, genomic DNA from a wild-type strain (N150) was used as template in PCR reactions with primers JGP1 and JGP3. The PCR product was then cloned into the BglII and XbaI sites of pKA122, to generate pJG1. To generate $cul4^{1-823}$, genomic DNA from a wild-type strain (N150) was amplified using primers JGP52 and JGP54 and the PCR product was cloned into the ApaI and SpeI sites of pKA67 to generate pJG2. Plasmids pJG1 and pJG2 were digested with NdeI and targeted to the *his-3* locus of strain N3892 by electroporation. His^{+} transformants were isolated for each construct and made homokaryotic through microconidiation (Ebbole & Sachs, 1990).

rbx1 Deletion Mutant

To generate a knockout mutant for the putative *rbx1* gene (NCU11300), fragments corresponding to the 5' UTR and 3' UTR were PCR amplified with primers JGP158/JGP159 and JGP162/JGP163 respectively using genomic DNA from a wild-type strain (N150) as template. These fragments also contained homology to the *PtrpC::hph* (hygromycin resistance) cassette (Honda & Selker, 2009). Additionally, a fragment containing *PtrpC::hph* and homology to the 5' and 3' UTR regions of NCU11300 was amplified with primers JGP160 and JGP161 using plasmid *p3xFLAG::hph+::loxP* (Honda & Selker, 2009) as template. To generate a knockout cassette for the *rbx1* gene (NCU11300 5'UTR-*PtrpC::hph*+-NCU11300-3'UTR), these three fragments were used as template in an overlap-extension PCR reaction using primers JGP158 and JGP161. This knockout cassette was transformed into strain N2930 by electroporation (Margolin et al., 1997). Replacement of the native *rbx1* gene with this hygromycin resistance cassette generated HygR transformants that were purified by microconidiation (Ebbole & Sachs, 1990). We were unable to obtain homokaryotic strains, suggesting that *rbx1* gene is essential. However, we were successful in enriching the nuclei harboring the deletion using the antibiotic (hygromycin) selection of microconidia; this enrichment was verified by Southern blotting using a probe corresponding to the 3' UTR region of NCU11300 (Fig. 8).

hH2A Constructs

The construction of epitope tagged H2A strains is briefly described here. Wildtype (N150) genomic DNA was used as template in PCR with primers 2338 and

2686 to amplify a 2.1 kb fragment containing the hH2A gene and 1.4 kb of 5' UTR. This PCR product was cloned into the NotI and EcoRI sites of a plasmid (pRS416+10XGly) (Honda & Selker, 2009) to generate plasmid pKA130. Plasmid pKA130 was digested with NotI + PacI and the 2.1 kb fragment was subcloned between the NotI and PacI sites of pCCG::C- Gly::3XFLAG (Honda & Selker, 2009) to obtain plasmid pKA133. In pKA133, the hH2A gene is separated from the 3XFLAG epitope by a 10XGly spacer and the expression of H2A-FLAG is driven by the native promoter. To change the conserved ubiquitination site (K122; Fig. 6), PCR-driven overlap extension was used with primers 2271, 2272, 2338 and 2686 and plasmid pKA130 as template (Heckman & Pease, 2007). After confirming the mutation by sequencing, the PCR product was cloned between the NotI and EcoRI sites of a plasmid (pRS416+10XGly) (Honda & Selker, 2009) to generate pKA137. Plasmid pKA137 was digested with NotI and PacI and the 2.1 kb fragment was subcloned between the NotI and PacI sites of pCCG::C- Gly::3XFLAG (Honda & Selker, 2009) to generate pKA139. Plasmid pKA133 was digested with XmnI and a 7.1 kb fragment containing the epitope-tagged hH2A gene along with the flanking *his-3* sequences was gel-purified and targeted to the *his-3* region of the host strain by electroporation. Several *his+* transformants were analyzed by Southern blotting (to confirm correct integration) and Western blotting (to detect H2A-FLAG) and strain N4197 was selected for further experiments. Similarly strain N4201 (expressing H2AK122A-FLAG) was constructed using plasmid pKA139. In order to replace the endogenous hH2A gene with *inl+*, we constructed plasmid pKA120 as follows. Genomic DNA from wild-type strain (N150) was used as template in PCR reactions with primers 2318 and 2319 to amplify 1.4 kb of 5' UTR and primers 2320 and 2321 to amplify 1 kb

of 3' UTR of the hH2A gene. The *inl* (myoinositol-1-phosphate synthase) plasmid pOKE1 was used as template with primers 1497 and 1498 to amplify a 2.6 kb fragment containing the wildtype *inl*+ gene. These three PCR products were mixed with DNA of linearized pRS416 (digested with BamHI and EcoRI), and transformed into yeast strain PJ49-6A (18). Plasmid DNA was isolated from *ura*+ colonies transformed into *E. coli* strain DH5αF. Plasmid pKA120 was isolated from a transformant, with BamHI and EcoRI and the 5.1 kb fragment was purified and transformed into a *inl*, *mus-52* strain (N2993) by electroporation (Margolin et al., 1997). To confirm correct integration, 15 *Inl*+ transformants were analyzed by Southern hybridization and strain N4195 was selected for further study. To obtain strains expressing only H2A-FLAG, strain N4197 was crossed with N4195 and progeny growing on minimal medium were screened by Southern hybridization to obtain strains N4528 and N4529. Similarly, to obtain strains expressing only H2AK122A-FLAG, strain N4201 was crossed with N4195 and progeny growing on minimal medium were screened by Southern hybridization to obtain strains N4533 and N4534.

Supplemental Information

COP9 Signalosome and DNA Methylation

The COP9 signalosome (CSN) is believed to regulate the ubiquitin ligase activity of cullin complexes by removal of NEDD8 (Choo et al., 2011; Hotton & Callis, 2008; J.-T. Wu et al., 2006). Persistence of neddylation in Neurospora signalosome mutants (*csn*) results in autoubiquitination and degradation of the CUL1/SKPFWD1 complex (Qun He

et al., 2005). We wished to determine if a similar persistence of NEDD8 on CUL4 in the *csn* mutants could lead to autoubiquitination and degradation of DCDC, leading to loss of DNA methylation. However, we observed normal DNA methylation in *csn* mutants (Fig. 5). Consistent with this observation, proteomic analysis of purified epitope-tagged DCDC (DIM-8-FLAG) from a *csn* mutant revealed the presence of all DCDC components (Appendix B). Treatment with cycloheximide inhibits protein synthesis and affects the stability of DCDC components CUL4 and DDB1in *csn* mutants (J. Wang et al., 2010). Again, we observed normal DNA methylation in cycloheximide treated *csn* mutant (Fig. 5), suggesting that DNA methylation may not require the continuous presence of DCDC at regions of DNA methylation.

Histone H2A Ubiquitination Is Not Required for DNA Methylation in Neurospora

Recently, it has been speculated that monoubiquitination of histone H2A lysine 119 (H2AK119ub) by CRL4B may direct DNA methylation in mammals (Yang et al., 2015). H2A monoubiquitination by BRCA-1 also mediates heterochromatin formation (Guerrero-Santoro et al., 2008; Kapetanaki et al., 2006; Zhu et al., 2011). To explore the possibility that H2A is a substrate for DCDC, we expressed epitope-tagged H2A (wild-type and putative ubiquitination site mutant) in wild-type and *cul4* strains but failed to detect ubiquitination in any of the transformants by Western blotting. We also developed a method to generate *in vivo* substitutions in H2A and constructed Neurospora strains that have all H2A with the potential ubiquitination site mutated (Fig. 6). DNA methylation was unaffected by H2AK122A substitution (Fig. 6). Similarly, DNA methylation was not affected by mutations in Neurospora genes encoding proteins that are known to

ubiquitinate H2A for DNA repair in mammals (Inoue, 2011; Ulrich & Walden, 2010; W. Zhou, Wang, & Rosenfeld, 2009), namely MMS2, RAD5, RAD6, RAD18 and RNF8 (Fig. 10).

Bridge to Chapter III

After demonstrating that CUL4 did not require core aspects of cullin E3 ubiquitin ligases, my next goal was to utilize a similar approach to explore the subunit contributions of the HCHC histone deacetylase complex. The HCHC contains multiple proteins that could function in its localization: the chromodomain proteins HP1 and CDP-2, which bind to H3K9me3, and the AT-hook protein CHAP, which binds to A:T-rich DNA. Through mutational analysis I discovered that the CDP-2 chromodomain is not required for HCHC function and does not operate redundantly with the HP1 chromodomain. I also found evidence that the A:T-rich DNA binding activity of CHAP functions in tandem with the HP1 chromodomain to properly establish heterochromatin.

CHAPTER III

DISSECTION OF THE DUAL CHROMATIN RECOGNITION MODES OF THE HCHC HISTONE DEACETYLASE COMPLEX IN *NEUROSPORA CRASSA*

This work was published in volume 113 of the journal *Proceedings of the National Academy of Sciences of the United States of America* in September 2016. This work was performed in collaboration with Shinji Honda, Vincent Bicocca, Michael Rountree, Ayumi Yokoyama, Eun Yu, Jeanne Selker, and Eric Selker. I generated deletions of the HP1 and CDP-2 chromodomains at their endogenous loci and tested the effect of these mutations on DNA methylation. I also generated strains to test redundancy of the HP1 chromodomain with CDP-2 and CHAP and performed DNA methylation-sensitive Southern blotting. Shinji Honda generated ectopically expressed mutants of CDP-2, HP1, HDA-1 and CHAP and tested for DNA methylation defects. Shinji Honda also performed the DNA adenine methyltransferase identification (DamID), yeast two-hybrid, and co-immunoprecipitation (Co-IP) experiments. Vincent Bicocca performed DamID sequencing (DamID-seq) and performed the CHAP *in vitro* binding assays. Michael Rountree performed bisulfite sequencing and generated HP1 mutants. Ayumi Yokoyama constructed mutants of CDP-2 and performed Co-IP experiments with HP1 and HDA-1. Eun Yu constructed strains for Co-IP and assisted with yeast two-hybrid experiments. Jeanne Selker performed the microscopy characterizing the frequency of chromatin bridges in mutant strain backgrounds. Eric Selker was the principle investigator for this work.

Introduction

DNA methylation is an epigenetic mechanism involved in fundamental biological processes such as transcriptional regulation, genome defense, X chromosome inactivation, and genomic imprinting (Heard & Disteche, 2006; Reik & Walter, 2001; Slotkin & Martienssen, 2007; Weber & Schübeler, 2007). In mammals, patterns of DNA methylation are established during embryonic development and are maintained during subsequent cell divisions (Reik, Dean, & Walter, 2001). Abnormal DNA methylation is associated with human disease, including cancer (Feinberg, 2007; Robertson, 2005), but the events leading to abnormal DNA methylation are not well understood. A full understanding of aberrant methylation will first require a more complete understanding of normal methylation. Nevertheless, revelations during the last decade have provided clues to guide further research. Most importantly, studies in fungi, plants, and animals have revealed that histone modifications and RNA signals can influence, if not outright control, DNA methylation (Cedar & Bergman, 2009; S. W.-L. Chan, Henderson, & Jacobsen, 2005; Rountree & Selker, 2010).

Research using the filamentous fungus *Neurospora crassa* first revealed a link between DNA methylation and histone H3 lysine 9 (H3K9) methylation, which is a molecular hallmark of constitutive heterochromatin (Tamaru & Selker, 2001). Subsequent genetic and biochemical studies uncovered a direct pathway from H3K9 methylation to DNA methylation. The DIM-5 (defective in methylation-5) lysine methyltransferase (KMT) catalyzes trimethylation of H3K9 (H3K9me3) (Tamaru et al., 2003), which is recognized and bound by the chromodomain (CD) of heterochromatin

protein 1 (HP1) (Freitag, Hickey, Khlafallah, Read, & Selker, 2004a). The DNA methyltransferase (DNMT) DIM-2 is directly recruited by HP1 through the chromoshadow domain of HP1 and two PxVxL-like motifs in DIM-2 (Honda & Selker, 2008).

In *N. crassa*, H3K9me3, HP1, and DNA methylation are co-localized and together define the regions of constitutive heterochromatin (Lewis et al., 2009). The centromere regions, generally rich in transposon relics, account for the largest regions of constitutive heterochromatin, but telomeres and interstitial islands of transposon relics also have some features of heterochromatin. Most of these regions are A:T-rich as a result of the genome defense system RIP (repeat-induced point mutation). RIP detects duplicated sequences and induces G:C to A:T mutations in these regions during the sexual phase of the *N. crassa* life cycle (Lewis et al., 2009; Selker, 1990; Selker et al., 2003). The resulting A:T-rich sequences serve as potent signals for triggering H3K9me3 and DNA methylation *de novo* (Lewis et al., 2009; Miao et al., 2000; Tamaru & Selker, 2003). We identified DIM-5, DIM-7, DIM-9, CUL4 (cullin 4), and DDB1 (DNA damage-binding protein 1) as components of a KMT complex, DCDC (DIM-5/-7/-9–CUL4– DDB1 complex), which is required for H3K9me3 and appears to operate by a two-step mechanism: DIM-7–dependent DIM-5 recruitment and CUL4/DDB1/DIM-9–dependent catalysis by the KMT DIM-5 (Lewis, Adhvaryu, Honda, Shiver, & Selker, 2010a; Lewis, Adhvaryu, Honda, Shiver, Knip, Sack, et al., 2010b).

We previously identified a histone deacetylase (HDAC) complex, HCHC, which contains HP1, CD protein 2 (CDP-2), the HDAC HDA-1, and a CDP-2/HDA-1–associated protein, CHAP (Honda et al., 2012). The HCHC complex works in parallel

with the DNMT complex DIM-2–HP1 to establish and maintain normal heterochromatin. In addition, the HCHC complex indirectly maintains proper DNA methylation at regions with moderate and heavy mutation by RIP, which respectively show hypo- and hyper-methylation in *cdp-2*, *hda-1*, or *chap* mutants (Honda et al., 2012). Here we describe detailed functional interrelationships and domain functions of the components of the HCHC complex.

Results

HCHC Plays an Important Role in Centromere Function.

We previously demonstrated that mutants lacking HP1, but not DIM-2, exhibit sensitivity to the microtubule inhibitor thiabendazole (TBZ) and the topoisomerase I inhibitor camptothecin (CPT) and suffer from chromosome segregation defects (Lewis, Adhvaryu, Honda, Shiver, Knip, Sack, et al., 2010b). Because HP1 is present in both the HCHC and DIM-2/HP1 complexes (Honda et al., 2012) and because centromere regions are hypermethylated in mutants defective in components of HCHC (Honda et al., 2012), we wished to test if mutants lacking other components of HCHC show these *hpo* (HP1 gene) phenotypes. We found that the *hda-1*, *cdp-2*, and *chap* mutants did not display sensitivity to CPT comparable to that observed for the *hpo* mutant (Fig. 11A), suggesting that HP1 has functions other than its role in the HCHC and HP1–DIM-2 complexes. Like *hpo* strains, mutants lacking HDA-1 exhibited strong sensitivity to TBZ, whereas *cdp-2* and *chap* mutants showed an intermediate level of TBZ sensitivity (Fig. 11A). Like *hpo* strains but unlike *dim-2* strains, all the HCHC mutants showed numerous chromosome

bridges (Fig. 11B) (Lewis, Adhvaryu, Honda, Shiver, Knip, Sack, et al., 2010b). These findings fit with our prior observation that HCHC mutants show centromeric silencing defects (Honda et al., 2012) and strengthen the conclusion that HCHC is important for centromere function.

Whole-Genome Bisulfite Sequencing Analysis of the HCHC Mutants.

DNA methylation of HCHC mutants was previously assessed in selected genomic regions by Southern hybridization and methylated DNA immunoprecipitation analyses (Lewis et al., 2009). To extend our understanding of the role of HCHC, we carried out whole-genome bisulfite sequencing (WGBS) of *cdp-2*, *chap*, and *hda-1* mutants. Consistent with our prior analyses (Honda et al., 2012), a heat map display of the WGBS data revealed both hypomethylated and hypermethylated regions in the three HCHC mutants (Fig. 12). In addition, when methylated regions were sorted by increasing size, we found that shorter regions, which are generally heavily methylated in wild-type HCHC (average of 47.6% of C residues are methylated in the 50 shortest regions), tend to show significantly reduced methylation in the HCHC mutants (averages of 13.9, 14.8, and 22.7% in *cdp-2*, *hda-1*, and *chap* mutants, respectively) (Fig. 13A). Conversely, longer regions, most notably centromeres, are more lightly methylated in wild-type strains (average of 25.9% in the longest 50 regions) but tend to show moderately more methylation in the HCHC mutants (average of 30.7, 32.0, and 35.0% in *hda-1*, *cdp-2*, and *chap* mutants, respectively) (Fig. 13A and B). Sequences near telomeres that are normally methylated were found to lose methylation in the mutants (Fig. 13B and Fig. 12). In addition, sequences with a low combined RIP index (CRI) (Selker et al., 2003)

tend to show reduced methylation in the mutants, whereas sequences with higher CRI scores show increased methylation (Fig. 13C). The borders of normally methylated regions typically lose methylation and show a contraction of boundary methylation in the HCHC mutants (Fig. 13D).

The CD of HP1 but Not That of CDP-2 Is Required for HCHC Complex Function.

We previously demonstrated that the CD of CDP-2 efficiently binds to H3K9me3 *in vitro* (Honda et al., 2012). Considering that the HCHC complex harbors two proteins containing this domain, we wished to investigate the possibility that the chromodomains might be partially or fully redundant. To do so, we generated constructs to produce epitope-tagged proteins bearing mutations changing or deleting residues known to be critical for the CD function (CDP-2^{W446G}, CDP-$2^{\Delta CD}$, and CDP-$2^{1\text{-}419}$) (Fig. 14A). All constructs were tagged with a C-terminal 3XFLAG epitope, and expression was driven by the native *cdp-2* promoter. We inserted the constructs at the *his-3* locus in a *cdp-2* mutant strain and confirmed that their expression levels were all comparable to that in the wild-type strain (Fig. 15A). Curiously, all the *cdp-2* constructs bearing CD mutations rescued the *cdp-2* defects, namely region-specific hypomethylation (Fig. 14B), global hypermethylation (e.g., at centromere regions) (Fig. 15B), and derepression of centromere silencing (Fig. 15C), suggesting that the CD of CDP-2 is dispensable.

These findings did not eliminate the possibility that the CDP-2 CD has a redundant function, perhaps with HP1. We therefore generated C-terminal HAT-FLAG epitope-tagged HP1 constructs, similar to those created for CDP-2, that contain mutations changing or deleting residues critical for HP1 CD function (hpo^{W98G} and $hpo^{\Delta CD}$) (Fig.

16A). These *hpo* promoter-driven constructs were inserted at the *his-3* locus in a *Δhpo* mutant strain. DNA methylation was entirely lost in the *Δhpo* transformation host strain but was fully restored with the *his-3* targeted hpo^{WT} construct (Fig. 16B). Surprisingly, both the HP1 CD mutant constructs, hpo^{W98G} and $hpo^{\Delta CD}$, restored a low level of DNA methylation, indicating that the CD region is not absolutely required for DNA methylation. Similarly, these CD mutants partially alleviated sensitivity to TBZ (Fig. S3C). However, the mutants still showed sensitivity to CPT and defective centromeric silencing (Fig. 16C and D).

The CDP-2 and HP1 CD mutations described above were expressed at the *his-3* locus. To test the effect of simultaneously compromising the chromodomains of both CDP-2 and HP1, we inserted the CD-deletion constructs at their respective endogenous loci (Fig. 14). The new *hpo* constructs were tagged with the LexA DNA-binding domain (LexADBD) epitope at the C terminus. We confirmed that the strain carrying the tagged hpo^{WT} construct exhibited normal DNA methylation, indicating that the tagged protein was functional (Fig. 14D). As in our results described above (Fig. 16B), we found that deletion of the HP1 CD, unlike the loss of the whole protein (Freitag, Hickey, Khlafallah, Read, & Selker, 2004a), resulted in reduced DNA methylation rather than a complete loss of DNA methylation (Fig. 14D). Deletion of the CDP-2 CD did not accentuate the DNA methylation defect of the HP1 CD mutant (Fig. 14E), suggesting that, despite its ability to bind methylated H3K9 *in vitro* (Honda et al., 2012), the CDP-2 CD does not act redundantly with the HP1 CD.

CDP-2 Interacts Directly with the Chromoshadow Domain of HP1.

To gain insights into how HCHC operates without the CDP-2 CD, we investigated the organization of the HCHC subunits and tested the function of their prominent domains (Honda et al., 2012). We performed a yeast two-hybrid assay and found that HP1 and CDP-2 interact directly and that this interaction requires the chromoshadow domain of HP1 (Fig. 17A). CDP-2 did not interact with the HP1^{Y244E} mutant, which has a single amino acid substitution in the HP1 chromoshadow domain that prevents both dimerization of HP1 and interaction with the DIM-2 tandem PxVxL-like motifs (Honda & Selker, 2008; Thiru et al., 2004). To determine which CDP-2 sequences interact with the HP1 chromoshadow domain, we generated and tested a series of CDP-2 fragments. We found that amino acids 8–24 of CDP-2 are sufficient for binding HP1 (Fig. 18A). Inspection of the CDP-2 sequence revealed a PxVxL-like motif, (I/F/V)x(I/V)x(I/L/V), at amino acids 14–18 that is conserved among filamentous fungi (Fig. 18B). We generated and tested a mutant construct with alanines substituted for conserved residues at 14 and 15 (IE/AA) in the motif and found that the change abolished interaction with HP1 (Fig. 17B and Fig. 18A). To verify the specific interaction, we deleted a second PxVxL-like motif, ΔPPITL, found at amino acids 33–37, adjacent to the first PxVxL-like motif, and confirmed that it did not abolish the interaction (Fig. 18A). We next created the corresponding CDP-2 mutant strains and tested this interaction *in vivo*. Each protein included a 3XFLAG epitope tag, and expression was driven by the endogenous promoter. In line with our yeast two-hybrid results, coimmunoprecipitation (co-IP) experiments revealed that the IE/AA mutation abolished interaction with HP1 (Fig. 17C). Interestingly, the ΔPPITL mutation also eliminated interaction with HP1 *in*

vivo even though it did not *in vitro* (Fig. 17C and Fig. 18A), suggesting CDP-2 might be similar to DIM-2 in requiring tandem PxVxL-like motifs to interact with HP1 (Honda & Selker, 2008). Together, these results support a model in which the N-terminal fragment of CDP-2 interacts directly with the chromoshadow domain of HP1.

CDP-2 and CHAP Interact Directly with HDA-1.

We further used the yeast two-hybrid assay to ask how other components of HCHC interact. We found that, in addition to interacting with HP1, CDP-2 interacts with HDA-1 but not with CHAP (Fig. 17A). Similarly, HDA-1 interacts with CHAP but not with HP1, and CHAP does not interact directly with HP1 (Fig. 17A). To identify the protein regions involved in the interactions, we generated and tested a series of CDP-2, HDA-1, and CHAP fragments. The experiments revealed that amino acids 24–54 of CDP-2 are sufficient for binding HDA-1 and that deletion of the PxVxL-related motif PPITL (amino acids 33–37) abolished its interaction with HDA-1 (Fig. 17B and Fig. 18C). *In vivo* co-IP analysis of this interaction, using the IE/AA and ΔPPITL constructs described above, revealed that only the PPITL motif is required for CDP-2's interaction with HDA-1 and that the IE/AA mutation had no effect on their interaction (Fig. 17D). Further yeast two-hybrid analysis showed amino acids 87– 474 of the HDA-1 HDAC domain were sufficient for binding CDP-2 (Fig. 17B and Fig. 18D), and amino acids 478–744 of the HDA-1 Arb2 (argonaute-binding protein 2) domain are sufficient for its direct interaction with CHAP (Fig. 17B and Fig. 18E). To test whether the AT-hook and zinc finger motifs of CHAP are involved in the interaction between HDA-1 and CHAP, we made CHAP point mutants [first AT-hook (ATh1); second AT-hook (ATh2); first

zinc finger (Zf1); and second zinc finger (Zf2)] (Fig. 19A) and found that the Zf1 of CHAP is important for its interaction with HDA-1 (Fig. 17B and Fig. 18F). Unfortunately, we were unable to validate the roles of CHAP's zinc fingers *in vivo*, because mutant constructs produced unstable CHAP protein (Fig. 19B). The yeast two-hybrid interactions of all the components of HCHC are summarized in Fig. 17B.

CDP-2 Recruits HDA-1 HDAC Activity to H3K9me3 Regions.

Based on the interaction map among the HCHC components (Fig. 17B), we hypothesized that CDP-2 might simply serve as a tether between HP1 and HDA-1, facilitating deacetylation of histones marked with H3K9me3. To test this idea, we first carried out co-IP experiments on extracts from strains with epitope-tagged HDA-1 and HP1 in *cdp-2*-null mutant strains and found that interactions between HDA-1 and HP1 indeed depend on CDP-2 (Fig. 20A). Interestingly, the interaction between HDA-1 and HP1 occurred in a *dim-5* mutant, indicating that formation of the HCHC complex can occur before HP1 binding to H3K9me3 (Fig. 20A). To elucidate further the role of CDP-2 in tethering, we performed DamID (DNA adenine methyltransferase identification) by generating wild-type and *cdp-2* mutant strains expressing HDA-1–Dam. DamID uses DpnI (which cuts specifically at adenine-methylated GATC sites) and DpnII (which cuts at GATC sites without adenine methylation) to assess adenine methylation catalyzed by Dam fusion proteins and can provide information on the genomic localization of proteins that are not detectable by ChIP (Lewis, Adhvaryu, Honda, Shiver, & Selker, 2010a; Vogel, Peric-Hupkes, & van Steensel, 2007). At all heterochromatic regions tested, expression of HDA-1–Dam in a wild-type background produced low- and some

intermediate- molecular-weight DpnI fragments, indicating that HDA-1–Dam localized to heterochromatin (Fig. 21A). Little DpnI digestion was detected at the euchromatic pan-1 gene. Compared with a wild-type strain, HDA-1–Dam localization to heterochromatin was reduced in *cdp-2* strains, providing further evidence that CDP-2 is required for proper targeting of HDA-1 (Fig. 21A).

In principle, the essential role of HDA-1 in HCHC may or may not depend on HDAC activity. To distinguish between these possibilities, we generated an *hda-1* construct with a point mutation causing an amino acid substitution of a residue critical for HDAC activity, HDA-1^{D263N} (Fig. 21B)(Sugiyama et al., 2007), and with a 3XFLAG epitope tag at the C terminus of the protein. The construct was driven by the native *hda-1* promoter and was inserted at the *his-3* locus of an *hda-1* mutant. Insertion of a wild-type control *hda-1– FLAG* construct restored nearly normal patterns of DNA methylation, indicating that the HDA-1–FLAG fusion was functional (Fig. 21C). In contrast, HDA-1^{D263N}–FLAG failed to complement the methylation defects (Fig. 21C), even though it was expressed as well as wild-type HDA-1–FLAG (Fig. 21D and E). Co-IP experiments verified that the mutation did not affect the stable formation of HCHC (Fig. 21D and E), implying that HDAC activity is required for the HCHC function. Taking these results together with the previous observation that mutants lacking CDP-2 show striking hyperacetylation of histones H3 and H4 at heterochromatic regions (Honda et al., 2012), we conclude that CDP-2 serves as a bridge between HP1 and HDA-1 to recruit HDAC activity to methylated H3K9 regions.

HP1 and CDP-2 Localize to Heterochromatin Independently of HDA-1 and CHAP

To investigate further the extent to which recruitment of HP1 and CDP-2 may depend on other members of the complex, we generated *hda-1* and *chap* mutants expressing HP1–GFP or CDP-2–GFP and examined localization of the GFP-tagged proteins by microscopy. Because CDP-2 is destabilized in the absence of other components of the complex (Fig. 20B–D), it was necessary to overexpress CDP-2 to test if its punctate localization depends on the other HCHC components. The nuclear foci that characterize normal HP1–GFP localization were lost when H3K9me3 was abrogated in a *dim-5* mutant but were evident in *cdp-2*, *hda-1*, and *chap* mutants (Fig. 22A), consistent with the model that HP1 recruits CDP-2, HDA-1, and CHAP to chromatin marked with H3K9me3. Similarly, CDP-2 localization was unaltered in *hda-1* and *chap* mutants but was dependent on HP1 and H3K9me3 (Fig. 22B). Furthermore, using the DamID assay, we verified that CDP-2 localization to heterochromatin depends on HP1 but not on HDA-1 and CHAP (Fig. 22C). These data suggest that CDP-2 is important for tethering HP1 to HDA-1/CHAP, as is consistent with our interaction map (Fig. 17B).

CHAP Is Required for the Residual DNA Methylation in the HP1 CD Deletion Strain

We next characterized the role of CHAP *in vivo* and found that mutants lacking CHAP had unstable interactions with the other HCHC components (Fig. 20A–C) and reduced HDA-1–Dam localization to heterochromatin (Fig. 21A), as is consistent with importance of CHAP for histone deacetylation at heterochromatic regions (Honda et al., 2012). We also found that the stability of CHAP and its localization to DNA with repeat-

induced point mutations were dependent on the other components of HCHC (Fig. 20D–F and Fig. 23A). Given the similar residual DNA methylation in the HP1 CD mutant and in *chap*-null mutant strains (Fig. 24), we hypothesized that chromatin binding of the HCHC complex may rely partly on CHAP. We therefore tested a strain with both the HP1 CD deletion and a *chap* deletion and found that it showed complete loss of DNA methylation at regions that lose methylation in the *hda-1* mutant (8:A6, 8:G3, and 2:B3) (Honda et al., 2012) but did not lose methylation at a region unaffected by *hda-1* (8:F10) (Fig. 24). Taken together, these data provide evidence that CHAP, in conjunction with the CD of HP1, facilitates the recruitment of HCHC to some heterochromatic regions.

The CHAP AT-Hook Motifs Are Required for Normal DNA Methylation

To evaluate the possible role of the AT-hooks of CHAP, we generated a series of constructs with point mutations to change critical residues in these motifs and with a 3XHA epitope tag at the C terminus of the protein (CHAP–HA) (Fig. 25A). All constructs were driven by the native *chap* promoter and were inserted at the *pan-2* locus of a *chap*-deletion strain. We confirmed that mutations in the AT-hook motifs ($CHAP^{ATh1}$, $CHAP^{ATh2}$, and $CHAP^{ATh1\&2}$) did not affect the level of CHAP protein (Fig. 23B) and that insertion of a wild-type *chap–HA* construct into a chap-deletion strain restored nearly normal patterns of DNA methylation, indicating that the CHAP–HA fusion is functional (Fig. 25B). Strains expressing $CHAP^{ATh1}$ showed moderate restoration of DNA methylation, and strains expressing $CHAP^{ATh2}$ exhibited almost full restoration. However, strains bearing mutations in both AT-hook motifs ($CHAP^{ATh1\&2}$) showed marked defects in DNA methylation (Fig. 25B). Co-IP experiments verified that

the AT-hook mutations do not affect the stable formation of HCHC (Fig. 23C). We conclude that the CHAP AT-hook motifs are required for normal DNA methylation, perhaps through the AT-rich DNA-binding activity expected of such motifs (Aravind & Landsman, 1998).

The CHAP AT-Hook Motifs Specifically Bind AT-Rich DNA with High Numbers of Repeat-Induced Point Mutations

To test whether the CHAP AT-hook motifs bind AT-rich DNA that has repeat-induced point mutations, we performed *in vitro* DNA-affinity purification with the recombinant CHAP N terminus (residues 1–274) containing the two AT-hook motifs and analyzed the purified DNA with high-throughput sequencing. To complement this approach, we also assessed the binding of CHAP *in vivo* with DamID sequencing using the CHAP–Dam strain. Together, these techniques gave us a detailed genomic view of the specific localization and binding of CHAP to AT-rich DNA that has repeat-induced point mutations, which is nearly coincident with methylated DNA regions (Fig. 26A and B). We carried out band-shift assays to test further the binding of CHAP to AT-rich DNA and the role of its AT-hooks, using two representative probe sequences containing distinct AT contents: the middle segment of the heterochromatic region peak 33 (probe 1, 75.1% A+T) and a segment adjacent to the region (probe 2, 43.5% A+T) (Fig. 26B). The CHAP AT-hook motifs bound strongly to the AT-rich DNA that has repeat-induced point mutations (probe 1) but not to the control region (probe 2), and the binding was essentially abolished by mutations of the AT-hook motifs (CHAP-$N^{ATh1\&2}$) (Fig. 26C and

D). We conclude that CHAP, through its AT-hook motifs, binds AT-rich DNA that has repeat-induced point mutations (Lewis et al., 2009).

Discussion

DNA methylation, a prototypical epigenetic mark, is widely thought to be stably maintained by a simple copying system at symmetric methylated sites, as proposed by Riggs (Riggs, 1975) and Holliday and Pugh (Holliday & Pugh, 1975) more than 30 years ago. However, it has become apparent that maintenance of methylation patterns reflects the product of a variety of processes involving a multitude of proteins. In addition to DNA methyltransferases and other enzymes that interact with DNA to convert or excise 5-methylcytosine (5mC) residues, chromatin remodelers and histone modification enzymes impact the distribution and intensity of DNA methylation (Du, Johnson, Jacobsen, & Patel, 2015). Indeed, in some organisms, such as *N. crassa*, DNA methylation is dependent on the methylation of a particular residue of histone H3, H3K9 (Tamaru & Selker, 2001). Other histone modifications, such as methylation of H3K4, phosphorylation of H3S10 (Adhvaryu & Selker, 2008; Adhvaryu, Berge, Tamaru, Freitag, & Selker, 2011), and histone acetylation, also influence DNA methylation (Selker, 1998; K. M. Smith et al., 2010). We previously demonstrated that HCHC mutants of *N. crassa* show increased acetylation of histone H3 and H4 at larger heterochromatin domains, such as centromeres, and speculated that the increased acetylation might provide an enhanced environment for the HP1-DIM-2 complex, leading to the increased DNA methylation observed in the large domains of constitutive

heterochromatin in centromere regions. Our WGBS analyses on a wild-type strain confirmed that shorter regions tend to be more methylated than longer regions (Fig. 13A), whereas HCHC mutants show hypo-methylation of shorter regions and hyper-methylation of longer regions (Fig. 13A and B). The current study also demonstrated that the AT-hook motifs of CHAP are important for proper DNA methylation and bind specifically to AT-rich DNA that has repeat-induced point mutations (Fig. 26), which is particularly prevalent at centromere regions. This finding raises the possibility that CHAP binding contributes to stronger recruitment of HCHC at centromeres, at the expense of the HP1-DIM-2 complex, leading to the characteristic low levels of DNA methylation in these regions. It is interesting that, in contrast to the importance of DNA methylation in silencing short heterochromatic regions, DNA methylation is unnecessary for silencing at centromere regions (Honda et al., 2012).

The HCHC complex possesses two CD proteins, HP1 and CDP-2, which one might imagine could operate semi-redundantly. Consistent with this possibility, we found that although the CD of CDP-2 binds efficiently to methylated H3K9 *in vitro* (Honda et al., 2012), this domain is not required for normal DNA methylation and centromere silencing *in vivo* (Fig. 14B and Fig. 15B and C). We therefore considered the possibility that the CDP-2 CD in the HCHC complex might mediate the association of this complex with methylated H3K9 in the absence of HP1 binding. However, the CDP-2 CD mutants did not show additional DNA methylation defects in the HP1 CD mutant background (Fig. 14E), suggesting that the CDP-2 CD does not work redundantly with the HP1 CD in HCHC. Instead, our findings suggest that CDP-2 serves as a bridge between HP1 and HDA-1, ensuring the proper recruitment of the HDA-1 HDAC domain to chromatin (Fig.

27B). We show that CDP-2, like DIM-2, interacts directly with the HP1 chromoshadow domain through the PxVxL-like motifs near the N terminus (Fig. 17B and C). This observation is consistent with our previous observation that HP1 forms physically and functionally distinct complexes with DIM-2 and CDP-2 (Honda et al., 2012).

We demonstrated that in the absence of the HP1 CD, *N. crassa* still has residual DNA methylation in the regions with repeat-induced point mutations that depend on HDA-1. This surprising residual DNA methylation is dependent on CHAP (Fig. 24), which apparently serves as an additional means to recruit HCHC that is independent of the chromodomains (Fig. 27D). Therefore, we propose that dual chromatin recognition of heterochromatin by the HP1 CD and by the CHAP AT-hook motifs is responsible for HCHC function (Fig. 27A). Curiously, we still observed DNA methylation in double mutants lacking the HP1 CD and CHAP at the region 8:F10, which has repeat-induced point mutations (Fig. 24), raising the possibility that another element of HP1 recognizes a heterochromatic signal. In mammals and fission yeasts, HP1 has been shown to bind to RNA through the hinge region in addition to binding methylated H3K9 through the CD (Keller et al., 2012; Muchardt et al., 2002). Although the RNAi pathway is not involved in heterochromatin formation *in N. crassa* (Freitag, Lee, Kothe, Pratt, Aramayo, & Selker, 2004b), bivalent recognition via the CD and hinge region of HP1 seems possible.

Although *N. crassa* has a relatively simple DNA methylation pathway centered on H3K9 methylation serving as a signal for the direct recruitment of the HP1-DIM-2 complex (Freitag, Hickey, Khlafallah, Read, & Selker, 2004a; Honda & Selker, 2008), reinforcing loops involving H3K9me3, HP1, and DNA methylation occur. Recent studies using *N. crassa* and *Arabidopsis* uncovered mutants that fail to modulate these

reinforcing loops properly (Honda et al., 2010; Saze, Shiraishi, Miura, & Kakutani, 2008). The mutants exhibit abnormal silencing of essential genes by aberrant DNA methylation and H3K9 methylation, resulting in growth defects. In *N. crassa*, aberrant H3K9me3 depends on DNA methylation, revealing the existence of feedback pathway from DNA methylation to H3K9me3 (Honda et al., 2010). In addition, our WGBS analyses revealed that HDA-1 and CHAP are required for the spreading of DNA methylation (Fig. 13D), presumably through HDAC activity and binding AT-rich DNA, respectively. In summary, we describe multifaceted interrelationships among AT-rich DNA that has repeat-induced point mutations, H3K9me3, HP1, histone deacetylation, and DNA methylation that together result in the observed establishment and maintenance of heterochromatic domains.

The *N. crassa* HCHC complex shares features with the *Schizosaccharomyces pombe* HDAC complex SHREC (Motamedi et al., 2008; Sugiyama et al., 2007), which also functions in centromeric silencing. Although there are obvious differences between the HDAC complexes in fission yeast and *N. crassa* (e.g., *N. crassa* HCHC does not contain a homolog of the chromatin remodeler Mit1), it would be interesting to know if mammals use a similar mechanism to control proper heterochromatin domains, especially at AT-rich pericentromeric heterochromatin.

Materials and Methods

N. crassa Strains and Molecular Analyses

All *N. crassa* strains and primers used in this study are listed in Appendices C and D, respectively. Strains were grown, crossed, and maintained according to standard procedures (Davis, 2000a). *N. crassa* strains were built according to methods described previously (Honda & Selker, 2009). DNA isolation, Southern blotting, Western blotting, co-IP, and fluorescence microscopy were performed as previously described (Honda & Selker, 2008). The following antibodies were used: anti-FLAG (Sigma, F3165; MBL, M185-3), anti-HA (University of Oregon monoclonal facility; Roche, 3F10; MBL, M180-3), anti-GFP (Abcam, ab290; MBL, 598), and anti-tubulin (Sigma, T6199). Specific HP1, CDP-2, HDA-1, and CHAP mutations were made with a QuikChange site-directed mutagenesis kit (Stratagene) and a PCR-based mutagenesis with the In-Fusion HD cloning system (Takara).

Assessment of Chromosome Bridges

The frequency of chromosome bridges was quantified using with GFP-tagged histone H2A (Lewis, Adhvaryu, Honda, Shiver, Knip, Sack, et al., 2010b). Conidia were plated on a thin layer of Vogel's medium solidified with 2% agar and supplemented with required nutrients and were grown at 32 °C overnight. A square of the culture was placed on a slide and covered with a drop of Vogel's medium and a coverslip. Hyphae observed using a 100× oil-immersion objective in a Zeiss Axioplan 2 fluorescence microscope with differential interference contrast (DIC) showed cytoplasmic streaming. Two

methods were used to count chromosome bridges that were visualized with a GFP filter. *(i)* For tips with at least four nuclei, those having a chromosome bridge were scored as positive. *(ii)* In other hyphae (in which the tips were not obvious), the number of bridges was recorded relative to the total number of nuclei observed. To combine the results from the two counting schemes, the number of tips multiplied by 4 was used as the number of nuclei for the first counting method. Results were expressed as the percentage of nuclei showing bridges relative to the total number of nuclei. For each nucleus there are two possible outcomes: having a bridge or not having a bridge. Thus, we used the statistical test for a binomial distribution. The 95% confidence intervals were calculated for the binomial parameter p, the probability of a bridge in a given strain, using the formula $\left(\sqrt{\frac{p(1-p)}{n}}\right)(1.96)$ where n is the total number of nuclei observed.

WGBS

WGBS was performed and reads were mapped as previously described (Klocko et al., 2015). Sequencing reads can be downloaded from the National Center for Biotechnology (NCBI) database (accession no. GSE81129). Normally methylated regions with a minimum size of 200 bp were determined using the RSEG software package (smithlabresearch.org/software/rseg/). To display the bisulfite sequencing data, the average 5mC level was determined for specified step-wise window sizes across the genome using the MethPipe program (smithlabresearch.org/software/methpipe/) (Song et al., 2013). The resulting file was renamed with an .igv file extension to allow display on the Integrated Genome Viewer (software.broadinstitute.org/software/igv/) (Robinson et al., 2011). Similarly, the MethPipe (ROI function) was used to calculate the average 5mC

level over the normally methylated regions found in the wild-type strain (N3752) as determined using RSEG software and sequences immediately flanking these regions. The CRI was calculated for 500-bp windows across the *N. crassa* genome using a custom Perl script (Lewis et al., 2009).

CHAP–DamID Sequencing

Whole-genome DamID sequencing was performed using a procedure adapted from Vogel et al., 2007. Briefly, genomic DNA from the Dam-tagged CHAP strain was digested with DpnI. Digested DNA was ligated to adapters and amplified using a biotin-tagged primer. The amplified DNA was fragmented by sonication to 100- to 500-bp products and purified using streptavidin-conjugated beads (Sigma). Bound DNA was eluted using a DpnII digestion. Purified DNA was prepared for sequencing using the Illumina TruSeq ChIP Sample Preparation Kit. Sequence alignments were performed as previously described (Jamieson, Rountree, Lewis, Stajich, & Selker, 2013), except that the reads were mapped to the *N. crassa* OR74A (NC12) genome (*N. crassa* Sequencing Project, Broad Institute of Harvard and MIT; www.broadinstitute.org/), and read densities then were averaged over 25-bp windows to generate all tiled data files. Sequencing reads can be downloaded from the NCBI database (accession no. GSE81129).

Construction of HA-Tagged CHAP Fusion Constructs Expressed at the *pan-2* Locus

We amplified a fragment of HA-tagged *chap* gene with its native promoter by PCR with primers 2090 and 2497 from the genomic DNA of a strain expressing CHAP–HA from its native locus (created using the knock-in system described above). The PCR

products were digested with NotI and XhoI, inserted into the *pan-2* targeting vector pRATT42b (the gift of R. Aramayo, Texas A&M University), linearized, and inserted at the *pan-2−::hph+::tk+* locus of the *chap*-null mutant (N3642).

Generation of Recombinant CHAP Proteins and Gel Mobility Shift Assays

The *chap* ORF (amino acids 1–274) was amplified with primers 3011 and 3069 and inserted between the EcoRI and BamHI sites of pMALc2 (New England Biolabs). The plasmids were transformed into *E. coli.* strain BL21, and recombinant proteins were purified as described by the manufacturer of pMALc2. Recombinant maltose binding protein (MBP)-CHAP$^{1–274}$ protein was incubated for 30 min at room temperature in a 20-μL volume of EMSA binding buffer [20 mM Hepes (pH 7.9), 50 mM KCl, 4 mM MgCl2, 25 μM ZnCl2, and 1 mM DTT], 1 μg of BSA, and a radiolabeled DNA probe. A 100-pM DNA probe was used for K_d determination. Double-stranded DNA probes were produced using PCR primers (probe 1: primers 3019 and 3020; probe 2: primers 2483 and 2484) in reactions supplemented with [α-^{32}P] dCTP. Following incubation, EMSA reactions were analyzed on 5–20% Mini-Protean TGX gels (Bio-Rad); after electrophoresis, gels were dried and autoradiographed.

DNA–Protein Affinity Purification

DNA affinity purification using recombinant MBP-CHAP was performed using a protocol adapted from (Jolma et al., 2010). Amylose resin (New England Biolabs) containing immobilized MBP-CHAP was incubated with sonicated wild-type genomic DNA (~250-bp fragments) in binding buffer [20 mM Hepes (pH 7.5), 80 mM NaCl, 37.5

mM Imidazole, 0.7 mM MgCl2, 0.35 mM EDTA, 0.7 mM DTT, and 17.8% glycerol] for 2 h at 4 °C. Beads were washed six times with 1 mL of wash buffer [10 mM Tris (pH 7.5), 50 mM NaCl, 1 mM MgCl2, 0.5 mM EDTA, and 4% glycerol]. Following washes, DNA was eluted with TES [20 mM Tris (pH 8.0), 10 mM EDTA, and 1% SDS] by heating for 10 min at 65 °C. Eluted samples were treated with proteinase K, and DNA was purified with MinElute columns (Qiagen). Purified DNA was prepared for high-throughput sequencing using the TruSeq ChIP Sample Preparation Kit (Illumina).

Construction of a C-Terminal Dam Fusion Vector for *his-3* Targeting and Fusion Constructs for CDP-2, HDA-1, and CHAP

Escherichia coli dam was amplified from pCmyc-Dam (Vogel et al., 2007) with primer 3058, which contains a PacI site and a 10×Gly tail, and primer 3059, which contains an EcoRI site. The PCR products were digested with PacI and EcoRI and inserted into PacI- and EcoRI-digested pCCG::C-3XFLAG (Honda & Selker, 2009) to replace the 3XFLAG region with the 10×Gly–Dam segment, yielding pCCG::C-Gly::Dam.

To express the CDP-2–Dam fusion construct from its endogenous promoter, the *cdp-2* coding region was transferred from pTTK26 with NotI and PacI into pCCG::C-Gly::Dam. We assembled FLAG- and Dam-tagged *hda-1* constructs for targeting to the *his-3* locus by PCR with primers 3062 and 2093 and cloned the product into pCR2.1 using a TA cloning kit (Invitrogen). A fragment of the *hda-1* promoter region was amplified by PCR with primers 2091 and 3086 and was transferred with NotI and SpeI into pCCG::C-Gly::3XFLAG (Honda & Selker, 2009) to replace the *ccg-1* promoter with

the *hda-1* promoter, yielding phda-1::C-Gly::3XFLAG. We amplified the *his-3* 3′-flanking sequence along with the *hda-1* promoter from phda-1::C-Gly::3XFLAG using primers 3131 and 3126. Similarly, the 5′ *his-3* region with a 3XFLAG or a Dam tag was amplified by PCR with primers 3125 and 3128 and pCCG::C-Gly::3XFLAG or pCCG::C-Gly::Dam, respectively, as templates. The three products, containing the 3′ *his-3* flanking sequence with the *hda-1* promoter, the 5′ partial *his-3* sequence with the epitope tag, and the cloned *hda-1* ORF sequence, were mixed and assembled by PCR with primers 3128 and 3131, were gel-purified, and were introduced at the *his-3* locus of the *hda-1*-null mutant by electroporation (Margolin et al., 1997). To express Dam-tagged CHAP from its endogenous promoter, a fragment of the *chap* coding region with its promoter was amplified by PCR, digested with NotI and PacI, and inserted into pCCG::C-Gly::Dam using the same enzymes, yielding pCHAP::C-Gly::Dam. The pCHAP:: C-Gly::Dam then was linearized and inserted at *his-3* in the *chap*-null mutant (Margolin et al., 1997).

Construction of the C-Terminal HAT/FLAG–Tagged HP1 CD Constructs Expressed at *his-3*

Site-directed mutagenesis using overlapping forward and reverse primers (3081 and 3082) was used to create a point mutation (T to G) in the CD region of HP1 resulting in a codon change of W to G at the 98th residue. The *his-3*–targeting plasmid 2899 (*phpo::hpo-HAT-FLAG*) was used as the template, and the creation of the point mutation was confirmed by sequencing.

To generate a deletion of the entire *hpo* CD, we amplified two fragments of the *hpo* gene by PCR with one fragment immediately upstream of the CD (primers 5246 and 5247) and the other immediately downstream of the CD (primers 5248 and 5249) using plasmid 2899 (*phpo::hpo-HAT-FLAG*) as the template. These fragments were combined through stitching PCR, generating a deletion of the HP1 CD. This stitched PCR fragment then was digested with BsiWI and PacI and was cloned into the BsiWI/PacI-digested plasmid 2899. The deletion of the CD was confirmed by sequencing.

These HP1 CD mutant constructs, along with the HP1 wild-type construct, were linearized and transformed into N5430 (*his-3; Δhpo strain*). *His+* transformants were selected and checked by Southern analysis for the proper integration of the HP1 constructs at the *his-3* locus. Positive transformants then were crossed to the N4909 (*cenVIR::bar; his-3; trp-2*) strain to generate homokaryotic strains containing *cenVIR::bar; his-3::hpo*$^{WT\ or\ CDmutant}$*; Δhpo::hph; trp-2*.

Construction of CDP-2, HDA-1, and CHAP Mutant Constructs.

We created the other mutant constructs by site-direct mutagenesis similarly with the following primer pairs: primers 3187 and 3188 for *cdp-2*$^{I14A,\ E15A}$; primers 3056 and 3057 for *cdp-2*^{W466G}; primers 3138 and 3139 for *cdp-2*$^{\Delta PPITL}$; primers 3171 and 3172 for *cdp-2*$^{\Delta CD(444–459aa)}$; primers 3054 and 3055 for *hda-1*^{D263N}; primers 2433 and 2434 for CHAP$^{ATh1(R210A)}$; primers 2435 and 2436 for CHAP$^{ATh2(R250A)}$; primers 2437 and 2438 for CHAP$^{Zf1(C280A)}$; and primers 2439 and 2440 for CHAP$^{Zf2(C327A)}$.

Construction of LexADBD-Tagged HP1 CD-Deletion Fusion Constructs Expressed at the Native *hpo* Locus.

We amplified the *hpo* gene with the CD deleted by PCR with primers 4525 and JGP123 from N5869. Additionally the LexADBD with an 8X glycine linker was amplified by PCR from plasmid 3015 using primers JGP62 and JGP63. The hygromycin resistance cassette *ptrpC::hph* was amplified from PCR from plasmid 2409 using primers JGP60 and JGP61. Also, the flanking region downstream of the *hpo* gene was amplified by PCR using primers JGP124 and JGP125. These PCR products were combined by PCR stitching and integrated at the native *hpo* locus of N5643.

Construction of CDP-2 CD-Deletion Constructs Expressed at the Native *cdp-2* Locus.

We amplified the CD-deleted *cdp-2* gene by PCR with primers N3064 and JGP281 from plasmid 2973 (created for ectopic CDP-$2^{\Delta CD}$ expression from the *his-3* locus). Additionally, the flanking region downstream of the *cdp-2* gene was amplified by PCR using primers JGP282 and 3145. These PCR products were combined through PCR stitching with a central *ptrpC::nat-1* antibiotic resistance cassette from plasmid 3130. This PCR product then was integrated at the native *cdp-2* locus of N2930.

Bridge to Chapter IV

Chapters II and III dissected the complexes controlling H3K9me3, DNA methylation, and histone deacetylation. My next goal was to better understand the interplay between

these modifications as well as explore the contributions of individual subunits. To address these goals, I developed *in vivo* protein tethering in Neurospora to dissect the establishment of heterochromatin targeted to a euchromatic locus. My findings suggest connections between heterochromatin features and support a central role of histone deacetylation by HDA-1 in heterochromatin spreading and gene silencing.

CHAPTER IV

INDUCTION OF H3K9ME3 AND DNA METHYLATION BY TETHERED HETEROCHROMATIN FACTORS IN *NEUROSPORA CRASSA*

This chapter contains unpublished, co-authored work exploring the control of H3K9me3, DNA methylation, and silencing using *in vivo* protein tethering. I was responsible for experimental design, data collection, and analysis of the resulting data. Eric Selker was the principle investigator for this work.

Introduction

Heterochromatic regions of eukaryotic genomes are typically comprised of gene-poor sequences, hypo-acetylated histones H3 and H4, tri-methylation of lysine 9 on histone H3 (H3K9me3), and DNA methylation (Bühler & Gasser, 2009; Grewal & Jia, 2007; Henikoff, 2000; Lewis et al., 2009). The hypoacetylated status of histones within heterochromatin is mediated by histone deacetylases (HDACs) and is generally associated with transcriptional repression (Ekwall, 2005). The proper assembly of heterochromatin and regulation of the underlying genes is important for centromere and telomere function, and for silencing parasitic transposable elements (Henikoff, 2000; Lewis et al., 2009). Moreover, aberrant DNA methylation is associated with human diseases, including cancer (Feinberg, 2007; Robertson, 2005), providing motivation to elucidate the establishment and maintenance of heterochromatin. Dissection of the pathway for heterochromatin formation is problematic in mammals and other higher

eukaryotes because of the essential nature of H3K9me3 and DNA methylation, and the redundancy of the factors responsible for these marks (Dodge et al., 2004; Okano et al., 1999; Peters et al., 2001; Ronemus et al., 1996; Tachibana et al., 2002). The filamentous fungus *Neurospora crassa* serves as a useful model system to investigate the workings of heterochromatin; it shows many of the features of heterochromatin found in higher organisms, but the underlying genes are generally neither essential nor redundant.

In Neurospora, constitutive heterochromatin is found at centromeric regions, telomeric regions, and at islands of heterochromatin characterized by relics of transposons rendered A:T-rich by the genome defense system RIP (repeat-induced point mutation) (Lewis et al., 2009). Segments of such RIP'd DNA serve as recruitment signals for *de novo* H3K9me3 and DNA methylation (Lewis et al., 2009; Miao et al., 2000; Selker, 1990; Tamaru & Selker, 2003). H3K9me3 depends on all members of the five-member complex DCDC (DIM-5/-7/-9, CUL4, DDB1 Complex). Results of an *in vivo* DamID study revealed that only the DIM-7 (defective in methylation-7) subunit is required to localize the lysine methyltransferase DIM-5, which is responsible for all H3K9me3 (Lewis, Adhvaryu, Honda, Shiver, & Selker, 2010a; Tamaru et al., 2003; Tamaru & Selker, 2001). H3K9me3 is recognized and bound by heterochromatin protein 1 (HP1) through its chromodomain (Freitag, Hickey, Khlafallah, Read, & Selker, 2004a). HP1 in turn acts as a scaffold to recruit a DNA methyltransferase (DIM-2), a putative histone demethylase (DMM) complex, and a histone deacetylase complex (HCHC) (Honda et al., 2010; 2012; Honda & Selker, 2008).

DIM-2 is recruited to heterochromatin through a direct interaction between its PXVXL-like motif and the chromoshadow domain of HP1, leading to methylation of

cytosines remaining in RIP'd DNA (Honda & Selker, 2008). Spreading of DNA methylation into euchromatin is prevented by the DMM (DNA methylation modulator) complex, which consists of a putative JmjC domain demethylase (DMM-1) and a DNA-binding protein (DMM-2) (Honda et al., 2010).

The HCHC complex is composed of HP1, the chromodomain protein CDP-2, the histone deacetylase HDA-1, and the AT-hook protein CHAP (Honda et al., 2012; 2016). Dissection of the HCHC complex components suggested that the histone deacetylation activity of HDA-1 selectively modulates H3K9me3 and DNA methylation levels (Honda et al., 2012; 2016). HCHC mutants show histone hyperacetylation and defects in centromeric silencing in centromere regions, and interestingly, also display hypermethylation of DNA in these regions, perhaps because of greater accessibility of the hyperacetylated chromatin to DIM-2 (Honda et al., 2012; 2016). In addition, HCHC mutants show hypomethylation of some small patches of interstitial heterochromatin associated with relatively weak RIP (Honda et al., 2016).

To improve our understanding of heterochromatin formation, including the interplay between the deacetylation of histones and the methylation of histones and cytosines *in vivo*, we utilized a protein tethering system to artificially localize individual components of the heterochromatin machinery to a euchromatic site. This allowed us to decipher the requirements for heterochromatin establishment and maintenance by bypassing the recruitment signals within heterochromatin. We found that several members of the heterochromatin machinery, including DIM-5, HP1, and HDA-1, are able to induce H3K9me3 and cytosine methylation at a euchromatic locus but require other members of the heterochromatin machinery. Further dissection of HP1-interacting

proteins led to the identification of histone deacetylase HDA-1 as a critical factor in the establishment of H3K9me3, DNA methylation, and silencing. Altogether, our results reveal a feedback mechanism between the histone deacetylation activity of HDA-1 and the other methylation-dependent hallmarks of heterochromatin.

Results

Tethering DIM-5 or HP1 Induces Heterochromatin

Previous work demonstrated requirements of members of the heterochromatin machinery for H3K9me3 and DNA methylation but important questions remained regarding the roles of individual proteins and the functional interplay between heterochromatic marks. To investigate the roles and requirements of heterochromatin machinery, we used an *in vivo* protein tethering system derived from the bacterial LexA transcriptional regulator to test the sufficiency of core heterochromatic components to induce ectopic heterochromatin at euchromatic loci (Hoshino & Fujii, 2009; Thliveris & Mount, 1992). The C-termini of DCDC components DIM-5, DIM-7, DIM-9, DDB1, and CUL4 as well as HP1 and the DNA methyltransferase DIM-2 were C-terminally-tagged with an 8x glycine linker, an SV40 antigen nuclear localization signal (NLS), and the LexA DNA-binding domain (LexADBD). All fusion constructs were engineered to replace the corresponding genes at their native loci and tested for functionality by scoring DNA methylation at heterochromatin locus 8:A6. All of the chimeras were functional, displaying essentially wild-type levels of DNA methylation (Fig. 28). The proteins were individually expressed in a strain containing four tandem copies of a LexA consensus

sequence (LexAO) (Hoshino & Fujii, 2009; Thliveris & Mount, 1992) integrated about 500 bp downstream of the euchromatic *his-3* locus (Fig. 29A). Each half-site of the palindromic LexA sequence serves as a binding site (Thliveris & Mount, 1992) to recruit the LexADBD, which in total allows for tethering of up to eight molecules of a given protein.

To test the sufficiency of each tethered component to induce heterochromatin formation, we carried out DNA methylation-sensitive Southern hybridizations with AvaI and BfuCI restriction digests and probed for the LexAO. We found that both tethered DIM-5 and HP1 were individually sufficient to induce DNA methylation at the LexAO (Fig. 29B). In contrast, tethered DIM-7, DIM-9, DDB1, CUL4 and DIM-2 failed to induce DNA methylation (Fig. 29B). The observed digestion patterns suggested that DIM-5 and HP1 induce domains of DNA methylation of up to approximately 1 kb and 3 kb, respectively (Fig. 29A-B). We observed comparable results at *trp-2,* a locus that shows a low level of cytosine methylation without a tethered protein (Fig. 30).

Tethered DIM-5 Requires All Components of DCDC

With the ability to bypass the native mechanisms of DIM-5 recruitment, we wished to determine if other DCDC members are required to activate tethered DIM-5. Thus, we tethered DIM-5 to the LexAO in strains lacking the other members of the DCDC and asked if cytosine methylation was induced. We found that all members of the DCDC were required for the tethered DIM-5-mediated induction of DNA methylation at the LexAO (Fig. 29C). Previous results of a DamID assay for localization of DIM-5 revealed that DIM-7 is the only member of the DCDC required to localize DIM-5 to

incipient heterochromatin (Lewis, Adhvaryu, Honda, Shiver, & Selker, 2010a). Notably, our findings demonstrate that the requirement of DIM-7 is not bypassed by tethering DIM-5, implying that DIM-7 serves one or more roles within the DCDC in addition to its apparent role in DIM-5 localization.

Tethered HP1 Depends on Histone Deacetylase Activity of HCHC to Induce H3K9me3 and DNA Methylation

To elucidate how tethered HP1 induces DNA methylation, we investigated if DIM-5 or HP1-associated complexes are necessary by testing for induction in various mutant strains. We also examined the necessity of a putative chromatin remodeler, MI-2, that associates with the HDA-1 homolog Clr3 in *Schizosaccharomyces pombe* (Sugiyama et al., 2007). Tethered HP1 was unable to induce DNA methylation at the LexAO in strains with a deletion of either *dim-5* or *hda-1* (Fig. 31A) implying that both H3K9me3 and deacetylation are required for induction of methylation. Additionally, the DNA methylation profile was altered, but not abolished, in strains lacking *dmm-1* or *mi-2*, implying that these HP1-interacting proteins are not absolutely required but can modulate the extent of the induced DNA methylation (Fig. 31A).

Because we found that HDA-1 is required for heterochromatin formation induced by tethered HP1, we also tested the contributions of the other HCHC subunits CDP-2 and CHAP. Deletion of *cdp-2* or *chap* reduced, but did not abolish, the induced DNA methylation (Fig. 31B). Thus, in contrast to HDA-1, HCHC components CDP-2 and CHAP are not essential for the artificial heterochromatin nucleated by tethered HP1.

Given that *dim-5* was required for induction of DNA methylation by tethered HP1 (Fig. 31A), we wished to verify the presence of H3K9me3 and determine its extent by chromatin immunoprecipitation (ChIP). Tethered HP1 resulted in strong enrichment of H3K9me3 at the LexAO (Fig. 31C). Since HP1 can directly recruit DIM-2, and the requirement of DIM-2 for induced heterochromatin cannot be addressed by assaying DNA methylation, we examined if the cytosine methylation catalyzed by DIM-2 serves a function in establishing H3K9me3 at the LexAO. We assayed H3K9me3 enrichment in strains lacking DIM-2 catalytic activity, either because of deletion of the gene or due to a point mutation in the DIM-2 catalytic domain (C926A) (Kouzminova & Selker, 2001). All constructs were tagged with a C-terminal 3XFLAG at the native *dim-2* locus and we confirmed the DIM-2 catalytic domain mutant expression level was comparable to that of wild-type DIM-2 (Fig. 32). Curiously, the loss of DIM-2 DNA methyltransferase activity decreased but did not abolish H3K9me3 enrichment at the LexAO (Fig. 31C).

To test if histone deacetylase activity is required for the H3K9me3 resulting from tethered HP1, we expressed a 3XFLAG-tagged, catalytically defective version of HDA-1 (D263N) (Honda et al., 2016) from the native *hda-1* locus. The expression level of this construct was comparable to that of wild-type HDA-1 (Fig. 32). H3K9me3 ChIP demonstrated that the catalytically dead HDA-1 abolished H3K9me3 at the LexAO resulting in background signal comparable to that with the strain bearing deletion of *hda-1* (Fig. 31C). Altogether, these observations indicate that DNA methylation enhances H3K9me3 establishment and suggest that HCHC deacetylase activity, localized by tethered HP1, may be sufficient to induce H3K9me3 and DNA methylation.

To better characterize the heterochromatin domains induced by tethered DIM-5 or HP1, as well as the impact of HCHC and DIM-2 activity, we carried out H3K9me3 ChIP followed by high throughput sequencing (ChIP-seq). We found that the extent of H3K9me3 induced by tethered HP1 around LexAO (Fig. 31D) was comparable to the extent of DNA methylation detected by Southern hybridization (Fig. 29A-B). Curiously, tethered HP1 induced an asymmetric domain of H3K9me3, which was strongest downstream of the LexAO, and depleted within the LexAO (Fig. 31D). We further observed that deletion of *dim-2* resulted in a reduction both in intensity and extent of the H3K9me3 domain induced by tethered HP1 (Fig. 31D). In a strain lacking HDA-1 catalytic activity, tethered HP1 resulted in almost no H3K9me3 enrichment proximal to the LexAO (Fig. 31D). These results are consistent with, and extend, our other observations of the DNA methylation (Fig. 29A-B) and H3K9me3 (Fig. 31C) induced by HP1.

Tethered HP1 Is Sufficient to Silence Nearby Genes Through HCHC Activity Independent of H3K9me3 and DNA Methylation

To test if the induced heterochromatin is functional for gene silencing, the *nat-1* gene (Goldstein & McCusker, 1999), which confers resistance to the antibiotic nourseothricin, was integrated adjacent to the LexAO binding sites at the *his-3* locus. We found that tethering HP1 to the LexAO was sufficient to silence *nat-1*, rendering the strain sensitive to nourseothricin. In contrast, a strain with tethered DIM-5 retained antibiotic resistance (Fig. 31E; Fig. 33A), which is consistent with our observations that tethered HP1, but not DIM-5, resulted in appreciable heterochromatin, evidenced by

DNA methylation, going into the *nat-1* gene (Fig. 33B). We conclude that the artificial localization of HP1 is sufficient to induce functional heterochromatic silencing in a region that is normally euchromatin.

To evaluate the contributions of H3K9me3, DNA methylation, and histone deacetylation in the repression of *nat-1*, we tested silencing in strains with tethered HP1 that lacked HCHC function (Δ*hda-1* or Δ*chap*), DNA methylation (Δ*dim-2*), or both H3K9 methylation and DNA methylation (Δ*dim-5*). Deletion of *hda-1* fully derepressed the *nat-1* gene and deletion of *chap* resulted in partial derepression (Fig. 31E). In contrast, loss of DNA methylation (Δ*dim-2*) or H3K9me3 (Δ*dim-5*) did not alleviate silencing (Fig. 31E). These data suggest that deacetylation activity of HCHC is a key factor in establishing heterochromatic silencing independent of H3K9me3 and DNA methylation.

DNA Methylation Induced by Tethered HP1 Does Not Require Its Chromodomain or the AT-Hook Domains of CHAP

Our finding that HCHC subunits are important for the DNA methylation induced by tethered HP1 (Fig. 31B) prompted us to examine contributions of specific domains of the proteins. First, we assessed the possible contributions of the HP1 chromodomain, which binds to H3K9me3, and the chromoshadow domain, which facilitates dimerization and cofactor interactions (Freitag, Hickey, Khlafallah, Read, & Selker, 2004a; Honda & Selker, 2008; Thiru et al., 2004) using strains bearing a deletion of the chromodomain (ΔCD) or a point mutation that disrupts the function of the chromoshadow domain (Y244E) (Fig. 34A) (Honda et al., 2016). All constructs were tagged with the LexADBD

at the native *hpo* locus and expression of the altered HP1 proteins was found to be comparable to that of wild-type HP1 (Fig. 34B). As expected, the chromodomain was largely dispensable for heterochromatin induced by tethered HP1; the construct resulted in a moderate level of induced DNA methylation (Fig. 34C). In contrast, the HP1 chromoshadow mutant construct failed to cause DNA methylation at LexAO (Fig. 34C), demonstrating that the requirement of this domain is not bypassed by tethering HP1.

The HCHC component CHAP contains two AT-hook domains that bind to A:T-rich DNA and may contribute to normal HCHC localization (Fig. 34A); changes in both AT-hooks of CHAP result in a nearly complete loss of HCHC-dependent DNA methylation (Honda et al., 2012; 2016). We attempted to assess if the AT-hooks function in HCHC localization by testing if tethering HP1 would rescue HCHC activity when both CHAP AT-hooks were mutated. A strain expressing CHAP with both AT-hook point mutations only displayed a modest reduction of DNA methylation at the LexAO relative to the complete deletion of *chap* (Fig. 34D) supporting the idea that the AT-hooks normally augment HCHC localization (Honda et al., 2016).

HDA-1 Catalytic Activity Is Sufficient to Nucleate Heterochromatin

To determine if HCHC, like HP1, can induce DNA methylation at the LexAO in a site that is normally euchromatic, we individually tethered the HCHC components HDA-1, CDP-2, and CHAP. All LexADBD-tagged HCHC members were functional at the native, HCHC-regulated, 8:A6 heterochromatic locus (Fig. 35A) (Honda et al., 2012). We found that tethered HDA-1, much like DIM-5, induced a symmetric domain of DNA methylation and H3K9me3 centered on the LexAO (Fig. 36). Tethered HDA-1 also

increased the level of DNA methylation present at the LexAO within the *trp-2* locus (Fig. 30). To test if HDA-1 catalytic activity is required for the induced DNA methylation, we generated a LexADBD-tagged HDA-1 with an amino acid change that should prevent its catalytic activity (D263N) (Honda et al., 2016) at the *hda-1* locus; expression of this construct was similar to that of the wild-type allele (Fig. 35B). The tethered catalytic null variant of HDA-1 failed to induce DNA methylation (Fig. 36A). These results imply that histone deacetylation catalyzed by HDA-1 is sufficient to establish H3K9me3 and DNA methylation. In contrast, the other HCHC members, CDP-2 and CHAP, did not induce DNA methylation (Fig. 35C).

HDA-1 and DIM-5 Modulate the Localization and Activity of DIM-2

Induction of H3K9me3 and DNA methylation by tethered HP1 required the HCHC complex (Fig. 31A&C), but this result did not rule out recruitment of other cofactor complexes by tethered HP1. We wished to address the possibility that DIM-2 recruited to the LexAO by tethered HP1 remains inactive without HCHC activity. The distribution of DIM-2 is not readily detected by standard ChIP, possibly due to interactions being transient, but DIM-2 localization can be evaluated by DamID (DNA adenine methyltransferase identification) (Lewis, Adhvaryu, Honda, Shiver, & Selker, 2010a). DamID utilizes the restriction enzymes DpnI (cutting specifically at adenine-methylated GATC sites) and its isoschizomer DpnII (cutting inhibited by adenine methylation) to monitor adenine methylation catalyzed by Dam fusion proteins to provide an indication of the genomic localization of the tagged protein (Vogel et al., 2007). To test the requirements for DIM-2 localization, we compared DIM-2 DamID results in

tethered HP1 strains with or without a deletion of *hda-1*. We found that tethered HP1 at the LexAO in a wild type background strongly recruited DIM-2-Dam, consistent with the observed DNA methylation (Fig. 37A; Fig. 29B). Because deletion of *hda-1* prevents H3K9me3 at the LexAO (Fig. 31C), this mutation abrogates the normal H3K9me3/HP1-mediated mode of DIM-2 localization and focuses on DIM-2-Dam localization mediated by tethered HP1. Interestingly, a Δ*hda-1* strain with tethered HP1 still showed strong localization of DIM-2, while control probes showed the expected loss of localization at an *hda-1*-dependent heterochromatic locus (8:A6) and no recruitment to a euchromatic locus (*pan-1*) (Fig. 37A; Fig. 38A). Thus, DIM-2 was present at the LexAO but it did not catalyze DNA methylation.

This observation suggested that the HCHC deacetylase activity directed by tethered HP1, or the subsequent recruitment of DCDC, and leading to H3K9me3 might promote DIM-2 activity. To investigate if H3K9me3 machinery is required for DIM-2 activity, we assayed DIM-2-Dam localization with HP1 tethered in a Δ*dim-5* background, which both disrupts the native mode of DIM-2 localization and the induction of DNA methylation by tethered HP1 (Fig. 31A). DIM-2-Dam still strongly localized to the LexAO in this strain lacking H3K9me3, without obvious localization to 8:A6 or *pan-1*. (Fig. 37B; Fig. 38B). These results support a model in which DIM-5 promotes the activity of DIM-2 independent of localization.

The relationship between HCHC activity and H3K9me3/DNA methylation (Fig. 3A-B) raised the possibility that tethered DIM-5 may similarly require histone deacetylation to establish DNA methylation. To evaluate this hypothesis, we tested the DNA methylation level in a strain with tethered DIM-5 in a Δ*hda-1* background. We

observed that DNA methylation induced by tethered DIM-5 required HDA-1 (Fig. 37C). To differentiate between a defect in DIM-2 activity and localization, we examined the distribution of DIM-2-Dam in a tethered DIM-5; Δ*hda-1* strain. Curiously, in contrast to the case with tethered HP1, we found that tethered DIM-5-mediated recruitment of DIM-2-Dam was dependent on *hda-1* (Fig. 37D; Fig. 38C), suggesting histone deacetylation is necessary for HP1/DIM-2-Dam recruitment. Together, these results support a model in which the chromatin context, mediated by DIM-5 and HDA-1, can modulate the activity and localization of DIM-2.

HDA-1 Is Not Required for *de novo* Heterochromatin Formation at Native Heterochromatin

Our finding that HDA-1 activity is sufficient to induce heterochromatin (Fig. 36) raised the interesting possibility that HCHC may be required for *de novo* heterochromatin formation throughout the genome. We already knew that disruption of the HCHC complex does not eliminate most heterochromatin but, in principle, the persistence of heterochromatin could be due to some undefined maintenance system (Honda et al., 2012; 2016). To determine if the HCHC complex is necessary for *de novo* heterochromatin formation, we generated a strain with deletions of both *dim-5* and *hda-1,* thereby removing existing H3K9me3 as well as disrupting HCHC-mediated histone deacetylation, and then re-introduced *dim-5-3XFLAG* driven by the native *dim-5* promoter at an ectopic (*trp-2*) locus to examine *de novo* heterochromatin formation in a strain that lacked *hda-1*. Strikingly, DNA methylation was rescued to levels that were consistent with a deletion of *hda*-1 alone at both HCHC-regulated loci (8:G3 and

CenVIIM) and an HCHC-independent region (8:F10) (Honda et al., 2012) when only DIM-5, and therefore the capacity to establish H3K9me3, was restored (Fig. 39A). These data suggest that the HCHC is not required for *de novo* heterochromatin formation, and supports a model in which H3K9me3, seeded by the DCDC, serves as a signal to recruit HCHC-dependent histone deacetylation and DIM-2-dependent DNA methylation, which in turn promotes the spreading of H3K9me3 (Fig. 39B).

Discussion

In general terms, the establishment of heterochromatin domains is thought to follow a step-wise model: (i) seeding events, which create an altered state at a locus, (ii) spreading of the altered state, and (iii) maintenance of the altered state over time independent of the initial stimulus (Bonasio, Tu, & Reinberg, 2010). In the present study, we developed and used an *in vivo* system to target heterochromatin machinery to normally active euchromatic loci to expand our understanding of the mechanisms underlying these stages of heterochromatin assembly in Neurospora. We provide evidence of uncharacterized functions within the heterochromatin establishment machinery and clarify mechanisms contributing to heterochromatin spreading.

Requirement of DIM-7 for Heterochromatin Formation Is Not Limited to Its Role Recruiting DIM-5

Previous work in Neurospora and *S. pombe* defined largely conserved complexes responsible for establishing H3K9me3, the DCDC and ClrC, respectively (Lewis,

Adhvaryu, Honda, Shiver, Knip, Sack, et al., 2010b; K. Zhang et al., 2008). Much like DIM-5, the ClrC subunit Clr4 is responsible for H3K9 methylation in *S. pombe* (Nakayama, Rice, Strahl, Allis, & Grewal, 2001). Additionally, in ClrC, a protein similar to DIM-7, Raf2/Dos2, directly interacts with Cul4, Rik1 (similar to DDB1), Raf1/Dos1 (homologue of DIM-9), and Stc1 (not represented in DCDC) (Kuscu et al., 2014; K. Zhang et al., 2008). All core members of both DCDC and ClrC are required for the establishment of heterochromatin (Hong, Villén, Gerace, Gygi, & Moazed, 2005; Horn et al., 2005; Lewis, Adhvaryu, Honda, Shiver, Knip, Sack, et al., 2010b). The presence of the canonical components of Cullin E3 ubiquitin ligases (Petroski & Deshaies, 2005) in both DCDC and ClrC raised the possibility that ubiquitination mediated by CUL4 may be required for heterochromatin formation. While a separate putative Cul4 E3 ubiquitin ligase, Cul4-Ddb1^{Cdt2}, promotes heterochromatin formation in *S. pombe* by targeting a presumed histone demethylase, Epe1, for degradation (Braun et al., 2011), no ubiquitination substrate of the ClrC or DCDC complexes has been identified. This hypothesis was further thrown into doubt by results demonstrating that core aspects of Cullin E3 ubiquitin ligases are not required for heterochromatin establishment in Neurospora (Adhvaryu et al., 2014). These observations raised the possibility that the subunits of the ClrC and DCDC may function in other aspects of the localization and/or activity of the H3K9 methyltransferases. Prior work indicated that Rik1 is involved in more than Clr4 localization, as Rik1 is required for heterochromatin induced by tethered Clr4 (Kagansky et al., 2009). We expanded on this approach by tethering DIM-5 and testing each component of the DCDC for dispensability. Our finding that all members of the DCDC are required for DNA methylation induced by tethered DIM-5 (Fig. 29C)

implies that each subunit has one or more function(s) independent of DIM-5 localization. This result was striking given that DIM-7 is the only DCDC component required for localization of DIM-5 to constitutive heterochromatin (Lewis, Adhvaryu, Honda, Shiver, & Selker, 2010a). These results raise the possibility that DIM-7 serves as an essential scaffold between DIM-5 and DIM-9/DDB1/CUL4 (Lewis, Adhvaryu, Honda, Shiver, Knip, Sack, et al., 2010b). Additionally, these observations underscore the value of relatively simple model systems, such as Neurospora and *S. pombe*, to define and dissect the complexes and mechanisms controlling heterochromatin.

Role of Histone Deacetylation in Establishment of Heterochromatin Domains

In many model systems, including fission yeast, flies, mice, and human cells, HP1, or one of its homologs, recognizes H3K9me3 and directly interacts with an H3K9 methyltransferase (Aagaard et al., 1999; Haldar, Saini, Nanda, Saini, & Singh, 2011; Melcher et al., 2000; Schotta et al., 2002). This relationship provides an attractive mechanism through which HP1 binding to H3K9me3, *via* its conserved chromodomain, serves to recruit the H3K9 methyltransferase and propagate heterochromatic modifications. Consistent with this interaction, tethered HP1 in fission yeast, flies, mouse, and human cells, led to H3K9 methylation and gene silencing at euchromatic loci (Hathaway et al., 2012; Hines et al., 2009; Y. Li, Danzer, Alvarez, Belmont, & Wallrath, 2003; Ragunathan, Jih, & Moazed, 2014; Seum, Delattre, Spierer, & Spierer, 2001; Smallwood, Estève, Pradhan, & Carey, 2007). Further, the H3K9 methyltransferases in the aforementioned model systems also, like HP1, possess a chromodomain, some with demonstrated H3K9me3 binding specificity, which provides an additional mode of

feedback for heterochromatin propagation (Aagaard et al., 1999; Chin, Patnaik, Estève, Jacobsen, & Pradhan, 2006; K. Zhang et al., 2008). These interactions may mask additional feedback mechanisms that are independent of the chromodomains of HP1 and H3K9 methyltransferases. To explore this possibility, we took advantage of the fact that the Neurospora H3K9 methyltransferase, DIM-5, lacks a chromodomain and does not interact with HP1. Interestingly, we did find evidence of additional feedback interactions. Specifically, we observed that direction of the HCHC histone deacetylase activity, through tethered HP1 or HDA-1, was sufficient to establish H3K9me3 and DNA methylation at a euchromatic locus (Figs. 2 & 3).

At native heterochromatin, disruption of the HCHC complex preferentially results in the reduction of H3K9me3 and DNA methylation levels at small, less A:T-rich regions (Honda et al., 2012; 2016). The relationship we observed through protein tethering, between histone deacetylation and H3K9me3, provides insights for these HCHC-dependent changes observed at native heterochromatin. It is not yet well understood how histone deacetylation can direct DCDC activity, but previous work has shown that disruptions of HDA-1 homologs including mammalian HDAC4 (Hohl et al., 2013) and *S. pombe* Clr3 (Yamada, Fischle, Sugiyama, Allis, & Grewal, 2005), the histone deacetylase subunit of the complex homologous to HCHC, SHREC (Sugiyama et al., 2007), are associated with decreased H3K9me3. Elimination of *S. pombe* Clr3 (Bjerling et al., 2002; Sinha, Gross, & Narlikar, 2017) or Neurospora HDA-1 (Anderson, Green, Smith, & Selker, 2010; Honda et al., 2012; K. M. Smith et al., 2010) are also associated with increased H3K14ac as well as generally increased acetylation of histones H2B, H3, and H4. Interestingly, changing the H3K14 residue to either a lysine acetylation mimic

(glutamine) or a mimic of unacetylated lysine (arginine) showed no defects in DIM-5 activity *in vitro* and only a modest DNA methylation defect *in vivo* (Adhvaryu et al., 2011). The lack of a clear, singular HDA-1 histone deacetylation target raises the possibility that an array of deacetylated histone residues together serve as a signal for H3K9me3 establishment. Such a signal may alter binding of conserved interaction domains that bind specifically to acetylated lysines, such as bromodomains (Zeng & Zhou, 2002), and therefore may displace these factors by histone deacetylation. Additionally, the recent characterization of conserved acidic domains (D. Wang et al., 2016) has raised the possibility of a reader protein specifically binding unacetylated lysine residues. Alternatively, several instances of non-histone substrates of histone deacetylases have been identified and are implicated in regulating target gene expression, subcellular localization, and catalytic activity (Glozak, Sengupta, Zhang, & Seto, 2005). For future studies, Neurospora should provide a powerful model system to better understand how the activity of HDA-1 serves as a signal to establish H3K9me3 in lieu of direct HP1/DIM-5 or DIM-5/H3K9me3 interactions.

Disruption of Neurospora HDA-1 (Honda et al., 2012; K. M. Smith et al., 2010) or *S. pombe* Clr3 (Yamada et al., 2005) is associated with defects in heterochromatic silencing. These results support a role of histone deacetylation in gene silencing, but fail to disentangle this activity from other changes within heterochromatin, such as H3K9me3 or DNA methylation levels. Our finding that artificial recruitment of the HCHC complex by tethering HP1 establishes silencing at a proximal reporter gene, even in strains lacking H3K9me3 or DNA methylation, (Fig. 31E) expands on this model by supporting histone deacetylation as a key driver in gene silencing and suggesting H3K9me3 and DNA

methylation are not directly responsible for the repressive environment within heterochromatin. This proposed distinction is also consistent with prior observations noting the counter-intuitive association of centromeric silencing defects associated with increased levels of H3K9me3 and DNA methylation in HCHC mutants (Honda et al., 2012).

Role of Chromatin Context in the Activation and Localization of DIM-2

Unlike fission yeast and flies, Neurospora heterochromatin sports DNA methylation like many higher eukaryotes (Elgin & Reuter, 2013; Grewal & Jia, 2007; Saksouk, Simboeck, & Déjardin, 2015). We realized that our *in vivo* tethering approach provided a framework to better understand the mechanisms controlling this modification. While directly tethered DIM-2 did not induce DNA methylation (Fig. 29B), DIM-2 recruited by tethered HP1 required the DCDC to establish DNA methylation (Figs. 2 & 4). The necessity of DCDC activity suggests that DIM-2, once localized, may require a particular chromatin context to be catalytically active. The ability to "read" chromatin context at a given region may be mediated by DIM-2 itself through the conserved bromo-homology (BAH) protein-protein interaction domain (Callebaut, Courvalin, & Mornon, 1999; Kouzminova & Selker, 2001), or by an associated cofactor, such as HP1 "reading" H3K9me3. Alternatively, DIM-2 may be controlled through allosteric regulation related to the DCDC H3K9 methyltransferase activity. Post-translational methylation of the human DNA methyltransferases DNMT1 and DNMT3 is essential for cytosine methyltransferase catalytic activity and protein stability (Jeltsch & Jurkowska, 2016). While possible DIM-2 post-translational modifications have yet to be addressed, it is

conceivable that DCDC may post-translationally modify the DIM-2 protein to regulate its DNA methylation activity. The presence of DNA methylation, dependent on a sole methyltransferase, makes Neurospora an attractive model system to address such regulatory mechanisms of DNA methyltransferases.

The similarities in the heterochromatin machinery, chromatin modifications, and underlying mechanisms between Neurospora and higher organisms coupled with the reduced complexity of the Neurospora machinery - for example the lack of direct HP1/DIM-5 and DIM-5/H3K9me3 interactions - make our *in vivo* protein tethering approach ideal to study relationships between histone deacetylation, H3K9me3, DNA methylation, and gene silencing. Of possible relevance, in human patients suffering from heart failure, a fetal gene program is reactivated as a stress response resulting in maladaptive remodeling of heart valves (Hohl et al., 2013). This disruption in gene regulation is associated with nuclear export of a mammalian HDA-1 homolog, HDAC4, and reduced H3K9me3 levels (Hohl et al., 2013). The connection we observed between HDA-1 histone deacetylase activity and H3K9me3 establishment may offer insights into mechanistic underpinnings of this relationship. Moreover, the ability to direct the heterochromatic silencing mediated by HDA-1 presents an opportunity to better understand the repression of endogenous retrovirus-like elements in mammals established by the HP1 and NuRD histone deacetylase-containing ESET-KAP1 complex (Matsui et al., 2010).

Materials and Methods

Neurospora Strains and Molecular Analyses

All Neurospora strains and primers used in this study are listed in Appendices C and D, respectively. Strains were grown, crossed, and maintained according to standard procedure (Davis, 2000b). DNA isolation, Southern hybridization, and Western blotting were performed as previously described (Honda & Selker, 2008). Western blot analyses were carried out with antibodies to the LexA DNA binding region (LexADBD; Millipore, 06-719), FLAG-conjugated peroxidase (FLAG-HRP; Sigma, A8592), and phosphoglycerate kinase 1 (PGK1; Abcam, ab113687). Secondary antibodies were used as previously described (Honda & Selker, 2008). Chemiluminescence resulting from the treatment with SuperSignal West Femto Substrate (Thermo Fisher Scientific, 34095) for anti-LexADBD and SuperSignal West Pico Substrate (Thermo Fisher Scientific, 34080) for anti-PGK1 and anti-FLAG-HRP was imaged using a LI-COR Odyssey Fc imaging system.

Nucleic Acid Manipulations

DamID was carried out as described (Lewis, Adhvaryu, Honda, Shiver, & Selker, 2010a; Vogel et al., 2007). Briefly, DNA samples were incubated with or without DpnI, which cuts adenine-methylated GATC sites. As a control for completely digested DNA, wild-type genomic DNA was incubated with the 5^{m}C-insensitive isoschizomer DpnII. Digested DNA was analyzed by Southern hybridization with probes for the noted loci.

ChIP was performed as previously described (Jamieson et al., 2015) using anti-H3K9me3 (Active Motif, 39161). For quantitative ChIP (qChIP), real-time PCR experiments on independent experimental replicates were performed in triplicate using FAST SYBR Green master mix (Kapa) with the listed primers (Table S2) and analyzed using a Step One Plus Real Time PCR System (Life Technologies). Relative enrichment of each modification was determined by measuring enrichment as a percent of the total input. The enrichment proximal to the LexA Operator was then scaled to relative enrichment at the *hda-1*-independent, heterochromatic Peak 33a (Honda et al., 2012).

H3K9me3 ChIP samples were prepared for ChIP-seq as previously described (Jamieson et al., 2015). Sequencing was performed using an Illumina HiSeq 4000 using single-end 75 nucleotide reads. Manipulations of sequencing data were executed with the Galaxy platform (usegalaxy.org) (Afgan et al., 2016). FASTQ sequencing files were converted to FASTQ-Sanger format using FASTQ Groomer (Blankenberg et al., 2010). The resulting files were mapped with default settings using Bowtie2 (Langmead & Salzberg, 2012) to a form of the corrected *N. crassa* OR74A (NC12) genome (Galazka et al., 2016) that was modified to include the LexAO sequence at the *his-3* locus. For visualization, the mapped reads (BAM format) were then processed using the "count" function in igvtools (Robinson et al., 2011) to generate a tiled data file (.tdf) displaying read density at 1 bp resolution for the genome. The resulting files were displayed using Integrated Genomics Viewer (IGV) (Robinson et al., 2011) as reads per million per nucleotide (RPM).

Generation of LexAO Constructs

The LexAO sequence was amplified by PCR using plasmid FCNLD/pMIR (Hoshino & Fujii, 2009) as template with primers #3757 and #3758 containing EcoRV and XhoI sites, respectively. The PCR product and pZero::3XFLAG::*hph*::*loxP* (Honda & Selker, 2009) were digested with EcoRV and XhoI then ligated to yield pZero::LexAOP::*loxP*::*hph*. We amplified a fragment containing four copies of the LexAO binding site from plasmid pZero::LexAOP::*loxP*::*hph* using primers #5514 and #5515. This fragment and plasmid pKA67 (Lewis, Adhvaryu, Honda, Shiver, Knip, Sack, et al., 2010b) were digested with EcoRI and XbaI and then ligated. The resulting plasmid, pLO-1, was linearized by NdeI-digestion and transformed into strain N3012 to generate *his-3*-targeted LexAO repeats. The resulting his^+ strain (N5643) was verified by Southern hybridization and Sanger sequencing.

The nourseothricin resistance cassette P_{trpC}::*nat-1* was amplified by PCR from plasmid pAL12-Lifeact (Lichius & Read, 2010) with primers #6239 and #6240 containing SacI and XmnI sites, respectively. This fragment and pZero::3XFLAG::*hph*::*loxP* (Honda & Selker, 2009) were digested with SacI and XmnI then ligated to yield pZero::3XFLAG::*nat-1*::*loxP*. To insert the *nat-1* reporter gene near LexAO, we amplified two fragments of the targeted region by PCR with one encompassing the LexAO (primers #5532 and #5533) and the other further downstream of the LexAO binding sites (primers #5534 and #5535) using strain N5643 genomic DNA as template. These fragments were combined through three-part stitching-PCR (Heckman & Pease, 2007) with plasmid pZero::3XFLAG::*nat-1*::*loxP*. This fragment

was integrated proximal to the LexAO sites of strain N5643. The resulting *his*$^{+}$ *nat-1*$^{+}$ progeny were verified by Southern hybridization and Sanger sequencing.

To insert the LexAO at an alternative euchromatic locus, *trp-2*, we amplified fragments of the *trp-2* region by PCR upstream of the target site (primers #4878 and #5541) and downstream of the target site (primers #5542 and #4865) using strain N3753 DNA as template. The region containing the LexAO repeats and P_{trpC}::*nat-1* was amplified with primers #5532 and #5535 from strain N6647. These fragments were combined through stitching-PCR as described above, and the product was integrated into the genome to generate a deletion of the *trp-2* open reading frame in strain N3012. The resulting *trp*$^{-}$*; nat-1*$^{+}$ progeny were verified by Southern hybridization and Sanger sequencing.

Construction of Strains Expressing LexADBD-Tagged Fusion Proteins from Their Native Loci

To express gene-of-interest fusions with 8x glycine linker, SV40 nuclear localization signal (NLS), and LexA DNA binding domain (LexADBD) from the native loci of the respective genes, we amplified a region immediately upstream of the stop codon using the following primer pairs: primers #5516 and #5517 (DIM-5), primers #5520 and #5521 (HP1), primers #5510 and #5511 (DIM-2), primers #5524 and #5525 (DIM-7), primers #5528 and #5529 (DIM-9), primers #4757 and #5686 (DDB1), primers #5675 and #5684 (CUL4), primers #3007 and #5536 (HDA-1*), primers #3064 and #5551 (CDP-2*), and primers #3070 and #5553 (CHAP*) with genomic DNA from strain N3753 as template. We also amplified the region immediately downstream of the

stop codon using the following primer pairs: primers #5518 and #5519 (DIM-5), primers #5522 and #5523 (HP1), primers #5512 and #5513 (DIM-2), primers #5526 and #5527 (DIM-7), primers #5530 and #5531 (DIM-9), primers #5687 and #5678 (DDB1), primers #5685 and #5676 (CUL4), primers #5537 and #5679 (HDA-1*), primers #5552 and #3145 (CDP-2*), and primers #5554 and #5540 (CHAP*) with genomic DNA from strain N3753 as template. The NLS-LexADBD fragments were amplified from plasmid LexA-d1EGFP (Hoshino & Fujii, 2009) with primers #3755 and 3756 containing AscI and XbaI sites, respectively. The fragment and pCCG::N-3XFLAG (Honda & Selker, 2009) were digested with AscI and XbaI then ligated to yield pCCG-1-Nx3FLAG-LexADB. Fragments containing the 8xGly-NLS-LexADBD construct (primers #5508 and #5509) and P_{trpC}::*hph* (primers #5506 and #5507) were amplified with plasmids pCCG-1-Nx3FLAG-LexADB and pZero::3XFLAG::*hph*::*loxP* (Honda & Selker, 2009) as templates, respectively. The 5' region, LexADBD tag, *hph* resistance cassette, and 3' region were combined through primary stitching-PCR reactions (*5' region + LexADBD; LexADBD + hph + 3' region*) followed by a final stitching-PCR reaction (*5' region-LexADBD + LexADBD-hph-3' region*) and integrated into strains N2930 or N5643 (N5643 derived strains denoted with *). The resulting hph^+ or his^+; hph^+* progeny, respectively, were verified by Southern hybridization and Sanger sequencing.

Using the methods described above, we created tethered constructs with mutations of key residues. As with HP1-LexADBD above, to generate $HP1^{Y244E}$, we amplified the *hpo* gene harboring the mutation from plasmid pMF308 (Honda & Selker, 2008). As described above, this PCR product was combined with the tag, resistance cassette, and 3' region through stitching-PCR and integrated at the native *hpo* locus of

strain N2930. The resulting *hph*$^{+}$ progeny were verified by Southern hybridization and Sanger sequencing.

As with HDA-1-LexADBD above, to generate HDA-1^{D263N}-LexADBD, we amplified the *hda-1* gene harboring the mutation from strain N3998 (Honda et al., 2016). This PCR product was combined with the tag, resistance cassette, and 3' region through stitching-PCR and integrated at the native *hda-1* locus of strain N5643. The resulting *hph*$^{+}$ progeny were verified by Southern hybridization and Sanger sequencing.

Generation of CHAP$^{ATh1/2}$ Mutants

To generate CHAP$^{ATh1/2}$, we amplified the *chap* gene harboring the mutation from plasmid pGEX5X-1-*chap*$^{\Delta th1\&2}$ (Honda et al., 2016) using primers #3063 and #5538. Additionally, the region immediately downstream of the *chap* stop codon was amplified with primers #5539 and #5540 with genomic DNA of strain N3753 as template. These PCR products were combined with P_{trpC}::*nat-1* from plasmid pZero::3XFLAG::*nat-1*::*loxP* through stitching-PCR and integrated at the native *hpo* locus of strain N2930. The resulting *nat-1*$^{+}$ progeny were verified by Southern hybridization, crossed to strain N6166, and evaluated by Sanger sequencing. Sequencing revealed that the resulting strain (GC330-3) harbored an additional missense mutation. To repair the DNA sequence, a fragment upstream of the mutation was amplified from DNA from a sibling strain, GC330-2, using primers #3063 and #5680. A fragment including the mutated region was amplified using primers #5681 and #5682 from strain N3753 genomic DNA. These fragments were combined by stitching-PCR to produce a 5' region containing only the AT-hook mutations. A new 3' region fragment was amplified from strain GC330-2 to

include the P_{trpC}::*nat-1* gene using primers #5683 and #5540. To build a new selectable marker for the repaired allele, P_{trpC} was first added by stitching-PCR between the 5' region and plasmid pZero::3XFLAG::*hph*::*loxP* (Honda & Selker, 2009) using primers #3063 and #5656. This fragment was combined by stitching-PCR with the *bar* gene, conferring resistance to BASTA (Avalos, Geever, & Case, 1989), from pBARKS1 (Pall, 1993) using primers #3063 and #1658 to generate a split-marker fragment, as described (Klocko et al., 2015) for the 5' region. Additionally, the 3' region fragment was combined with pBARKS1 (Pall, 1993) by stitching-PCR using primers #1659 and #5540 to generate a 3' split-marker fragment, as described (Klocko et al., 2015). To generate a BASTA-sensitive strain, a sibling of the original strain (GC330-6) was outcrossed to N3752 to generate strain GC342-4. Both split-marker fragments were simultaneously transformed into strain GC342-4. The resulting *nat-1*$^{+}$;*bar*$^{+}$ progeny were verified by Southern hybridization and Sanger sequencing.

Generation of 3XFLAG-Tagged HDA-1 and DIM-2 Catalytic Mutants

As with HDA-1-LexADBD (above), to generate HDA-1^{D263N}-3XFLAG, we amplified the *hda-1* gene harboring the mutation from strain N3998 (Honda et al., 2016) with primers #3007 and #2077. Additionally, we amplified the region immediately downstream of the *hda-1* stop codon with primers #2078 and #2079 using genomic DNA from strain N150. These PCR products were combined with the *10xGly*::*3XFLAG*::P_{trpC}::*hph* cassette from circular plasmid pZero::3XFLAG::*hph*::*loxP* (Honda & Selker, 2009) by stitching-PCR and integrated at the native *hda-1* locus of strain N2930. The resulting *hph*$^{+}$ progeny were verified by Southern hybridization.

To generate a catalytic mutant of DIM-2 tagged with 3XFLAG, we amplified the *dim-2* gene harboring the mutation from strain N1909 (Kouzminova & Selker, 2001) with primers #4447 and #2013. Additionally, we amplified the region immediately downstream of the *dim-2* stop codon with primers #1989 and #1990. These PCR products were combined with *10xGly::3XFLAG::*P_{trpC}*::hph* as above and integrated at the native *dim-2* locus of strain N2930. The resulting *hph*$^{+}$ progeny were verified by Southern hybridization.

Generation of 3XFLAG-Tagged DIM-5 Expressed from *trp-2*

To express an ectopic copy of the *dim-5* gene fused to the 3XFLAG epitope tag from the *trp-2* locus, we amplified regions corresponding to 5' of the *trp-2* ORF (primers #4878 and #5555), the ORF and approximately 1100 base pairs upstream of the *dim-5* gene (primers #5677 and #1993), and a region 3' of the *trp-2* ORF (primers #5542 and #4865) from strain N3753 genomic DNA. The *trp-2* 5' region, *dim-5* fragment, and the P_{trpC}::*nat-1* cassette from plasmid pZero::3XFLAG::*nat-1*::*loxP* were combined by stitching-PCR using primers #4878 and #4883 to generate a 5' split-marker construct as described (Klocko et al., 2015). The *trp-2* 3' region and the P_{trpC}::*nat-1* cassette from plasmid pZero::3XFLAG::*nat-1*::*loxP* were combined by stitching-PCR using primers #4884 and #4865 to yield a 3' split-marker construct as described (Klocko et al., 2015). These fragments were simultaneously transformed into both strains N3944 and N6637. The resulting *nat-1*$^{+}$ progeny were verified by Southern hybridization and made homokaryotic through microconidiation (Ebbole & Sachs, 1990).

CHAPTER IV

CONCLUDING SUMMARY

In Chapter II, I utilized contemporary genetic tools to dissect the contributions of a putative, functional sub-complex (DIM-9/DDB1/CUL4) within the DCDC H3K9 methyltransferase complex. To this end, I targeted conserved, core aspects of Cullin E3 ubiquitin ligase complexes to test if these DCDC components functioned in this capacity in heterochromatin formation. The findings in Chapter II demonstrate that core aspects of these complexes are dispensable for heterochromatin formation, yet are required for the response to the mutagen methyl methanesulfonate (MMS), indicating compromised DNA repair processes.

These results provide evidence for non-canonical role(s) of CUL4 in heterochromatin formation. These findings favor a model in which these components may contribute to DIM-5-mediated H3K9me3 through alternative mechanisms, such as promoting associations amongst subunits within the DCDC or regulation of H3K9 methyltransferase activity. Given that all DCDC members are required for H3K9me3 and DNA methylation, it will be important for future studies to decipher how DIM-9, DDB1, and CUL4 contribute to DIM-5 activity and more broadly, heterochromatin establishment.

In Chapter III, I deleted the conserved chromodomains of endogenous HP1 and CDP-2 to evaluate potential redundancy in H3K9me3 binding within the HCHC complex. The deletion of the HP1 chromodomain resulted in a reduction but not a complete loss of DNA methylation at heterochromatic loci. In contrast, the deletion of the

CDP-2 chromodomain had no DNA methylation phenotype and no additional defect when combined with the HP1 chromodomain deletion. These observations show the HP1 chromodomain is not absolutely required to localize its associated complexes and curiously the CDP-2 CD, with demonstrated H3K9me3 binding specificity, is dispensable for HCHC function. In contrast, deletion of both the HP1 chromodomain and the *chap* gene resulted in a DNA methylation phenotype specifically at HCHC-dependent loci similar to an *hda-1* deletion. Taken together with the contributions of the other authors, these results support a model in which HP1 binding to H3K9me3 through its chromodomain and CHAP interacting with A:T-rich DNA through its AT-hook domains provide tandem mechanisms of heterochromatin recognition and serve to promote HCHC function.

These results provide the foundation for understanding HCHC function in heterochromatin. In this publication, we clarify the fundamental subunit interactions and localization mechanisms of the HCHC and the impact of these features on aspects of heterochromatin. In particular, we observe a core role of the HCHC in the establishment of the classic heterochromatin hallmarks H3K9me3 and DNA methylation as well as implicate HCHC function in proper centromere function and the faithful segregation of chromosomes. In the future, it will be of particular importance to better define the H3K9me3-dependent, but HP1 chromodomain-independent, process resulting in establishment of DNA methylation at incipient heterochromatin. The requirement of the HP1 protein for DNA methylation implicates other domains within the HP1 protein, such as the hinge region that bridges the chromo- and chromoshadow domains, in facilitating this activity.

In Chapter IV, I developed and demonstrated a novel application of *in vivo* protein tethering in Neurospora, derived from the bacterial LexA DNA binding domain and LexA Operator consensus sequence, which allowed for the targeted induction of heterochromatin at euchromatic loci. I found that induction of H3K9me3 and DNA methylation by tethered DIM-5 required all members of DCDC, providing evidence that DIM-7 fulfills role(s) independent of DIM-5-localization. Further, I found that directing HCHC activity, either by tethering HP1 or HDA-1, established H3K9me3, DNA methylation, and gene silencing. Silencing induced by tethered HP1 did not require H3K9me3 or DNA methylation but did require HCHC activity. Further, I demonstrated that HCHC activity is not required for *de novo* heterochromatin at native loci implicating HCHC in heterochromatin spreading/maintenance. Also, exploiting this protein tethering approach, I showed that DIM-5 is required for DIM-2-mediated establishment of DNA methylation independent of DIM-2 localization.

These results represent the first application of protein tethering in Neurospora to systematically dissect heterochromatin establishment and provide evidence of complex interplay between heterochromatic machinery and modifications. My findings take advantage of the well-defined H3K9 methyltransferase complex in Neurospora to expand on our understanding of the components involved in H3K9me3 deposition. In the future, it will be interesting to further elucidate the contributions of the DCDC components to DIM-5 activity. Further, this study exploits features of Neurospora heterochromatin to study feedback mediated by HCHC activity without confounding interactions between DIM-5/HP1 and DIM-5/H3K9me3 present with their respective homologs in other common model systems. To the best of our knowledge, these findings represent the first

evidence of the sufficiency of HDA-1 activity to establish H3K9me3 and serve to refine our model by further implicating deacetylation, along with establishment of DNA methylation, in H3K9me3 spreading. It will be critical to build on this foundation to determine how HDA-1-mediated deacetylation is integrated as a signal to promote H3K9me3 establishment. Also, it will be valuable to harness protein tethering to identify specific HDA-1 substrates, disentangling these targets from secondary effects driven by changing levels of other modifications, such as H3K9me3 and DNA methylation. Additionally, the ability of tethered HP1 to silence proximal genes independent of H3K9me3 and DNA methylation, yet dependent on *hda-1,* supports the concept of histone deacetylation as a key driver of silencing at heterochromatic loci. The utility in isolating this silencing mechanism, apparently driven by HCHC, from other features of heterochromatin should provide a valuable system to more precisely understand the mechanistic underpinnings of heterochromatic silencing and the role of *hda-1* in this process.

APPENDIX A

FIGURES

Figures for Chapter II

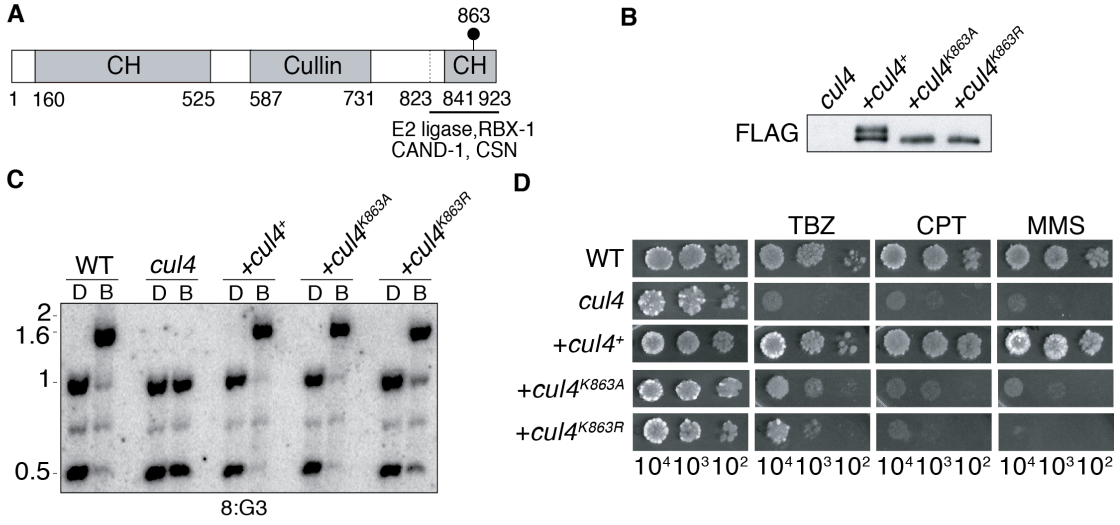

Fig. 1. Neddylation of CUL4 is dispensable for DNA methylation but not for DNA repair. (A) Schematic of CUL4 showing the NEDD8 attachment site (K863), cullin and cullin homology (CH) domains, and C-terminal region thought to interact with NEDD8 attachment machinery, E2 ligase, RBX1, CAND1, and CSN. (B) Western blots of extracts from an untransformed *cul4*^{RIP1} strain and *cul4*^{RIP1} strains expressing the indicated FLAG-CUL4 constructs. The strains are listed in Appendix C. (C) DNA methylation analysis of wild-type (WT) and *cul4*^{RIP1} strains and *cul4*^{RIP1} strains expressing the indicated FLAG-tagged CUL4 constructs at the *his-3* locus. DNA was digested with 5-methylcytosine-sensitive BfuCI (lanes B) or its 5-methylcytidine-insensitive isoschizomer, DpnII (lanes D), and the Southern blot was probed for methylated region 8:G3 (Selker et al., 2003); size standards (in kb) are indicated on the (left). Equivalent results were obtained for methylated region 8:A6 (Selker et al., 2003) (Fig. 3). (D) Sensitivity of neddylation site mutants to DNA-damaging agents. Serial dilutions of conidia (indicated at the bottom) were tested on medium with or without MMS (0.015%), CPT (0.3 μg/ml), or TBZ (0.5 μg/ml).

N. crassa	CUL4	854	TQAAIVRIMKSRKKMAHAQL	873
S. pombe	Pcu4	671	LQASIVRVMKQKEKMKHDDL	690
C. elegans	Cullin 4	777	IDAAVVRIMKARKQLNHQTL	896
D. melanogaster	Cullin 4	758	IDAAIVRIMKMRKTLSHNLL	777
A. thaliana	Cullin 4	679	IDAAIVRIMKTRKVLSHTLL	698
H. sapiens	CUL-4A	696	IDAAIVRIMKMRKTLGHNLL	715
H. sapiens	CUL-4B	749	IDAAIVRIMKMRKTLSHNLL	768

Fig. 2. NEDD8 attachment site is conserved in CUL4. Alignment of a conserved region in the carboxy termini of Cullin 4 proteins from various eukaryotes including *Neurospora crassa* (Lewis, Adhvaryu, Honda, Shiver, Knip, Sack, et al., 2010b), *Schizosacchromyces pombe* (BAA32520, accession number at NCBI), *Caenorhabditis elegans* (AAA68791), *Drosophila melanogaster* (NP_001163084), *Arabidopsis thaliana* (CAC85265) and *Homo sapiens* (CUL-4A: Q13619 and CUL-4B: Q13620). Identical residues are colored blue, NEDD8 is attached to the lysine that is indicated in red.

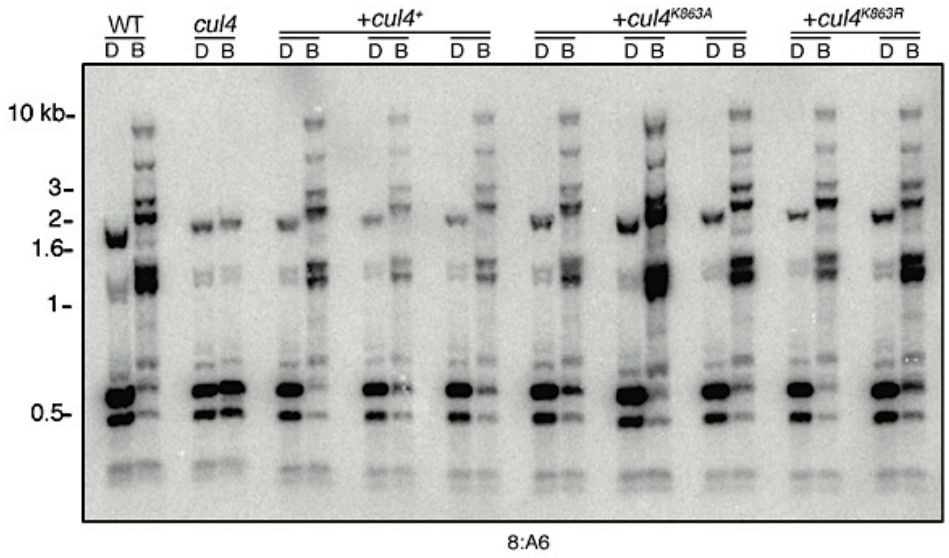

Fig. 3. DNA methylation analysis of wildtype (WT), *cul4* and transformed *cul4* strains expressing the indicated untagged CUL4 constructs. DNA was digested with 5mC-sensitive BfuCI (B) or its 5mC-insensitive isoschizomer DpnII (D) and the Southern blot was probed for methylated region 8:A6 (Selker et al., 2003); kb size standards (left). Equivalent results were obtained for other methylated regions (5:B8). Strains are listed in Appendix C.

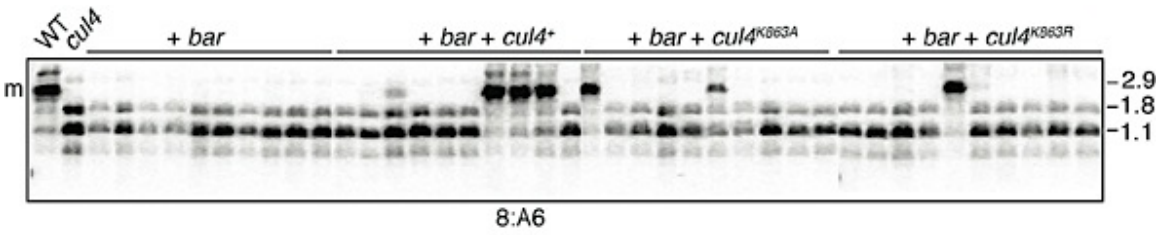

Fig. 4. *cul4* neddylation-site mutant alleles complement DNA methylation in a *cul4* deletion mutant. A *cul4* deletion mutant (N3169) was transformed by electroporation (Margolin et al., 1997) with a PCR product encoding basta resistance (*bar*) or co-transformed with PCR products encoding basta resistance (*bar*) and wildtype ($cul4^{+}$) or neddylation-site mutant ($cul4^{K863A/R}$) alleles. DNA from multiple Bar^{+} transformants were digested with 5mC-sensitive AvaII and the Southern blot was probed for methylated region 8:A6 (Selker et al., 2003); Methylation of AvaII site prevents digestion in wildtype strain (2.9 kb band labeled 'm'), while lack of DNA methylation in *cul4* mutant permits digestion by AvaII resulting in two fragments (1.8 and 1.1 kb). Transformation with either wildtype ($cul4^{+}$) or neddylation-site mutant alleles ($cul4^{K863A/R}$) resulted in complementation.

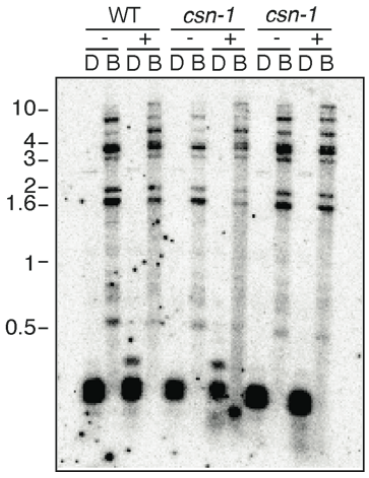

Fig. 5. COP9 Signalosome (CSN) is not required for DNA methylation. Normal DNA methylation in *csn-1* mutant. DNA from wildtype strain (N150) or two *csn-1* strains was digested with BfuCI (B) or DpnII (D) and the Southern blot was probed for methylated region 8:A6 (Selker et al., 2003); kb size standards (left). Cultures were grown in absence (-) or presence of 10 μg/ml cycloheximide (+). Strains are listed in Appendix C.

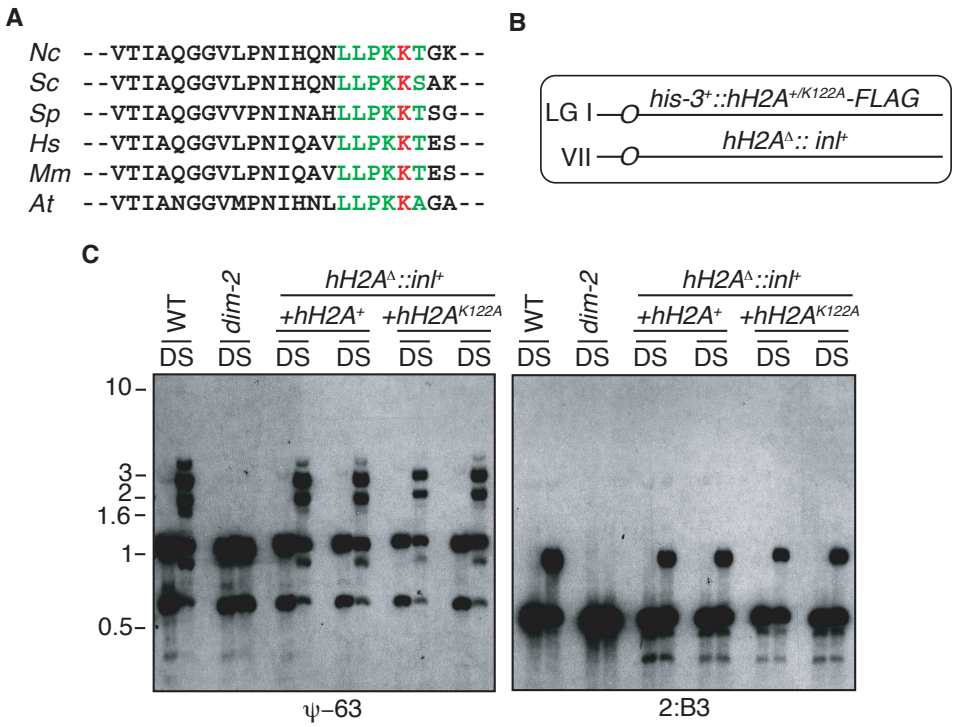

Fig. 6. Histone H2A ubiquitination is not required for DNA methylation in Neurospora. (A) Alignment of H2A C-terminal tails from various eukaryotes including *Neurospora crassa* (Hays, Swanson, & Selker, 2002), *Saccharomyces cerevisiae* (CAA81267.1; accession number at NCBI), *Schizosaccharomyces pombe* (NP_588180.1), *Homo sapiens* (NP_003502.1), *Mus musculans* (CAA83210.1) and *Arabidopsis thaliana* (NP_200275.1). The conserved recognition sequence is highlighted in green and the conserved site that is ubiquitinated in some organisms is red. (B) Genotype of strains expressing epitope-tagged wildtype (H2A-FLAG) or ubiquitination site mutant (H2AK122A-FLAG). The endogenous gene was replaced with a selectable marker (*inl*$^{+}$). (C) DNA methylation is normal in the H2AK122A mutant. DNA from wildtype (WT), *dim-2* mutant and strains of indicated genotypes was digested with *Sau*3AI (S) or *Dpn*II (D) and the Southern blot was probed for methylated regions Y-63 and 8:G3 (Selker et al., 2003); kb size standards (left). Absence of DNA methylation in the *dim-2* (Kouzminova & Selker, 2001) mutant results in identical pattern for DpnII and Sau3AI. Strains are listed in Appendix C.

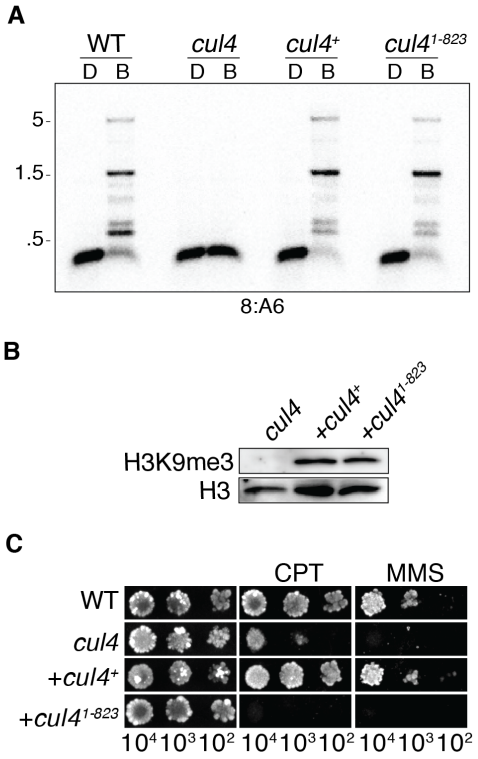

Fig. 7. The CUL4 C terminus is not required for DCDC function. (A) Normal DNA methylation in a CUL4 C terminus deletion mutant. DNA methylation was tested for the wild-type (WT) strain, a *cul4*^{RIP1} strain, and *cul4*^{RIP1} strains bearing either wild-type *cul4* allele or the C terminus truncation allele (the strain contained *cul4* residues 1 to 823 [*cul4*$^{1-823}$] and a deletion of residues 824 to 923; Fig. 1A), as described in the legend to Fig. 1C. Strains are listed in Appendix C. (B) H3K9me3 is unaffected by deletion of the C terminus of CUL4. Nuclear extracts from the indicated strains were probed by Western blotting to detect global trimethylated H3K9 or histone H3 levels. N3892, N3893, N5299. (C) The CUL4 C-terminal deletion abrogates DNA repair. Strains of the indicated genotypes were tested as described in the legend to Fig. 1D.

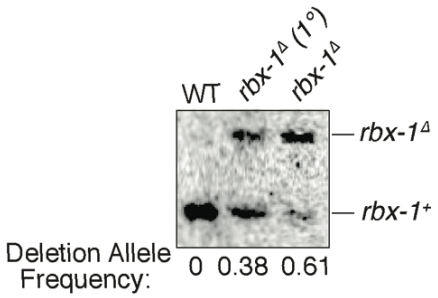

Fig. 8. Generation of *rbx1* deletion mutant. The endogenous allele was replaced with a hygromycin resistance selection cassette and the primary transformant (1°) was purified by microconidiation. The fraction of nuclei bearing the deletion was assessed by comparing the relative intensity of bands for the deletion and endogenous allele. The *rbx1* gene appears to be essential and we were unable to obtain a homokaryon. Strains are listed in Appendix C.

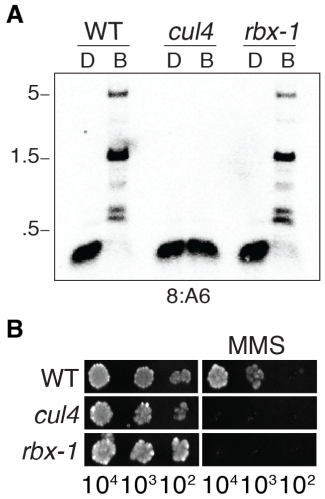

Fig. 9. RBX1, the putative RING protein for CUL4 complexes, is not required for control of DNA methylation by DCDC. (A) Normal DNA methylation in an *rbx1* deletion strain. DNA methylation was tested for the wild type (WT), a *cul4*^{RIP1} strain, and the *rbx1* deletion mutant, as described in the legend to Fig. 1C. (B) Compromised DNA repair in the *rbx1* mutant. Serial dilutions of conidia from strains of the indicated genotype were tested on medium with or without MMS (0.015%). The strains are listed in Appendix C.

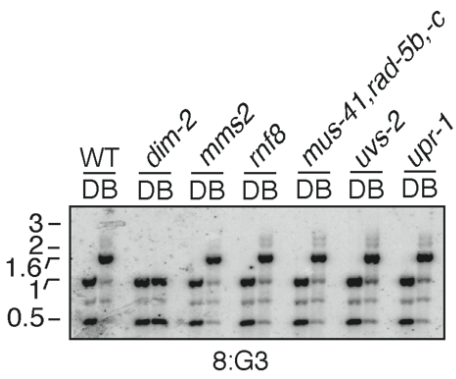

Fig. 10. DNA methylation is normal in various DNA repair mutants. DNA was digested with BfuCI (B) or DpnII (D) and the Southern blot was probed for methylated region 8:G3 (Selker et al., 2003); kb size standards (left). Strains are listed in Appendix C.

Figures for Chapter III

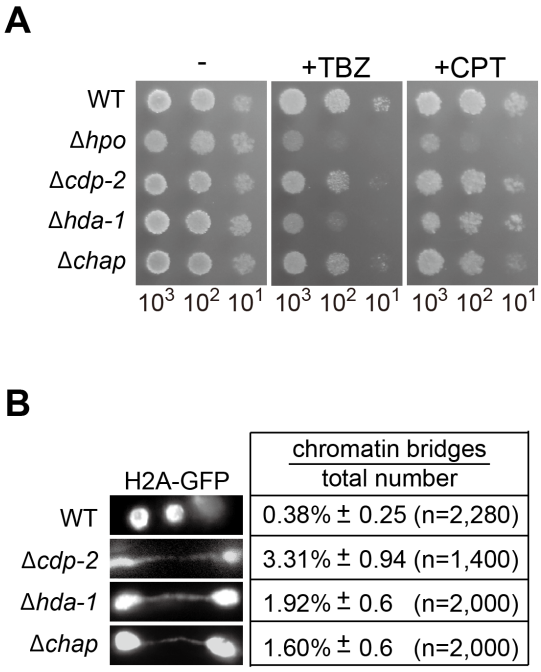

Fig. 11. HCHC is important for centromere function. (A) Serial dilutions of conidia from each of the indicated strains were spot-tested on medium with or without TBZ or CPT. Strains: N3753, N4922, 775, 903, and 949. (B) The distribution of the nuclear marker H2A-GFP in growing hyphae in wild-type, *cdp-2*, *hda-1*, and *chap* strains were examined microscopically. The frequency of observed chromatin bridges and the total number of nuclei are shown beside each representative micrograph. Strains: N5015, N5017, N5024, and N5026.

Fig. 12 (see next page). WGBS profiles for WT and HCHC mutants. The average 5mC levels were calculated for 500-bp windows across the genome from the WGBS data derived for wild-type strains and the HCHC mutants (Chapter III: Materials and Methods) and displayed by the Integrative Genomics Viewer using the heatmap function. Genes (green vertical lines) are displayed on the x axis below the DNA methylation heatmap profiles. Methylated regions called by RSEG (Chapter III: Materials and Methods) are indicated by black bars above the wild-type row. *N. crassa's* seven linkage groups are not displayed to scale. Strains: N3752, N3615, N3612, and N3435.

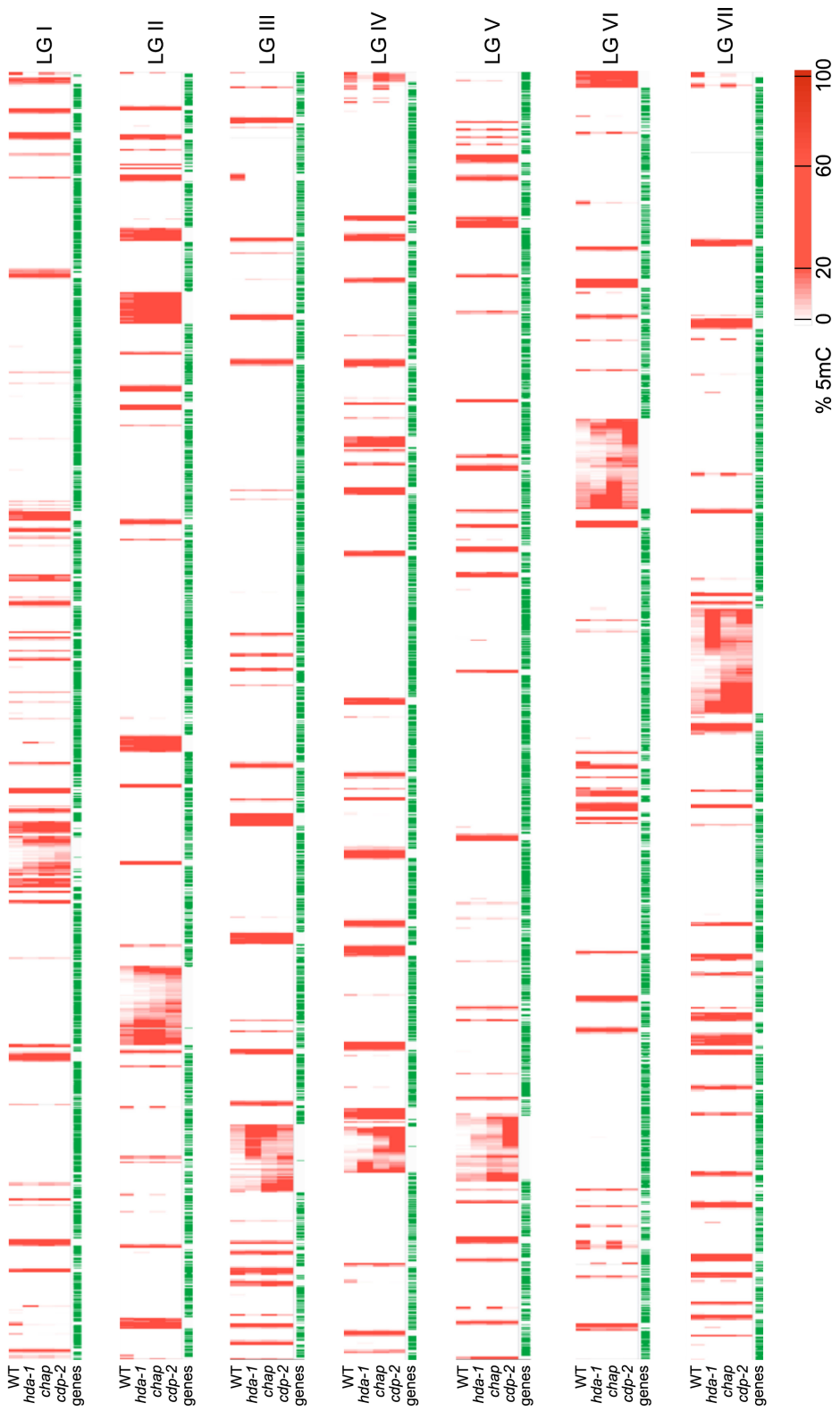
LG I
LG II
LG III
LG IV
LG V
LG VI
LG VII
WT
hda-1
chap
cdp-2
genes
% 5mC
0
20
60
100

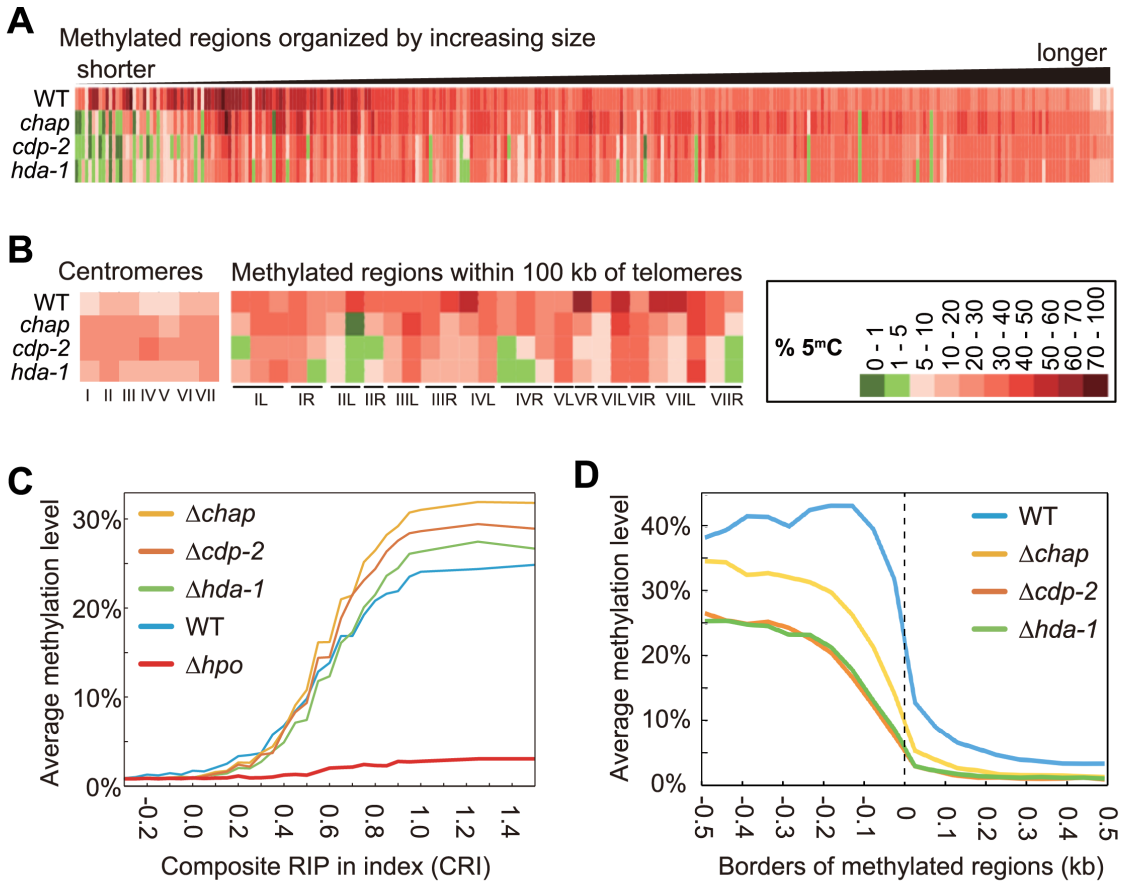

Fig. 13. WGBS analysis of HCHC mutants. (A) Heat map analyses showing the relative level of 5mC for all methylated regions, sorted from shortest to longest, for wild-type strains and the HCHC mutants. (B) Heat map analyses showing the relative level of 5mC at centromeres and methylated regions within 100 kb of telomeres for wild-type strains and HCHC mutants. (C) The CRI (x axis) and average methylation level (y axis) were calculated for 500-bp windows across the genome (Chapter III: Materials and Methods) and then were plotted for wild-type strains and each of the HCHC mutants. A mutant lacking HP1 (*Δhpo*) is used as a control for complete loss of DNA methylation. (D) Average methylation levels were calculated for 50-bp windows across the borders of methylated regions (Chapter III: Materials and Methods) and then were plotted for wild-type strains and HCHC mutants. Strains: N3752, N3615, N3612, N3435, and N4922.

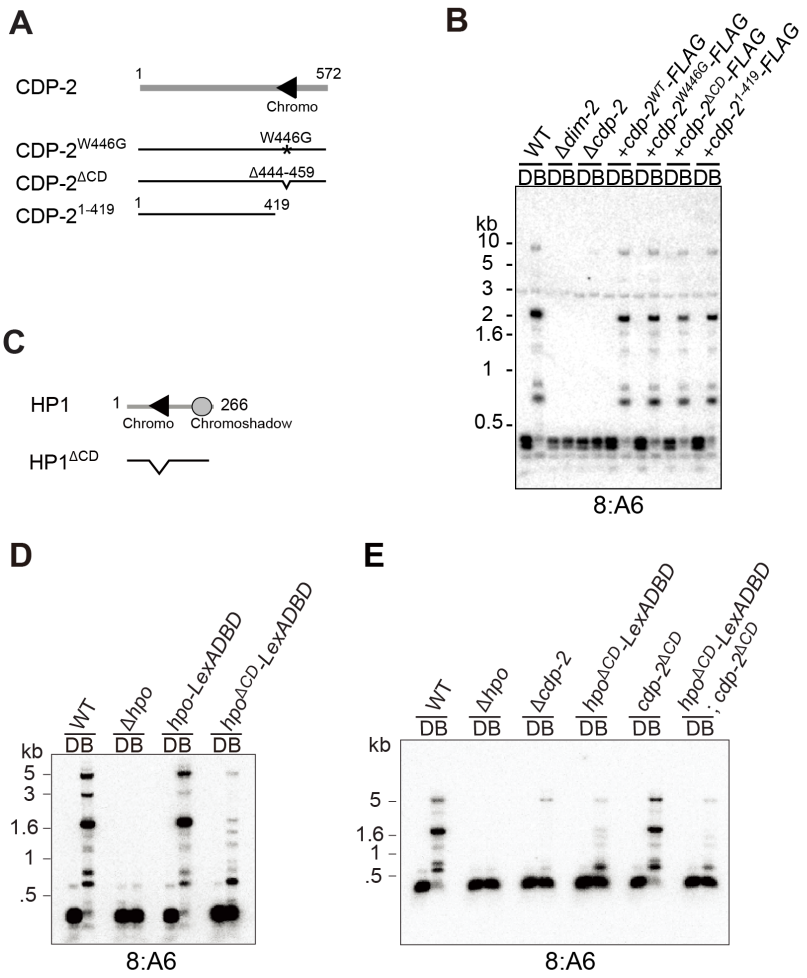

Fig. 14. The HP1 CD but not the CDP-2 CD is required for normal DNA methylation. (A) Diagram of the CDP-2 mutations tested. Tryptophan 446 is predicted to be an aromatic cage residue essential for binding to H3K9me (Fischle et al., 2005; Nielsen et al., 2002). (B) Introduction of CDP-2 CD mutant constructs complements DNA hypomethylation defects at the 8:A6 methylated region in *cdp-2*–null mutants. Genomic DNA of the indicated strains was digested with 5mC-sensitive BfuCI (B) or its 5mC-insensitive isoschizomer DpnII (D) and was gel-fractionated, and DNA methylation was analyzed by Southern hybridizations with the 8:A6 probe, a region that is methylated in wild-type strains (Selker et al., 2003). The positions of size standards are shown at left. Strains: N150, N1877, N3615, N4006, N3992, N4088, and N4089. (C) Diagram of the HP1 CD mutation tested. (D) The introduction of the HP1 CD-deletion gene partially restores DNA methylation at the 8:A6 methylated region. Strains: N3753, N5580, N6166, and N6390. (E) The residual DNA methylation of the 8:A6 region in the HP1 CD-deletion mutation is not affected by the CDP-2 CD deletion. Strains: N3753, N5580, N3615, N6390, N6393, and N6394.

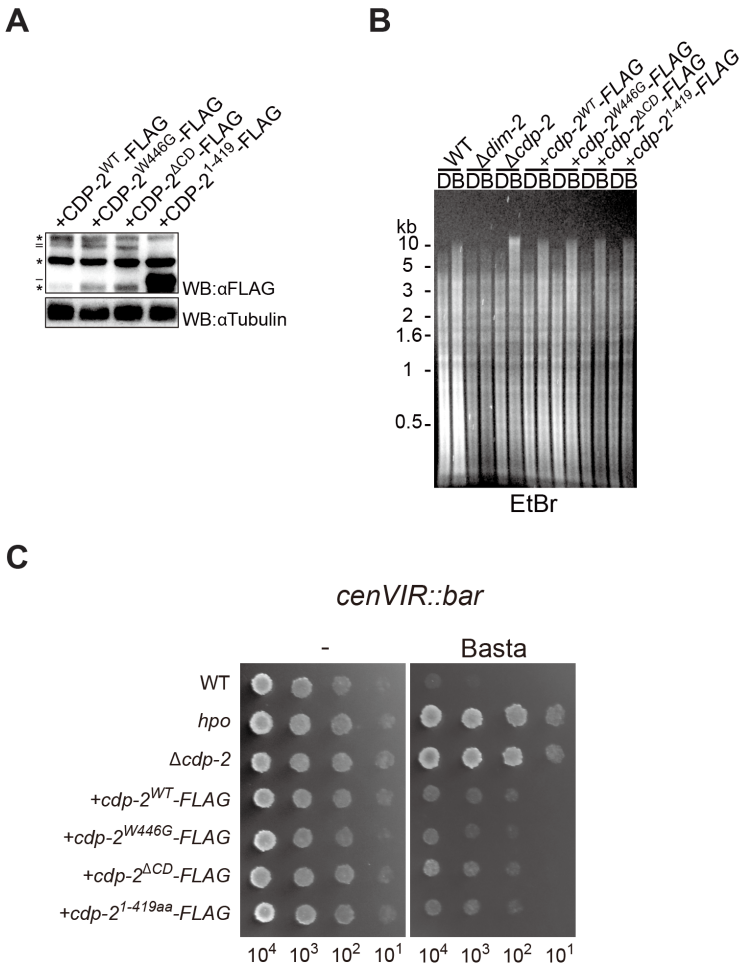

Fig. 15. The CDP-2 CD is dispensable for normal HCHC function. (A) Expression of *cdp-2* mutants was assessed by Western blotting with antibodies against FLAG. β-Tubulin was used as a loading control. Strains: N3343, N3992, N4088, and N4089. (B) Effects of *cdp-2* mutations on global DNA methylation by ethidium bromide (EtBr) staining. Genomic DNA of indicated strains was digested with 5mC-sensitive BfuCI (B) or its 5mC-insensitive isoschizomer, DpnII (D) and were gel-fractionated, and the products were visualized by EtBr straining. The positions of size standards are shown at left. The enhanced, more slowly migrated DNA (~10 kb) in *cdp-2*–null mutants indicates hypermethylation, but insertion of the CDP-2 CD mutants complements the methylation defects. Strains: N623, N1877, N3135, N3343, N3992, N4088, and N4089 (C) Effects of *cdp-2* mutations on centromere silencing. Serial dilutions of conidia from each of the indicated strains harboring a centromeric *bar* construct were spot-tested on medium with or without basta. Strains: N4890, N4891, N4915, 888, 890, 892, and 894.

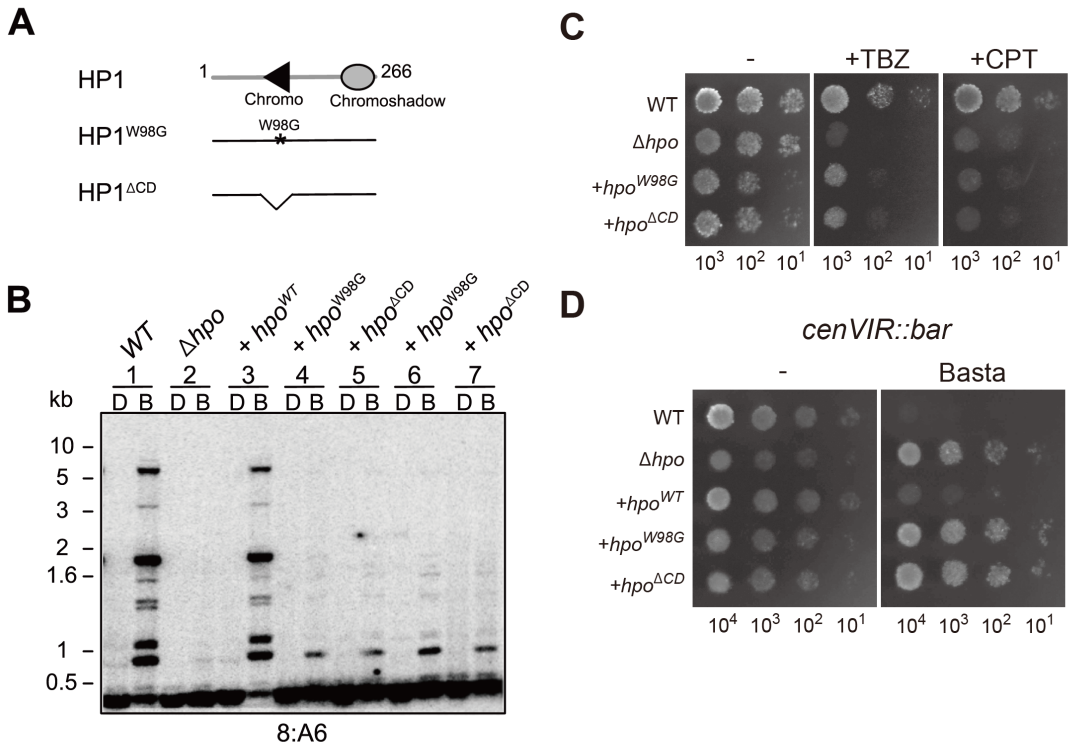

Fig. 16. The HP1 CD is required for centromeric silencing and for most but not all DNA methylation. (A) Diagram of HP1 and the CD mutation (tryptophan 98 to glycine) and deletion tested. Tryptophan 98 is predicted to be essential for binding to H3K9me (Fischle et al., 2005; Nielsen et al., 2002). (B) Southern analysis of the normally methylated 8:A6 region (Selker et al., 2003) demonstrating that insertion of either the *hpo* CD point mutation (lanes 4 and 6) or the *hpo* CD deletion (lanes 5 and 7) results in a partial restoration of the methylation lost at 8:A6 in a *hpo*-deletion strain (lane 2), whereas insertion of the wild-type *hpo* allele (lane 3) restores 8:A6 methylation to levels seen in a wild-type strain (N4909, lane 1). Genomic DNAs were digested with the 5mC-sensitive BfuCI (B) restriction enzyme or its 5mC-insensitive isoschizomer, DpnII (D). The positions of size standards are shown at left. Strains: N4909, N4922, N5898, N5869, N5870, N5871, and N5872. (C and D) Strains harboring the *hpo* CD mutation (hpo^{W98G}) or CD deletion ($hpo^{\Delta CD}$) slightly restore TBZ sensitivity but fail to restore CPT sensitivity or to silence the *cenVIR::bar* marker properly. Serial dilutions of conidia from each of the indicated strains were spot-tested on medium with the indicated drugs. Strains: N4890, N4922, N5898, N5869, and N5871.

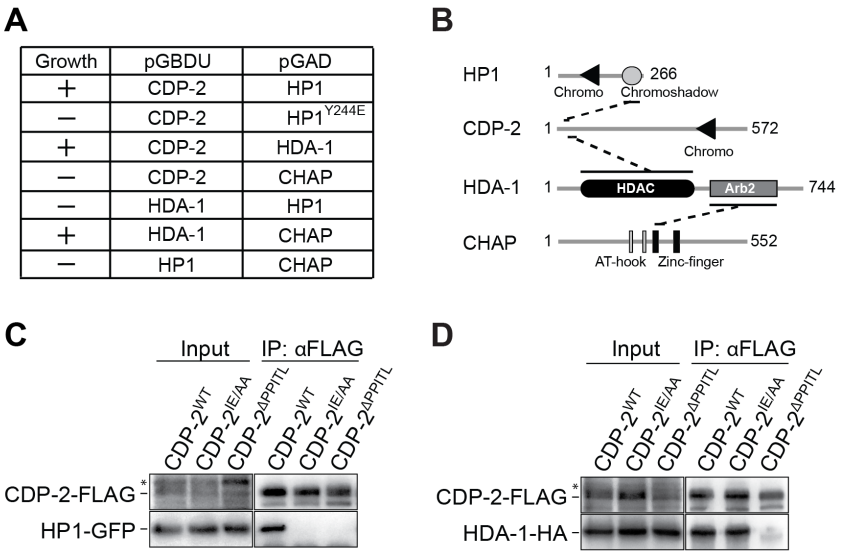

Fig. 17. HCHC component interactions. (A) Summary of yeast two-hybrid results for HCHC components expressed pairwise in yeast as galactose (Gal)-binding domain fusions (pGBDU) or Gal-activation domain fusions (pGAD). The indicated constructs were co-transformed into the PJ69-4A yeast cells. Transformants were tested on synthetic defined (SD) agar plates without adenine, histidine, leucine, or uracil; growth results are shown at left. (B) Diagram summarizing interactions between components of the HCHC complex. Detailed analyses are presented in Fig. 18. The chromoshadow domain of HP1 interacts with the most N-terminal PxVxL-like motif of CDP-2. An adjacent PxVxL-like motif on CDP-2 interacts with the HDAC domain of HDA-1. The Arb2 domain of HDA-1 interacts with the first zinc-finger motif of CHAP. (C and D) Verification of the interaction of CDP-2 with HP1 and HDA-1 via the N-terminal PxVxL-like motifs of CDP-2 *in vivo*. Co-IP experiments were performed with anti-FLAG antibodies in strains with the indicated tagged proteins. Input and immunoprecipitation samples were fractionated and analyzed by Western blotting with antibodies against the indicated epitopes. The asterisk indicates nonspecific bands. Strains: N3808, N3836, 3440, 3443, 3445, and 3447.

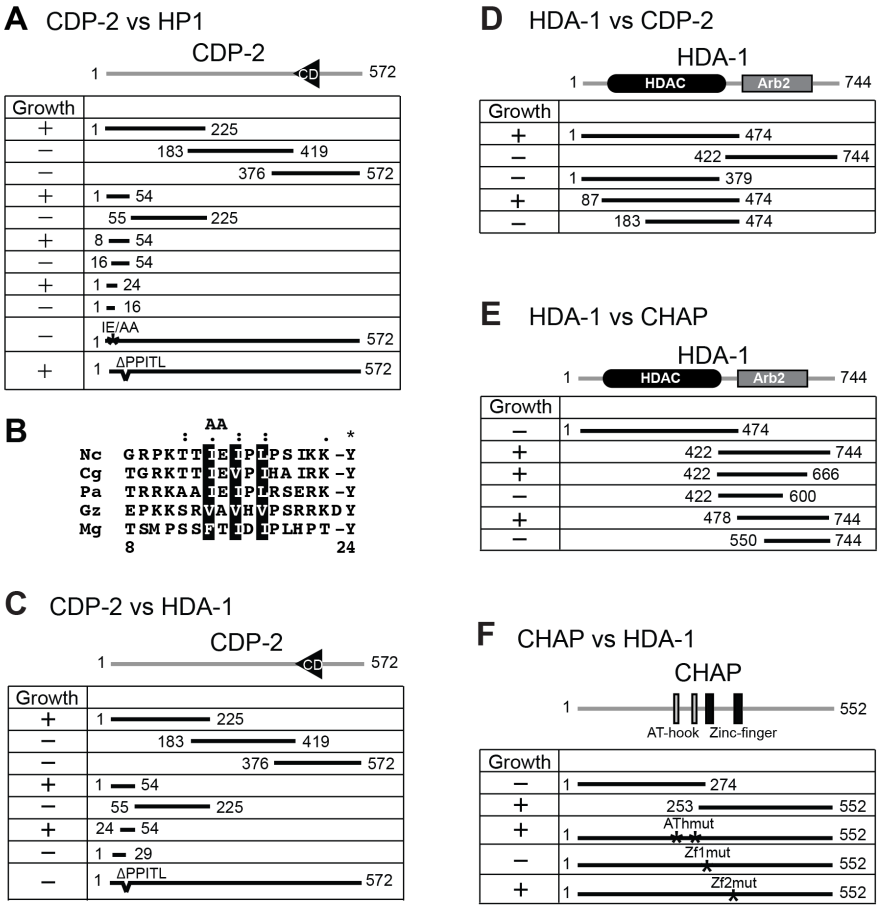

Fig. 18. Yeast two-hybrid analyses among truncated or mutated components of HCHC. (A) Schematic diagram of tested truncated or mutated derivatives of CDP-2 fused to the Gal DNA-binding domain. All constructs were co-transformed with pGAD-HP1 prey-vector into the PJ69-4A yeast cells (James, Halladay, & Craig, 1996). (B) Sequence comparison of the HP1-interacting fragment of CDP-2 from *N. crassa* (Nc) and the corresponding region of its counterparts in *Chaetomium globosum* (Cg, accession number XP_001220390), *Podospora anserina* (Pa, XP_001912830), *Gibberella zeae* (Gz, XP_385206), and *Magnaporthe grisea* (Mg, XP_001414497). The residue identical in all CDP-2 proteins is indicated by an asterisk. Colons and periods indicate strong and weak conservation, respectively. Residues similar to the PxVxL consensus sequence implicated in HP1 binding are shown in white on a black background. Residues replaced by alanines (IE/AA) are indicated above. (C–F) Schematic diagrams of tested truncated or mutated derivatives of CDP-2, HDA-1, and CHAP fused to the Gal DNA-binding domain.

Fig. 19 (see next page). Sequence alignment of *N. crassa* CHAP with homologs from other filamentous fungi and de-stabilization of the CHAP zinc finger motif mutant proteins. (A) Proteins were aligned with the Clustal X algorithm. Highly and partially conserved residues are indicated by asterisks and colons, respectively. The predicted AT-hook and zinc finger motifs are indicated by thick lines. The residues that are conserved among species and are critical resides (the arginine residue for the AT-hook motif and the cysteine residue in the zinc finger motif) were changed to alanine (ATh1, R210A; ATh2, R250A; Zf1, C280A; Zf2, C317A). The accession numbers of the proteins are *Chaetomium globosum*, XP_001225541; *Podospora anserina*, XP_001909682; *Magnaporthe grisea*, XP_370514; *Gibberella zeae*, XP_384555; *Sclerotinia sclerotiorum*, XP_001585520; and *Botryotinia fuckeliana*, XP_001554742. (B) The CHAP zinc finger motif mutant proteins are unstable. Expression of *chap* mutants was assessed by Western blotting with antibodies against HA. β-Tubulin was used as a loading control. Strains: N3818, N3825, N3827, and N3846.

A

AT-hook motif

A (R210A, ATh1)

```
Neusopora crassa          KKRGRPFGWR PGL--SYAAM RGNPVPPPRP KV-------- ---------P KQPKAPSEVK
Chaetomium globosum       KKRGRPVGWR RGHG-SYAAM RSGLPPGSAT PQ-------- ---------P KPKKPAGEQK
Podospora anserina        KQRGRPRGWR PGQ--AYSTS TPGSTTSKKV KKSVGRPL-- -------GSG KAGRPSGKLK
Magnaporthe grisea        KKRGRPKGWK PGMPYSTTSN RPASEAAKLA REDYLRKHPE AVAPVARGRP RTAAPKGPPK
Gibberella zeae           RGRGRPKGST NKLKGLPGTA AAGRQARQVK PR-------- ---------P YPEGFVGFPK
Sclerotinia sclerotiorum  RKRGRPPKDY TAVVSSTNSD ILTAKGQKSS NSK------- --------KP NSQSDDNPPK
Botryotinia fuckeliana    KRRGRPPKDH TALSGSNESD SFTTKDQKLK SLK------- --------NQ NSQSDDNPPK
                          : ****             :                                  .  *
```

AT-hook motif

A (R250A, ATh2)

Zinc finger motif

A (C280A, Zf1)

```
Neusopora crassa          R----RGRPP KKPHELPREI FSKLTPRYIR FLCEWEGCPA ELHNFETLRK HVLVVHGDY-
Chaetomium globosum       P----RGRPG RKPAPTARQL YLKLNPHFVA FRCEWEDCPA ELQNVETLRR HLLVVHGRP-
Podospora anserina        PDGESRGRPG RKPAQTARDQ YKKLNPRFPV FICEWEGCPA QLHNLETLRK HIFIVHGQPE
Magnaporthe grisea        P----RGRPP RKPPQTPRQV LNSLERRYVP FLCEWKDCKA ELQNMDTLRR HVRKVHGRE-
Gibberella zeae           R----RGRPP KPQPPPPREL YNRTNVQFFP FLCEWMDCKA ELHNLETLRR HVYKVHGDS-
Sclerotinia sclerotiorum  R----RGRPP KKP---LEVE IPLPNPPFQI YGCEWDKCPA KLHNLDTLRM HLSKVHGKR-
Botryotinia fuckeliana    K----RGRPP KQPS--PEAD IEPPNPNFLV YDCEWDKCPA KLHNLATLRM HLFKVHGKR-
                               ****  :      .          :   : ***  * * :*:*. ***  *:  ***
```

Zinc finger motif

A (C327A, Zf2)

```
Neusopora crassa          --RQPHQHHL LSAREQPQE- ---PKTCKWA SCHSKRLQSE LPPLTLP--- --------TR
Chaetomium globosum       --SRSSSTSL SPSPVAQQQN HTITLPCRWA SCTCTPLHS- ---------- ---------R
Podospora anserina        VSPAPSSSSS AVARPDEKHS DDGLIVCKWA KCISSPTPR- ---------- --------FQ
Magnaporthe grisea        ---------- ---------- ----EVCRWS TCASSGSTEV FG-------- --------TN
Gibberella zeae           ---------- ---------- ----VECLWG KCGRLEEPPE FE-------- --------DD
Sclerotinia sclerotiorum  ---------- ---------- ENGMFNCLWK GCTKVQTPND G-SMSSSELR ITTKYRFENE
Botryotinia fuckeliana    ---------- ---------- ENDKFQCLWK GCVAAAQHTE NENTLASESG IRKLREFEDE
                                                        * *   *
```

```
Neusopora crassa          SHFEAHVNES HLIPFLWHVG DGPRNTSIES PLSEKPLTIT SALPSQPLSS SSISHLDVTT
Chaetomium globosum       ESFASHIDTA HLLPIRWHVG DGPRNT---- ---------- -TPPPKP--- ----------
Podospora anserina        DDFRTHVEEV HLVPFAWHCG DGPQNT---- ---------- -SVSPKP--- ----------
Magnaporthe grisea        DEFIGHVEHA HLVPFQWHMG FGYSNET--- ---------- -PIPSRIK-- ----------
Gibberella zeae           EGFNDHVEEA HLVPLSWHVG DGPNNLAER- ---------- -GLKKEE--- ----------
Sclerotinia sclerotiorum  DDWKRHVEKK HVIRFAWHMG DGPRNS---- ---------- --LDGPR--- ----------
Botryotinia fuckeliana    DKWKRHIERK HITRYAWHMG DGPMNS---- ---------- --LDGLN--- ----------
                          . :  *::   *:    ** *  *  *
```

```
Neusopora crassa          TTTTNTTTTS TAIKLQPLPP YLFDTSGNQV TPSVRDQLYE NDDDKRRRRV RLERVHFLRD
Chaetomium globosum       -TTTKTTTP- ------QLPT YLFNAAGEQV TPSITTQQIE NEDERKRRAA RVNRVLLLRD
Podospora anserina        ----EVMLP- ------ALPK YLFDEEGRQV TPSVADQQLE TDEDKRRRVS KIAALTEKAN
Magnaporthe grisea        ---ADEDAP- -------VPA YLLDENGMQV TPWIKEIEIE DQVTRLARRR KLRLALKWMN
Gibberella zeae           ----KNDDD- -------IPD YLKDEHGNQV TPSIRDQEEE DLLTWRKNRR KLKELLIRMN
Sclerotinia sclerotiorum  ----KYDAS- ------ALPP YLFDKNGVQV TPSVKDQQIE YGDPKETSAQ RFKRTISGLD
Botryotinia fuckeliana    ----RPKSP- ------TVPS YLFDKNGNQV TPSVEDQKIE DGDPKQNSKK RFKRVISGLD
                                     :*  ** :  * ** ** :     *             :.       :
```

```
Neusopora crassa          ENAAPEPVYT QAERDAMEAS LAAKKKKQDE FWEYYEKVMG PVVEVTVLAA DQEDLEVPEN
Chaetomium globosum       RHAPDEPDYG PRELEIVGEA LAAKQKRQRM LREYAER--- ---------- ---------G
Podospora anserina        ENAPDEPEYD EKQMELIIAF MEKRNLRQRE LKKYAEWVTG ---------- --------EG
Magnaporthe grisea        DEAPLE-DGD NSEEEASS-- ---------- ---------- ---------- ----------
Gibberella zeae           DNLPDRDDEE GDAKQQDA-- ---------- ---------- ---------- ----------
Sclerotinia sclerotiorum  FVLNPIYNSN YASPIQSVAK DGGENNEVHS SNDGEDDGND ---------- ---------T
Botryotinia fuckeliana    FVLKPIYTSN FTLPTE---- -PGEE-EVHG NGKAHSEKEL ---------- ---------K
```

```
Neusopora crassa          ASGNLSKEVK RKMLSCGWDP QWRGLYQD
Chaetomium globosum       CVG------- ------GWLP --------
Podospora anserina        VILPVEEKEE RD----KWRG RMR-----
Magnaporthe grisea        ---------- ---------- --------
Gibberella zeae           ---------- ---------- --------
Sclerotinia sclerotiorum  NMEDIGNIGE IEDIDPIF-- --------
Botryotinia fuckeliana    RAEGNGDETD MEDIEPDF-- --------
```

B

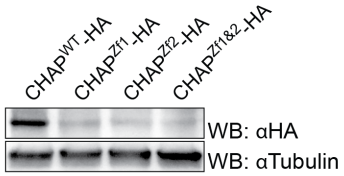

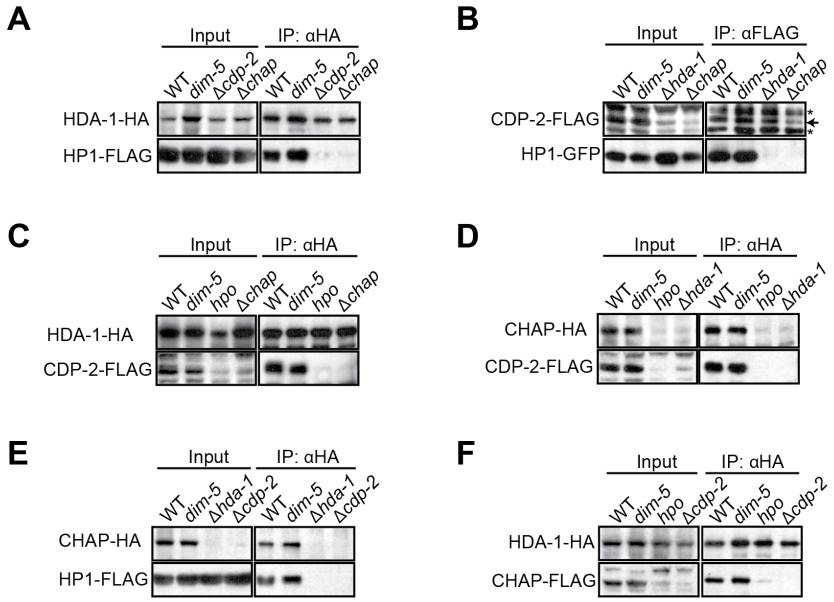

Fig. 20. Co-IP analyses among each component of the HCHC complex *in vivo*.
Extracts from the indicated tagged strains were immunoprecipitated with anti-HA or anti-FLAG antibodies. Input and immunoprecipitation samples were fractionated and analyzed by Western blotting with antibodies against the tagged proteins. The asterisk indicates nonspecific bands, and the arrow indicates a specific band. Strains: (A) N3704, N3735, N3733, and N3720; (B) N3836, N3835, N3838, and N3839; (C) N0808, N3852, N3853, and N3802; (D) N3803, N3842, N3843, and N3719; (E) N3805, N3800, N3717, and N3804; (F) N3730, N3806, N3841, and N3728.

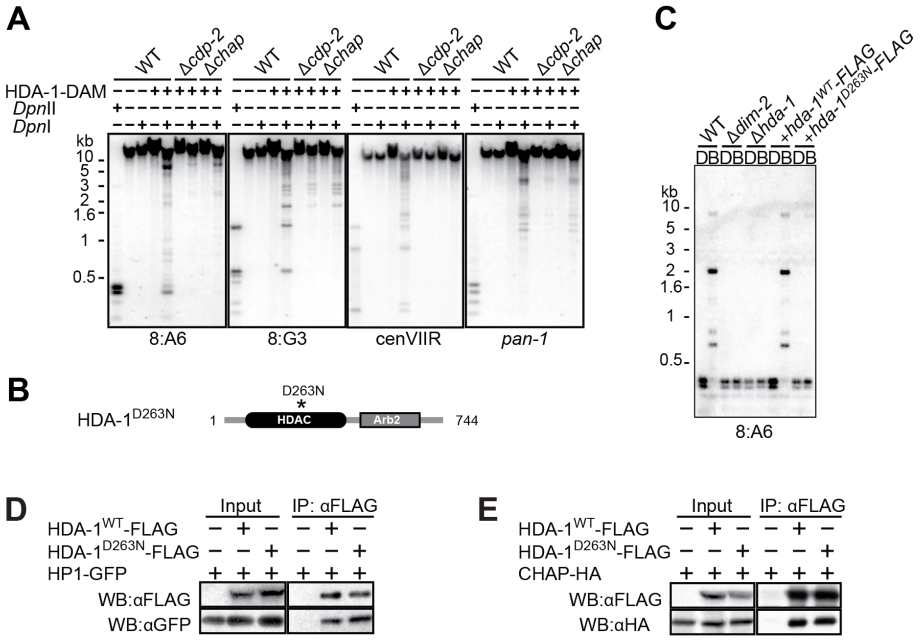

Fig. 21. HCHC function depends on the HDA-1 HDAC. (A) Sequence-dependent localization of HDA-1–Dam depends on CDP-2 and CHAP. Genomic DNA from a wild-type strain with (+) or without (−) HDA-1–Dam, as well as wild-type, *cdp-2*, and *chap* strains expressing HDA-1–Dam, were incubated with (+) or without (−) DpnI, which cuts adenine-methylated GATC sites. As a control for completely digested DNA, genomic DNA from the wild-type strain was incubated with the 5mC-insensitive isoschizomer DpnII. Digested DNA was used for Southern hybridizations with probes for the methylated regions 8:A6, 8:G3, and cenVIIR as well as a euchromatic gene, *pan-1*. Strains: N3752, N3995, N4023, and N4082. (B) The position of the point mutation in the HDA-1 catalytic domain. Asparagine 263 is predicted to be essential for the HDAC activity (Sugiyama et al., 2007). (C) The introduction of the *hda-1* gene with the catalytic mutation does not complement DNA methylation defects in *hda-1*–null mutants. The experiment was carried out as described in Fig. 14B with the 8:A6 methylated region (Selker et al., 2003). Strains: N623, N1877, N3610, N3997, and N3998. (D and E) The HDA-1 catalytic mutation does not disrupt the HCHC complex. Co-IP experiments were performed with anti-FLAG antibodies in strains with (+) or without (−) the indicated tagged proteins. Input and immunoprecipitation samples were fractionated and analyzed by Western blotting with antibodies against the indicated epitopes. Strains: N3321, N4002, N4043, N3377, N4000, and N4699.

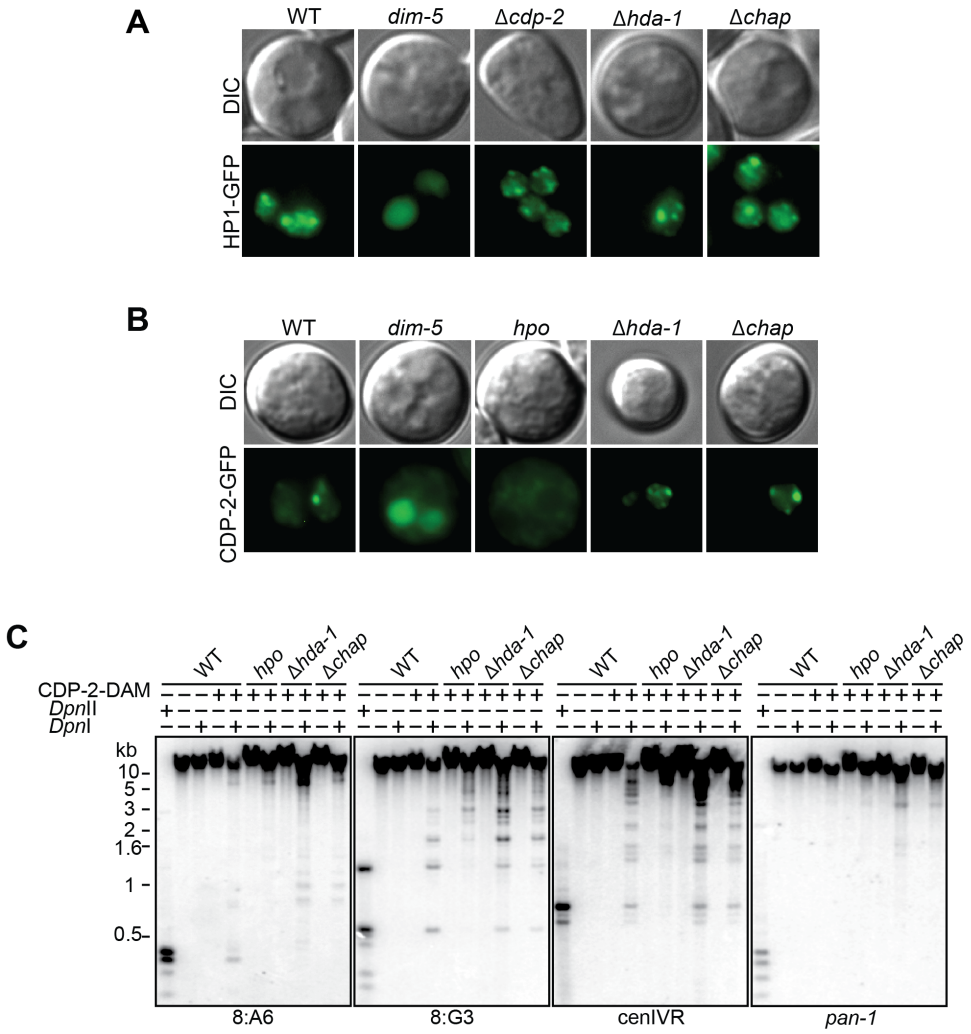

Fig. 22. HP1 and CDP-2 localize to heterochromatin independently of HDA-1 and CHAP. (A) Punctate localization of HP1–GFP is independent of other HCHC components. Conidia of the indicated strains were examined microscopically using visible light (DIC) or UV fluorescence. Strains: N3321, N3431, N3649, N3757, and N3759. (B) CDP-2–GFP localization is independent of HDA-1 and CHAP. Strains: N3790, N3792, N3794, N3911, and N3913. (C) CDP-2 localization depends on HP1 but not on HDA-1 and CHAP. Genomic DNA from the wild-type strain, which does not express HDA-1–Dam, and wild-type, *hpo*, *hda-1*, and *chap* strains which express CDP-2–Dam were incubated with (+) or without (−) DpnI, which cuts adenine-methylated GATC sites. As a control for completely digested DNA, genomic DNA from the wild-type strain was incubated with its 5mC-insensitive isoschizomer DpnII. Digested DNA was used for Southern hybridizations with probes for the methylated regions 8:A6, 8:G3, and cenIVR and the euchromatic gene *pan-1*. Strains: N150, N4011, N4013, N4083, and N4085.

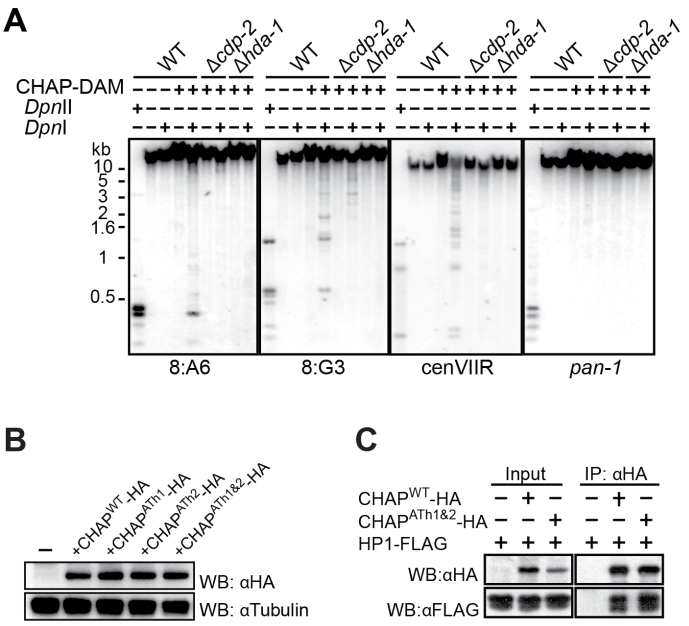

Fig. 23. CHAP localization to heterochromatin depends on the other components of HCHC. (A) Sequence-dependent localization of CHAP–Dam depends on HDA-1 and CDP-2. DNA isolated from the indicated strains was analyzed by Southern hybridizations as in Fig. 14B. Strains: N4045, N4687, and N4690. (B) Expression of *chap* AT-hook motif mutants was assessed by Western blotting with antibodies against HA. β-Tubulin was used as a loading control. Strains: N3752, N3818, N3820, N3822, and N3845. (C) Normal HCHC complex formation in the CHAP AT-hook motif mutants. Co-IP experiments were performed with anti-HA antibodies in strains with (+) or without (−) the indicated tagged proteins. Input and immunoprecipitation samples were fractionated and analyzed by Western blotting with antibodies against the indicated epitopes. Strains: N3319, N3730, and N3986.

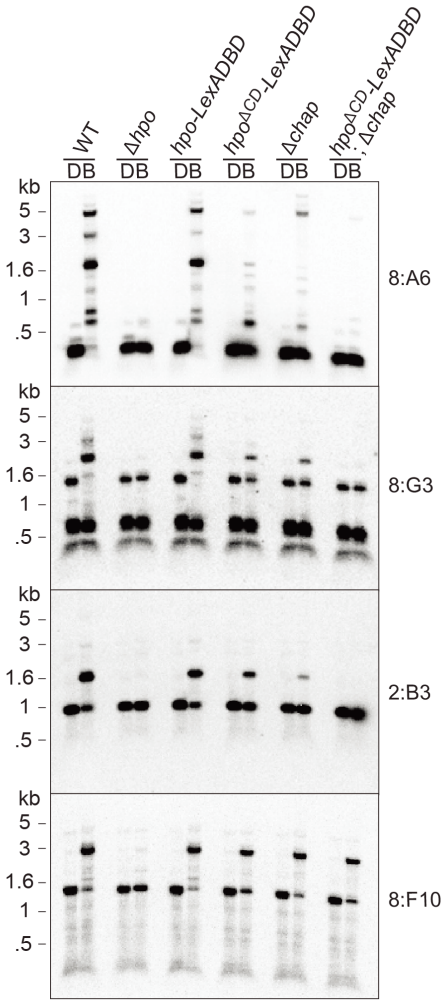

Fig. 24. CHAP is essential for the residual DNA methylation in the HP1 CD mutant. Southern blot analysis was carried out as in Fig. 14B. The three upper panels are the hypomethylated 8:A6, 8:G3, and 2:B3 regions, and the bottom panel is the intact methylated 8:F10 region in *hda-1*–null mutants. Mutants lacking the HP1 CD or CHAP show the residual DNA methylation at the 8:A6, 8:G3, and 2:B3, whereas the double mutants show complete loss of DNA methylation. DNA methylation at the 8:F10 region is unchanged in mutants lacking the HP1 CD and/or CHAP. Strains: N3753, N5580, N6166, N6390, N6392, and N6391.

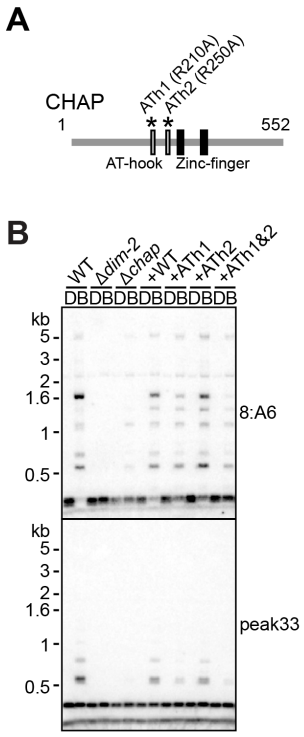

Fig. 25. The CHAP AT-hook motifs are required for DNA methylation. (A) Diagram of the CHAP AT-hook motif point mutations tested. (B) Effects of *chap* AT-hook motif mutations on DNA methylation at 8:A6 region and peak 33 (Honda et al., 2012). DNA isolated from indicated strains was analyzed by Southern hybridizations as in Fig. 14B. Strains: N3752, N1877, N3643, N3818, N3820, N3822, and N3845.

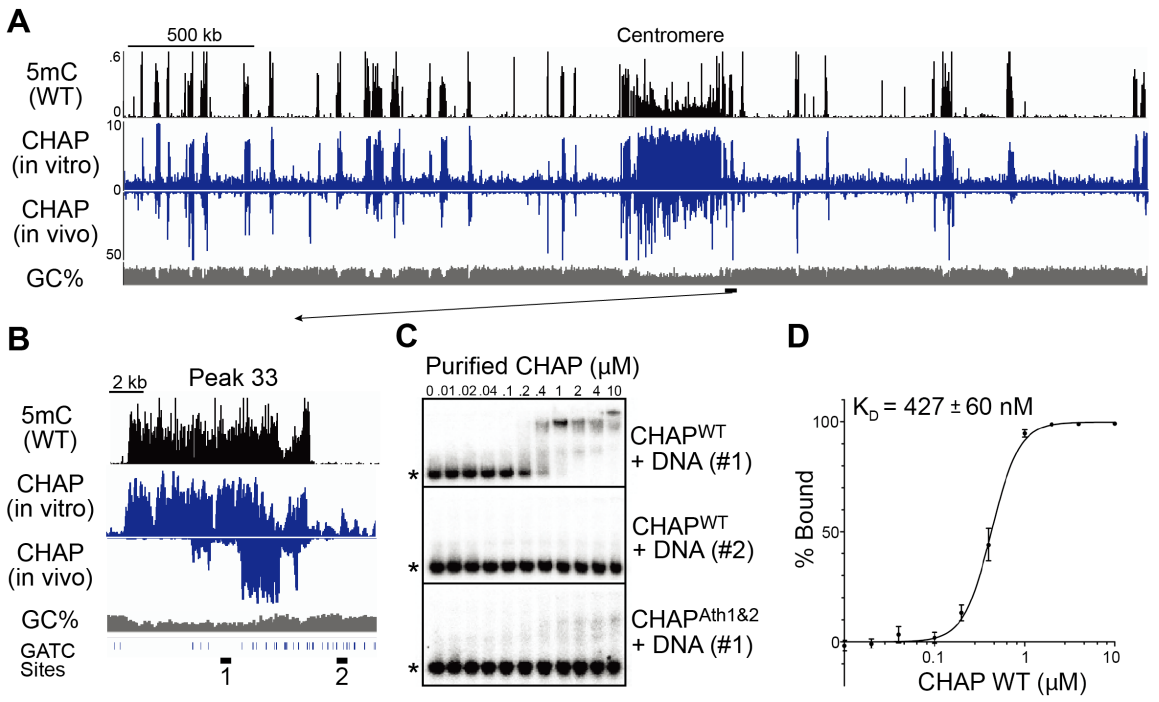

Fig. 26. The CHAP AT-hooks specifically bind to DNA that has repeat-induced point mutations. (A) Genome-wide distribution of DNA methylation (5mC) in the wild-type stain (Top Row), *in vitro* CHAP-binding distribution mapped with DNA affinity-purified by the recombinant wild-type N-terminal CHAP protein (Middle Row), and *in vivo* CHAP distribution determined by DamID sequencing with CHAP–Dam (Bottom Row). The bottom row indicates GC content. Strains: N3752 and N4045. (B) Distribution of DNA methylation and CHAP localization at the peak 33 region. GATC sites are indicated at the bottom to explain the gaps in CHAP localization as determined by DamID sequencing and to illustrate the limitations of the technique. The horizontal black bars and numbers identify the regions used for gel mobility shift assays. (C) The CHAP AT-hook motifs bind AT-rich DNA that has repeat-induced point mutations. Gel mobility shift assays were performed using recombinant wild-type N-terminal CHAP protein ($CHAP^{WT}$-N) or CHAP AT-hook mutant protein ($CHAP^{ATh1\&2}$-N). Probe regions 1 and 2 shown in B were amplified with radiolabeled dCTP by PCR and tested for binding as indicated by the gel shift. (D) Dissociation constant for N-terminal CHAP protein ($CHAP^{WT}$-N) and the probe for AT-rich DNA that has repeat-induced point mutations (probe 1) ($n = 3$).

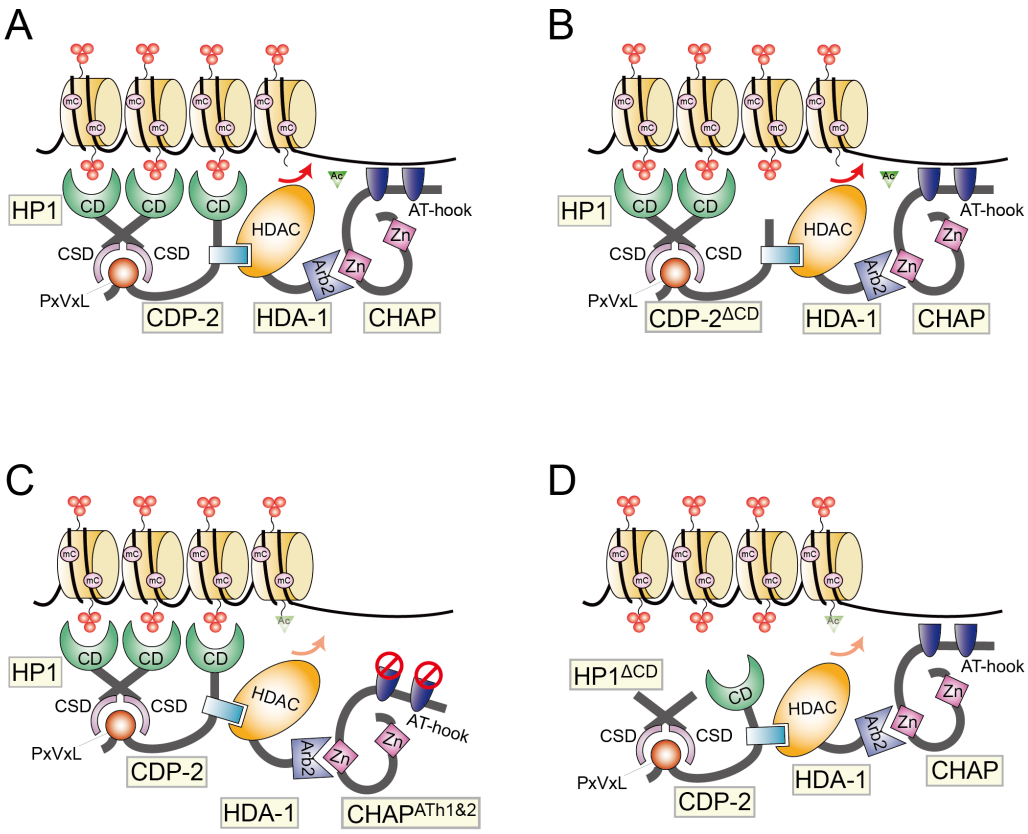

Fig. 27. Model for the interrelationship of the components of HCHC. (A) The HP1 chromoshadow domain (CSD) is predicted to dimerize, creating a binding pocket for the PxVxL-like motif of CDP-2. The adjacent region of CDP-2 interacts with the HDA-1 HDAC domain. The HDA-1 Arb2 domain interacts with the CHAP zinc finger motif (Zf). The CD of HP1 and CDP-2 and the CHAP AT-hooks bind to trimethylated H3 (red spheres) and DNA that has repeat-induced point mutations (black line), respectively. Proper formation and chromatin recognition by HCHC is required for the full HDA-1 HDAC activity, which removes acetyl groups (AC) from chromatin. (B–D) The CDP-2 CD is not required for the HCHC function (B), but the CHAP AT-hooks and the HP1 CD are important (C and D). mC, methyl-cytosine.

Figures for Chapter IV

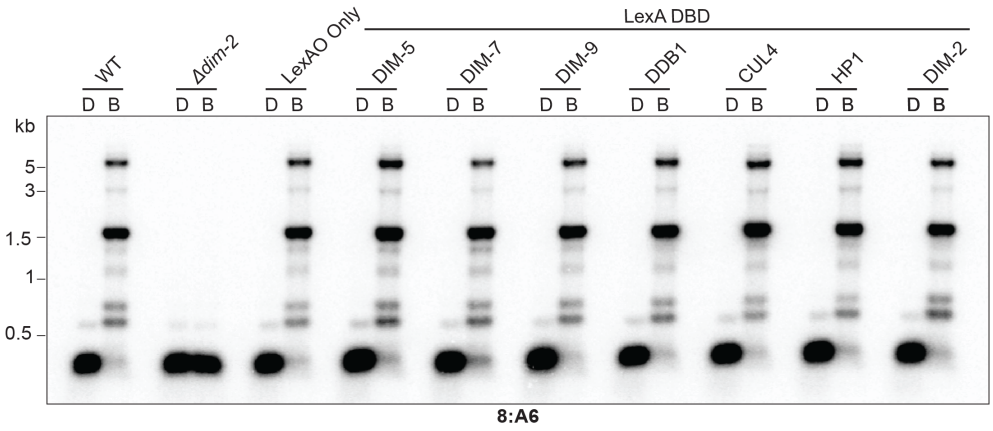

Fig. 28. LexADBD-Tagged H3K9me3 and DNA Methylation Components Are Functional. DNA methylation assayed by Southern hybridization with 5^{m}C-sensitive BfuCI or its 5^{m}C-insensitive isoschizomer DpnII and probed for the 8:A6 constitutive heterochromatic region (Selker et al., 2003). The positions of size standards are noted to the left. Strains (left to right): N3753, N1853, N5649, N5644, N6924, N5647, N6867, N6865, N6166, N6921.

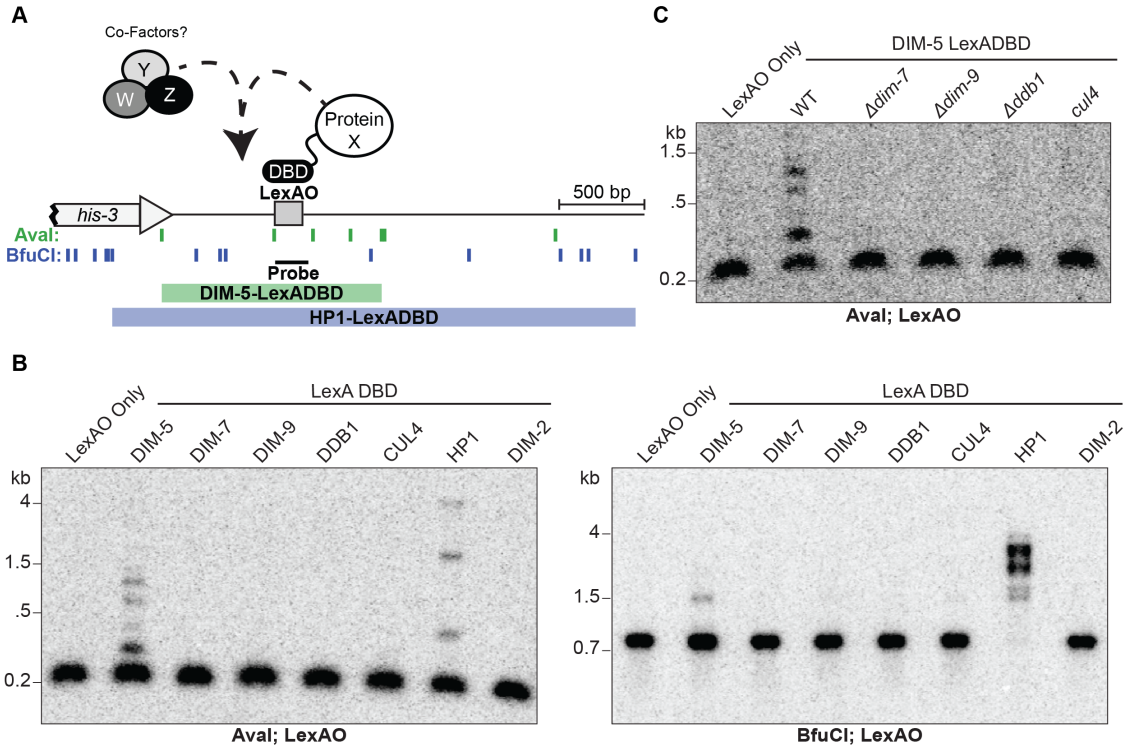

Fig. 29. Tethered DIM-5 or HP1 Is Sufficient to Induce Heterochromatin at a Euchromatic Locus. (A) Schematic of tethering experimental approach with map showing restriction sites for 5^{m}C-sensitive restriction enzymes AvaI (green) and BfuCI (blue) and position of Southern hybridization probe (black bar). The LexAO consists of four repeats of a LexA consensus sequence (Thliveris & Mount, 1992) integrated downstream of the *his-3* locus. The inferred DNA methylation domains for each tethered component based on the observed banding pattern from Fig. 29B are shown below. (B) DNA methylation is induced at the LexAO by tethering DIM-5 or HP1. Genomic DNA of the indicated strains was digested with 5^{m}C-sensitive AvaI or BfuCI, resolved by agarose gel electrophoresis and analyzed by Southern hybridization, probing for the LexAO (black bar). The positions of size standards are noted to the left of each autoradiogram. Strains (left to right): N5649, N5644, N6924, N5647, N6867, N6865, N6166, N6921. (C) All members of the DCDC are required for DNA methylation induced by tethered DIM-5. AvaI-specific Southern hybridization performed as in Fig. 29B. Strains (left to right): N5649, N5644, N6613, N6615, N6614, N6616.

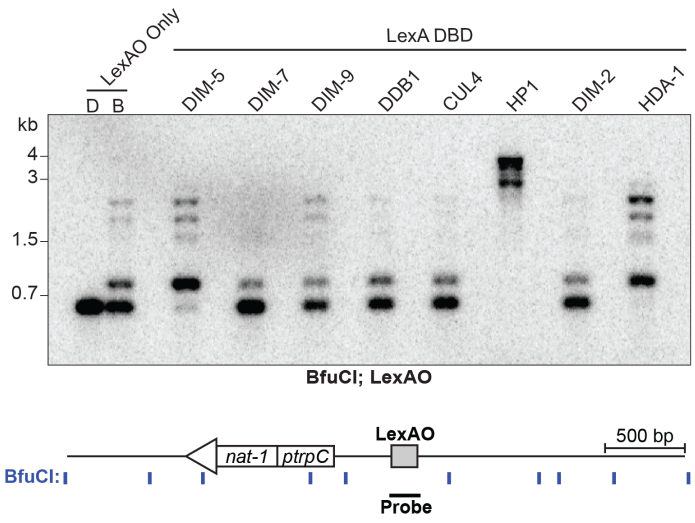

Fig. 30. Tethered DIM-5, HP1, and HDA-1 are Sufficient to Induce DNA Methylation at *trp-2*. BfuCI-specific Southern hybridization was carried out as in Fig. 29B. Strains (left to right): N6640, N6641, N6925, N6646, N6868, N6866, N6642, N6922, N6643.

Fig. 31 (see next page). Tethered HP1 Requires HDA-1 for Induction of Ectopic H3K9me3, DNA Methylation, and Gene Silencing. (A) Southern hybridization analysis (as in Fig. 29B) of proteins in HP1-associated complexes for their possible role in induced cytosine methylation at BfuCI sites. Strains (left to right): N6166, N6619, N6620, N6621, N6622, N5649. (B) Requirement of HCHC complex members for tethered HP1-induced DNA methylation assessed by BfuCI-specific Southern hybridization (as in Fig. 29B). Strains (left to right): N5649, N6166, N6626, N6622, N6627 (C) Tethered heterochromatin machinery induces H3K9me3 and requires cytosine methylation and HDA-1 activity. Relative enrichment of H3K9me3 at the LexAO was assessed by Chromatin Immunoprecipitation (ChIP) using a heterochromatic locus that is unchanged in a Δ*hda-1* strain (Peak 33a; (Honda et al., 2012)) as an internal control; ratios of enrichment measured for Peak 33a and the LexAO region were normalized to ratios obtained without immunoprecipitation (total input) and data presented are mean and standard deviation (SD) of three independent biological replicates. Strains (left to right): N5649, N6166, N6691, N6624, N6623, N6692, N6625, N6622. (D) ChIP-sequencing tracks showing the induction H3K9me3 of the indicated strains at the LexAO as well as static Peak 33a control locus. Schematic of LexAO and Peak 33a regions are shown with black bars denoting qPCR amplicons used in Fig. 31C. Enrichment of reads is displayed using the Integrative Genomics Viewer (Robinson et al., 2011), with the y-axis representing the number of reads per million per nucleotide (RPM). Strains (top to bottom): N5649, N6166, N6623, N6622. (E) Schematic of *nat-1* gene insertion, conferring resistance to nourseothricin, adjacent to LexAO tethering site. Serial dilutions of conidia from each strain harboring the reporter construct were spot-tested on histidine-containing medium or an equivalent medium containing 133μg/ml nourseothricin. Approximate numbers of spotted conidia are indicated below the images. Strains (top to bottom): N3756, N6610, N6611, N6630, N6631, N6632, N6633.

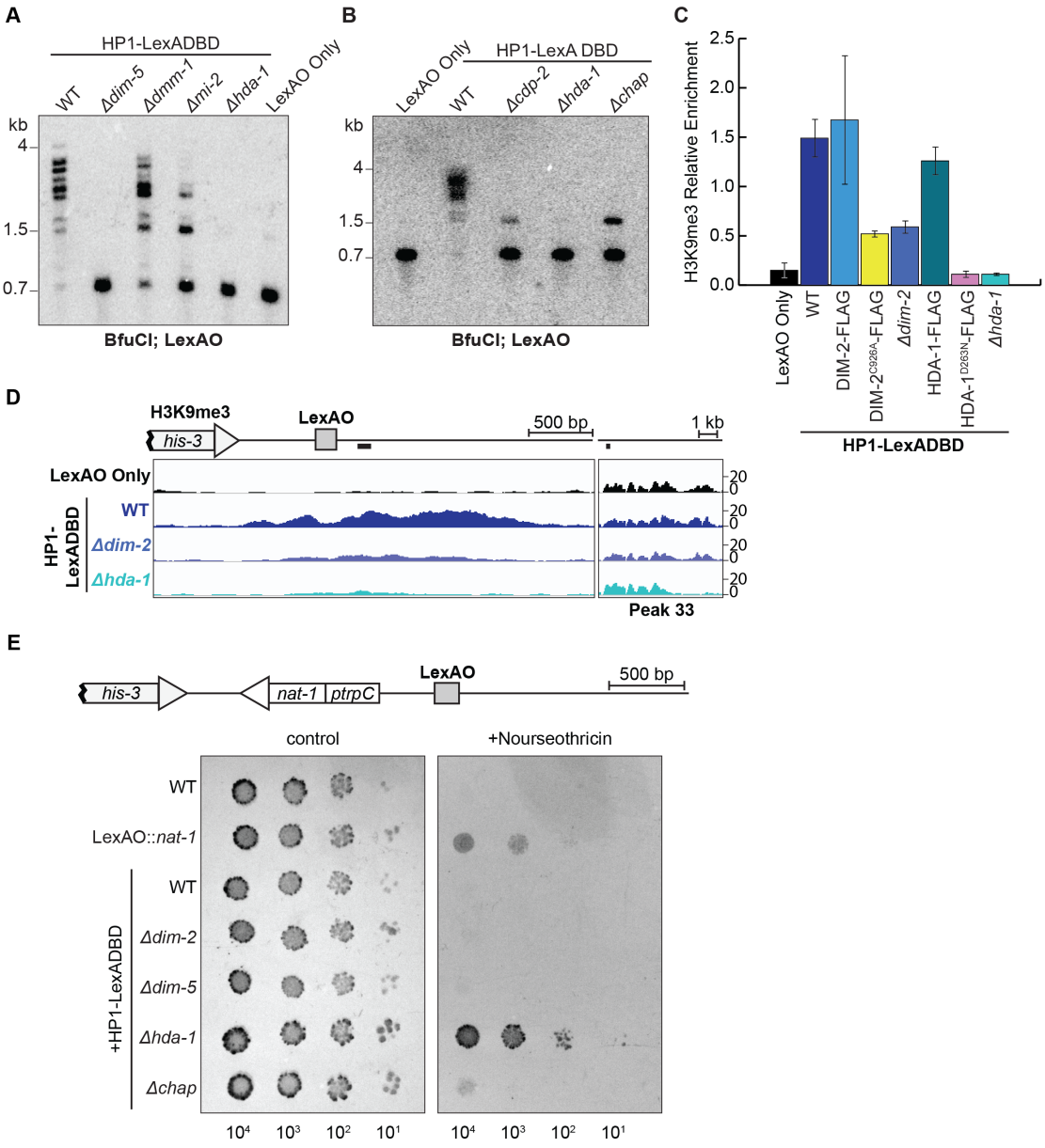
A
HP1-LexADBD
WT
Δdim-5
Δdmm-1
Δmi-2
Δhda-1
LexAO Only
kb
4
1.5
0.7
BfuCl; LexAO
B
LexAO Only
HP1-LexA DBD
WT
Δcdp-2
Δhda-1
Δchap
kb
4
1.5
0.7
BfuCl; LexAO
C
H3K9me3 Relative Enrichment
2.5
2.0
1.5
1.0
0.5
0.0
LexAO Only
WT
DIM-2-FLAG
DIM-2C926A-FLAG
Δdim-2
HDA-1-FLAG
HDA-1D263N-FLAG
Δhda-1
HP1-LexADBD
D
H3K9me3
his-3
LexAO
500 bp
1 kb
LexAO Only
HP1-LexADBD
WT
Δdim-2
Δhda-1
20
0
Peak 33
E
his-3
nat-1
ptrpC
LexAO
500 bp
control
+Nourseothricin
WT
LexAO::nat-1
+HP1-LexADBD
WT
Δdim-2
Δdim-5
Δhda-1
Δchap
10⁴
10³
10²
10¹

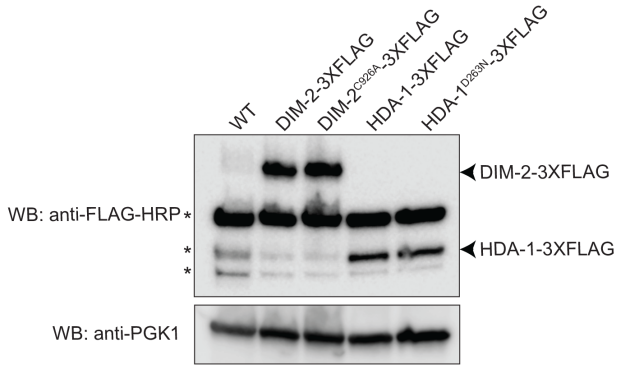

Fig. 32. Protein Expression Levels of DIM-2 and HDA-1 Catalytic Mutants. α-FLAG and α-phosphoglycerate kinase (PGK1; loading control) Western blots of *dim-2* and *hda-1* mutants from whole cell extracts. α-PGK1 was used as a loading control. Non-specific bands are indicated on left side with asterisks (*). Strains (left to right): N5649, N6691, N6624, N6692, N6625.

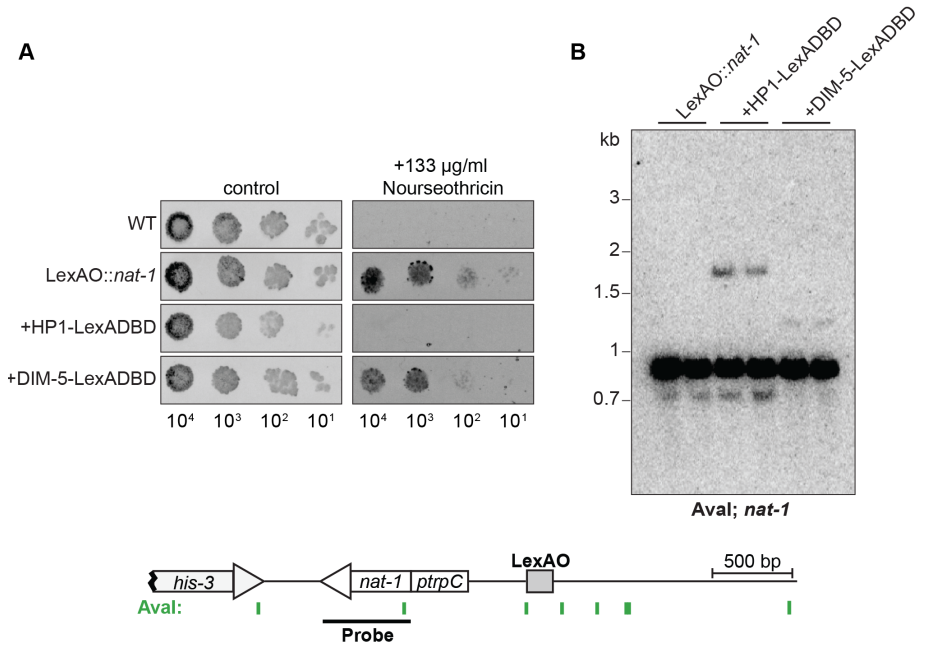

Fig. 33. Tethered DIM-5 Is Not Sufficient to Establish Silencing or DNA Methylation of *nat-1*. (A) Tethered HP1, but not tethered DIM-5, represses a proximal *nat-1* reporter gene. Silencing of *nat-1* gene assayed as in Fig. 31E. Strains (top to bottom): N3756, N6610, N6648, N6612 (B) Tethered DIM-5 fails to establish DNA methylation within *nat-1* gene. AvaI-specific Southern hybridization done as in Fig. 29B except probed for *nat-1*. Schematic of AvaI sites and probe used for Southern hybridization are illustrated below. Strains (left to right): N6610, N6647, N6611, N6648, N6612, N6649.

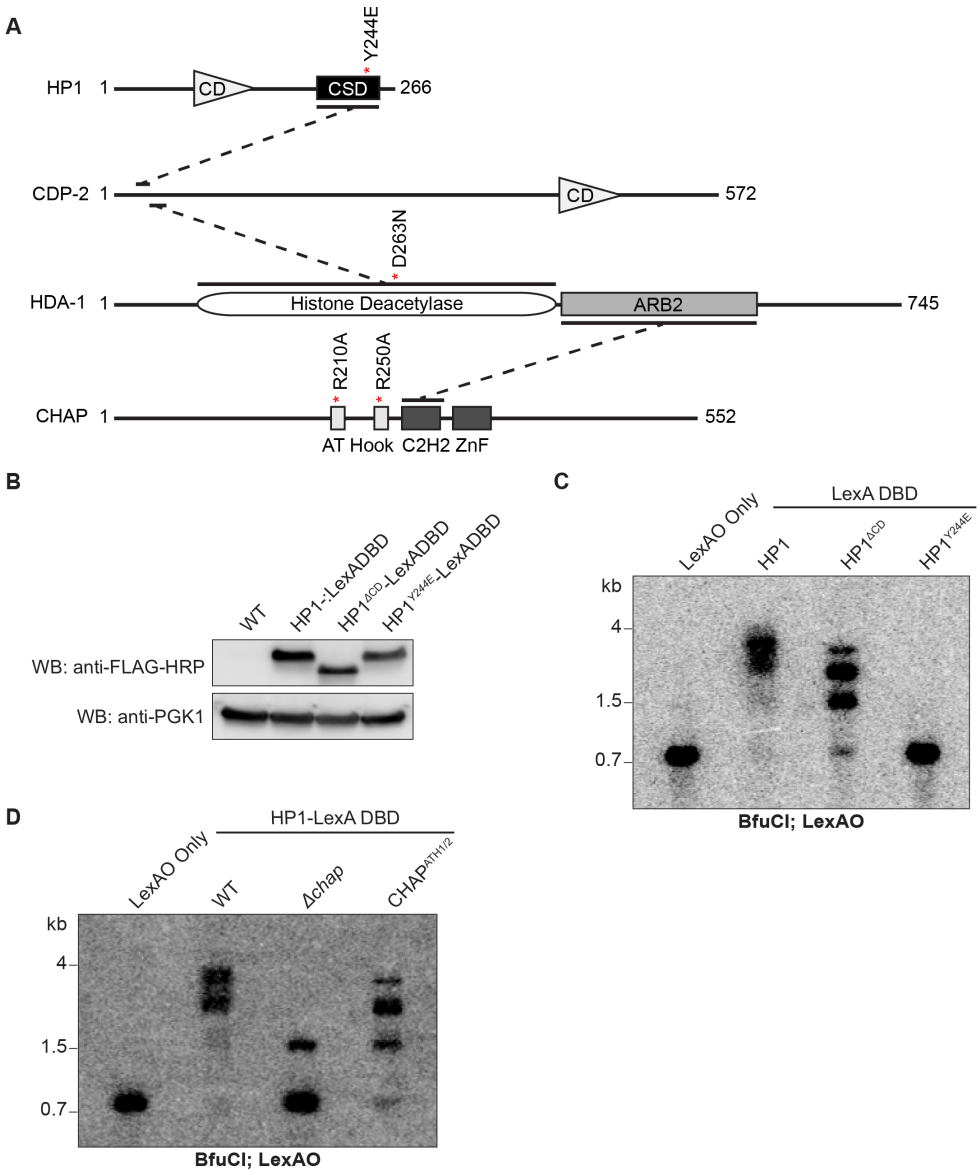

Fig. 34. Tethered HP1 Does Not Require the HP1 Chromodomain or CHAP AT-Hook Domains to Induce DNA Methylation. (A) Schematic of protein-protein interactions within the HCHC (adapted from (Honda et al., 2016)) and mutations of key functional domains. Mutations of HP1, HDA-1, and CHAP are indicated by red asterisks. Previously characterized interacting domains are shown by dashed lines (Honda et al., 2016). (B) Expression of tethered HP1 catalytic mutants. α-LexADBD Western blots of *hpo* mutants from whole cell extracts. As in Fig. 32, α-PGK1 was used as a loading control. Strains (left to right): N5649, N6166, N6390, N6635. (C) Unlike the HP1 chromoshadow domain, the chromodomain is not required for DNA methylation induced by tethered HP1. BfuCI-specific Southern hybridization (as in Fig. 29B). Strains (left to right): N5649, N6166, N6390, N6635 (D) CHAP AT-hook domains are not required for DNA methylation induced by tethered HP1. BfuCI-specific Southern hybridization (as in Fig. 29B). Strains (left to right): N5649, N6166, N6627, N6636.

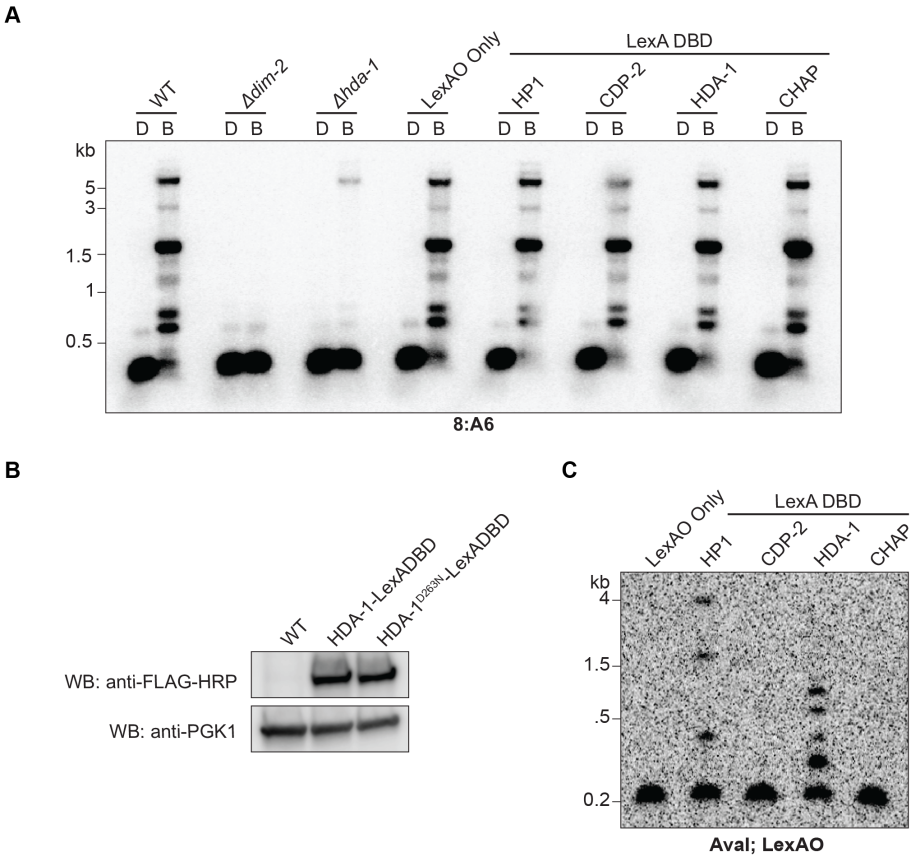

Fig. 35. HP1 and HDA-1 but Not CDP-2 and CHAP Are Sufficient to Induce DNA Methylation. (A) LexADBD-tagged HCHC components are functional. DpnII and BfuCI-specific Southern hybridizations, as in Fig. 28. Strains (left to right): N3753, N1853, N3435, N5649, N6166, N6662, N6628, N6663 (B) Expression of tethered HDA-1 catalytic mutants. α-LexADBD Western blots of *hda-1* catalytic mutant from whole cell extracts. As in Fig. 32, α-PGK1 was used as a loading control. Strains (left to right): N5649, N6628, N6629 (C) Neither tethered CDP-2 nor CHAP induces DNA methylation at the LexAO. AvaI-specific Southern hybridization done as in Fig. 29B. Strains (left to right): N5649, N6166, N6662, N6628, N6663.

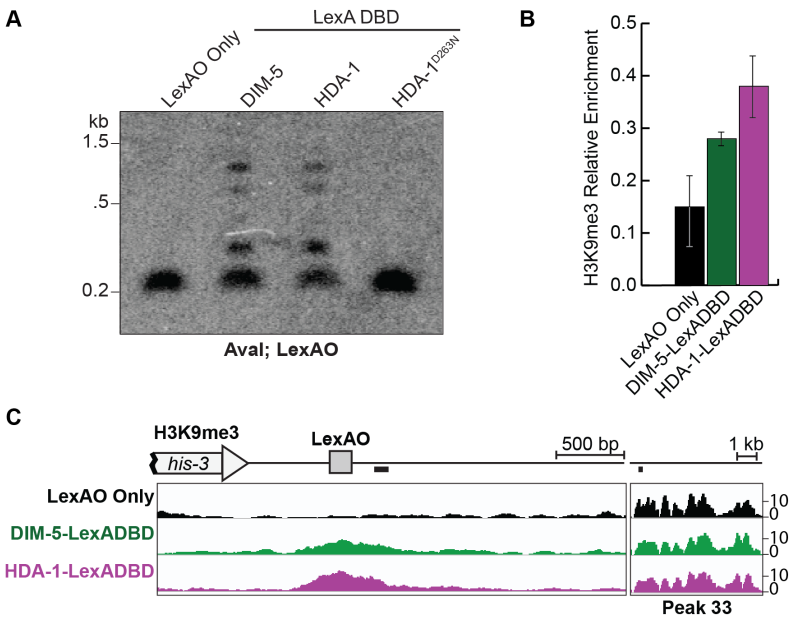

Fig. 36. HDA-1 Catalytic Activity Is Necessary to Induce H3K9me3 and DNA Methylation. (A) Tethered HDA-1 catalytic activity is required for induced DNA methylation. DNA methylation was evaluated (as in Fig. 29B) by AvaI-specific Southern hybridization. Strains (left to right): N5649, N5644, N6628, N6629. (B) Tethered HDA-1 and DIM-5 establish comparable H3K9me3 enrichment near the LexAO (assessed as in Fig. 31C). Strains (left to right): N5649, N5644, N6628. (C) Tethered HDA-1 and DIM-5 induce similar domains of H3K9me3. ChIP-sequencing tracks of H3K9me3 were assessed as in Figure 2D. Strains (top to bottom): N5649, N5644, N6628.

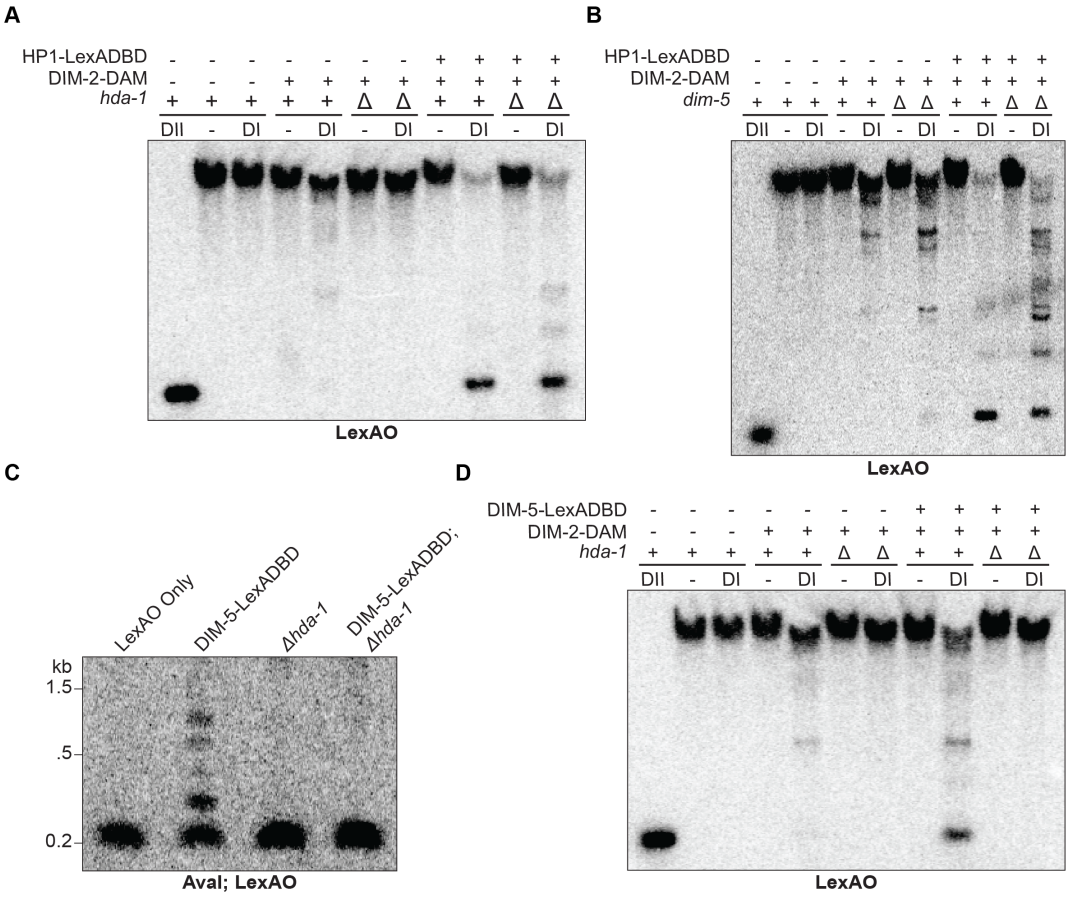

Fig. 37. DamID Analysis of DIM-2 Localization at Tethered Heterochromatin Machinery. (A) DIM-2-Dam localization to the LexAO by tethered HP1 is independent of *hda-1*. Genomic DNA of the indicated strains was digested with DpnI (DI), cleaving adenine-methylated GATC sequences, or subjected to a mock digestion without enzyme (-). As a control for completely digested DNA, genomic DNA from the wild-type strain was digested with the DpnI isoschizomer DpnII (DII), which cuts GATC sequences without methylated adenines. Strains (left to right): N5649, N6656, N6657, N6658, N6659. (B) Localization of DIM-2-Dam to the LexAO by tethered HP1 does not require *dim-5* (approach as in Fig. 37A). Strains (left to right): N5649, N6652, N6869, N6871, N6870. (C) DNA methylation induced by tethered DIM-5 depends on *hda-1* as detected in AvaI-specific Southern analysis (Fig. 29B). Strains (left to right): N5649, N5644, 6650, N6651. (D) DIM-2-Dam localization to the LexAO by tethered DIM-5 requires *hda-1* (as in Fig. 37A). Strains (left to right): N5649, N6652, N6653, N6654, N6655.

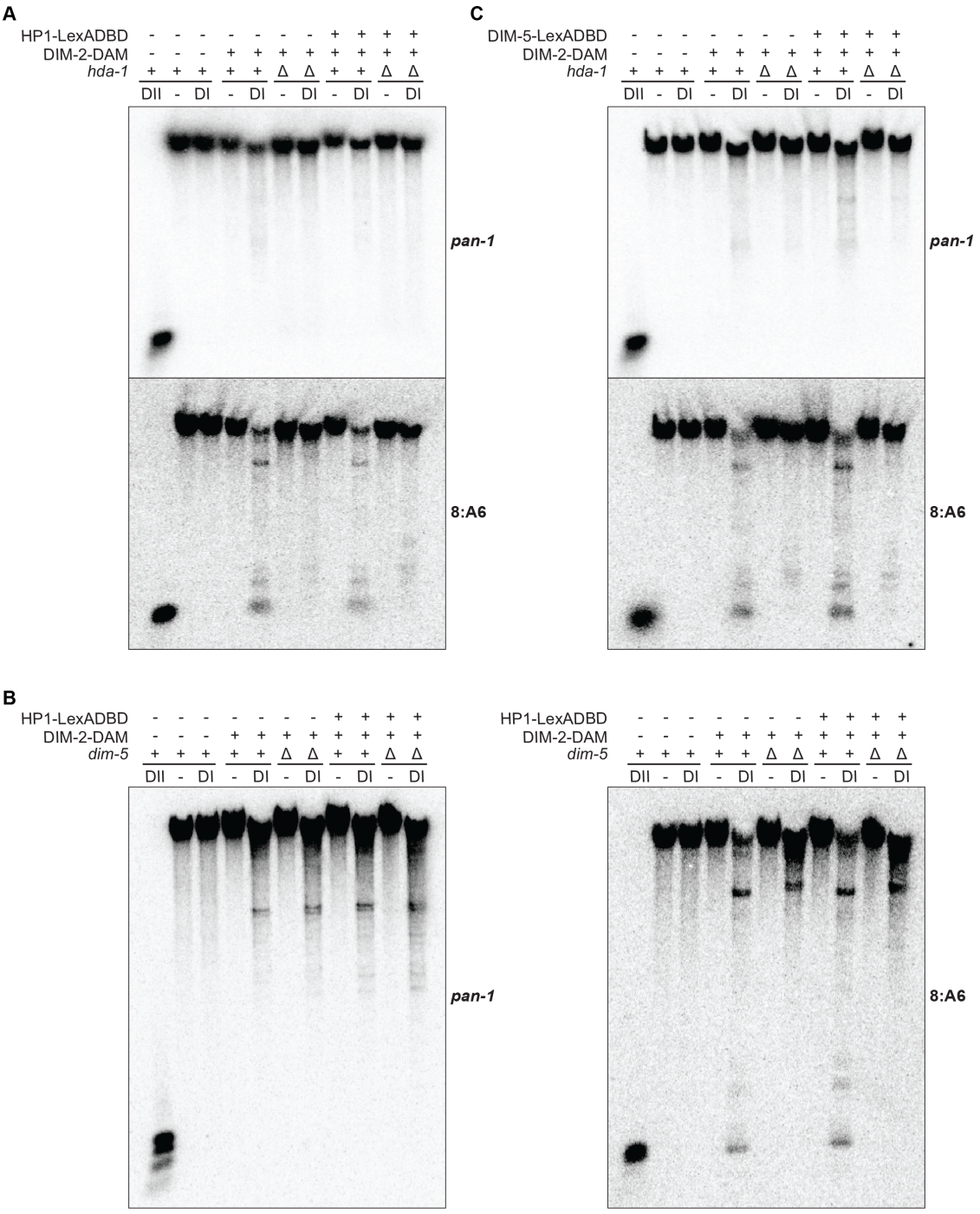

Fig. 38. Localization of DIM-2-Dam to Native Heterochromatin or Euchromatin. DamID experiments from Fig. 37 probed with alternative regions to examine DIM-2-Dam localization with tethered HP1 and deletions of (A) *hda-1* or (B) *dim-5* as well as (C) tethered DIM-5 with a deletion of *hda-1*. DpnII and DpnI-specific Southern hybridizations were carried out as in Fig. 37 except probed for the HCHC-dependent heterochromatic locus 8:A6 (Honda et al., 2012) or the euchromatic locus *pan-1*. Strains are identical to those used in Fig. 37.

Fig. 39 (see next page). *De novo* Heterochromatin Formation in *N. crassa*. (A) *hda-1* is not required for *de novo* heterochromatin formation. Genomic DNA of the indicated strains was digested with 5^{m}C-insensitive DpnII (D) or its 5^{m}C-sensitive isoschizomer BfuCI (B) and probed for *hda-1*-regulated regions (8:G3 and CenVIIM) or an *hda-1*-independent region (8:F10) (Honda et al., 2012). The positions of size standards are noted to the left. Strains: N3753, N3944, N3435, N6637, N6638, N6639. (B) Model for the relationship between histone deacetylation by the HCHC complex, DNA methylation, and H3K9me3 machinery in heterochromatin establishment. A:T-rich DNA (orange lines), harboring histone acetylation (blue triangles), serves as a signal to recruit the DCDC and establish H3K9me3 (red hexagons). H3K9me3 is bound by the HP1 chromodomain to localize the HCHC histone deacetylase complex and the DIM-2 DNA methyltransferase. Histone deacetylation promotes establishment of heterochromatic silencing and, together with DNA methylation (pink hexagons), leads to additional H3K9me3, which in turn can promote additional histone deacetylation and DNA methylation.

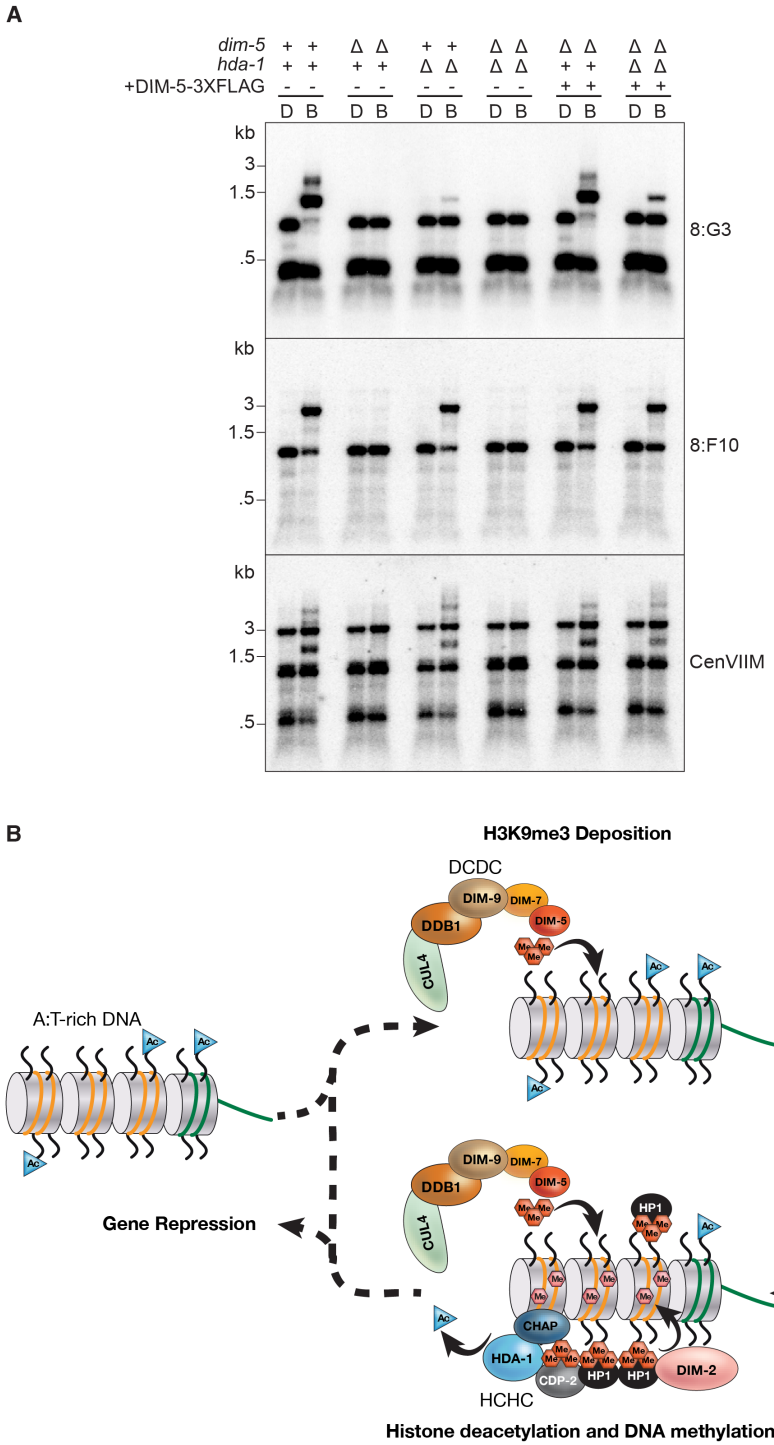
A
dim-5
hda-1
+DIM-5-3XFLAG
D B D B D B D B D B D B
kb
3
1.5
.5
8:G3
8:F10
CenVIIM
B
H3K9me3 Deposition
DCDC
DIM-9
DIM-7
DIM-5
DDB1
CUL4
A:T-rich DNA
Gene Repression
HP1
CHAP
HDA-1
CDP-2
DIM-2
HCHC
Histone deacetylation and DNA methylation

APPENDIX B

DATA TABLES

Table 1. Mass-spectroscopic analyses of DCDC from CUL4 neddylation-site and signalosome mutants[1].

			DIM-9-FLAG	DIM-8-FLAG	
			WT	*cul4*^{K863A}	*csn-1*
Gene Locus	**Description**	**MW (kDa)**	**Number of Peptides**	**Number of Peptides**	**Number of Peptides**
NCU06605	DIM-8/DDB1	128.6	72	216	181
NCU00272	CUL4	112.9	54	160	73
NCU01679	WD40 protein	68.97	0	74	19
NCU01656	DIM-9 (WD40 protein)	136.7	70	40	42
NCU01290	CBF5	52.8	0	40	0
NCU03668	WD40 protein	88.1	0	25	5
NCU04152	DIM-7	74.2	22	19	22
NCU04799	PABP	82.3	0	15	1
NCU02151	WD40 protein	75.9	0	14	13
NCU06598	Fungal specific protein	103.6	7	12	2
NCU08951	H/ACA ribonucleoprotein complex subunit 2	26.8	0	10	1
NCU07735	Grp1p	37.8	0	6	0
NCU01197	Ssd1	148.3	0	6	0
NCU06459	Negative regulator of differentiation 1	85.7	0	5	0
NCU06210	60S ribosomal protein L28e	159.8	0	3	0
NCU04402	DIM-5	37.5	1	2	0
NCU01634	Histone H4	11.3	0	2	0
NCU02437	Histone H2A	14.1	0	2	0
NCU05513	RCC-1	65.6	0	2	0
NCU05347	Histone H2A.Z	15.3	0	1	0
NCU03309	NEDD-8	8.8	4	0	1

[1] DIM-8-FLAG was purified from a CUL4-neddylation site mutant (*cul4*^{K863A}) or a COP9 signalosome mutant (*csn-1*). Purification of DIM-9-FLAG from a wild-type strain recovered all DCDC members (highlighted in red), similar to identification of DCDC with FLAG-CUL4 (13). Strains are listed in Appendix C.

APPENDIX C

STRAIN TABLES

All strains are *N. crassa*.

Chapter II

Strain	Genotype	Used in Figure/Table	Source
N150	*mat A*	1C,D;3-6;7A-C;8;9A,B;10	Our lab
N623	*mat A his-3*		Our lab
N625	*mat a his-3*		Our lab
N3016	*mat a Sad-1 his-3*		Our lab
N1860	*dim-2*	6;10	Our lab
N2930	*mat A his-3; Δmus-52::bar*$^{+}$		Our lab
N2993	*mat A his-3; Δmus-52::bar*$^{+}$*; Δinl*		Our lab
N3169	*mat a; Δcul4::hph*$^{+}$	4	FGSC#12374
N3892	*mat a Sad-1 his-3; cul4*^{RIP1}	1B-D;3-4;7A,B,C;9A,B	(Lewis, Adhvaryu, Honda, Shiver, Knip, Sack, et al., 2010b)
N3893	*mat a Sad-1 his-3*$^{+}$*::cul4* $^{+}$*; cul4*^{RIP1}	1D;3;7B,C;9A	
N3894	*mat a Sad-1 his-3*$^{+}$*::cul4* $^{+}$*; cul4*^{RIP1}	3	
N3896	*mat a Sad-1 his-3*$^{+}$*::flag-cul4*$^{+}$*; cul4*^{RIP1}	1B,C	
N3898	*mat a Sad-1 his-3*$^{+}$*::flag-cul4*^{K863A}*; cul4*^{RIP1}	1B,C	This study
N3970	*mat a; dim-9-flag::loxP::hph*$^{+}$*::loxP*	Appendix B	This study
N4269	*mat a Sad-1 his-3*$^{+}$*::cul4*^{K863R}*; cul4*^{RIP1}	1D;3	This study
N4270	*mat a Sad-1 his-3*$^{+}$*::cul4*^{K863R}*; cul4*^{RIP1}	3	This study
N4279	*mat a Sad-1 his-3*$^{+}$*::cul4*^{K863A}*; cul4*^{RIP1}	1D;3	This study
N4280	*mat a Sad-1 his-3*$^{+}$*::cull*^{K863A}*; cul4*^{RIP1}	3	This study
N4286	*mat a Sad-1 his-3*$^{+}$*::flag-cul4*^{K863R}*; cul4*^{RIP1}	1B,C	This study
N4195	*mat A his-3; Δmus-52::bar*$^{+}$*; Δinl; ΔhH2A::inl*$^{+}$		This study
N4197	*mat a his-3*$^{+}$*::hH2A-FLAG; ΔSad-2::hph*$^{+}$ *Δ mat a his-3*$^{+}$*::hH2A*^{K122A}*-FLAG; ΔSad-2::hph*$^{+}$		This study
N4201	*Δinl*		This study
N4528	*his-3*$^{+}$*::hH2A-FLAG; ΔhH2A::inl*$^{+}$	6	This study
N4529	*his-3*$^{+}$*::hH2A-FLAG; ΔhH2A::inl*$^{+}$	6	This study
N4533	*his-3*$^{+}$*::hH2A*^{K122A}*-FLAG; ΔhH2A::inl*$^{+}$	6	This study
N4534	*his-3*$^{+}$*::hH2A*^{K122A}*-FLAG; ΔhH2A::inl*$^{+}$	6	This study
N4616	*Δmms2::hph*$^{+}$	6	This study
N5029	*his-3*$^{+}$*::cul4*^{K863A}*; cul4*^{RIP1}*; dim-8-flag::loxP::hph*$^{+}$*::loxP*	Appendix B	This study
N5030	*Δcsn-1::hph*$^{+}$*; dim-8-flag::loxP::hph*$^{+}$*::loxP*	Appendix B	This study
N5112	*Δcsn-1::hph*$^{+}$	5	FGSC #11281
N5113	*Δcsn-1::hph*$^{+}$	5	FGSC #11282
N5523	*mat A; Δrbx1::hph*$^{+}$*; his-3; Δmus-52::bar*$^{+}$	8;9A,B	This study
N5292	*mat a; Sad-1 his-3*$^{+}$*::flag-cul4*$^{1-823}$*; cul4*^{RIP1}		This study
N5299	*mat a; Sad-1 his-3*$^{+}$*::cul4*$^{1-823}$*; cul4*^{RIP1}	7B-D	This study
	Δuvs-2::hph^{+}	10	FGSC #11445
N4656	*Δrnf8::hph*$^{+}$	10	FGSC #11916
	Δupr-1::hph^{+}	10	FGSC #15992
	mus-41, rad-5b,-c	10	(Kawabata, Kato, Suzuki, & Inoue, 2007)

Chapter III

Strain	Genotype	Reference
N150	*mat A*	FGSC #2489
N623	*mat A his-3*	FGSC #6103
N1877	*mat a his-3*; Δ*dim-2::hph*$^+$	(Kouzminova & Selker, 2001
N2264	*mat a his-3*; *dim-5 leu-2 pan-1*	(Tamaru & Selker, 2001)
N2556	*mat a his-3*; *hpo*^{RIP2}	(Freitag, Hickey, Khlafallah, Read, & Selker, 2004a)
N2700	*mat a his-3 cdp-1*^{RIP1}	This study
N2930	*mat A his-3* Δ*mus-52::bar*$^+$	(Honda & Selker, 2008)
N3135	*mat a* Δ*cdp-2::hph*$^+$	FGSC #11771
N3319	*mat a his-3*; *hpo-3xFLAG::loxP::hph*$^+$*::loxP*	(Honda & Selker, 2008)
N3320	*mat A his-3*; *hpo-3xFLAG::loxP::hph*$^+$*::loxP*	(Honda & Selker, 2008)
N3321	*mat a his-3*; *hpo-gfp::loxP::hph*$^+$*::loxP*	(Honda & Selker, 2008)
N3322	*mat A his-3*; *hpo-gfp::loxP::hph*$^+$*::loxP*	(Honda & Selker, 2008)
N3343	*mat a his-3*$^+$*::P*$_{cdp-2}$*::cdp-2-3xFLAG* Δ*cdp-2::hph*$^+$	(Honda et al., 2012)
N3365	*mat a his-3*; *hda-1-3xFLAG::loxP::hph*$^+$*::loxP*	This study
N3366	*mat A his-3*; *hda-1-3xFLAG::loxP::hph*$^+$*::loxP*	This study
N3367	*mat A his-3*; *hda-1-3xHA::loxP::hph*$^+$*::loxP*	This study
N3368	*mat a his-3*; *hda-1-3xHA::loxP::hph*$^+$*::loxP*	This study
N3375	*mat a his-3*; *chap-3xFLAG::loxP::hph*$^+$*::loxP*	This study
N3376	*mat A his-3*; *chap-3xFLAG::loxP::hph*$^+$*::loxP*	This study
N3377	*mat A his-3*; *chap -3xHA::loxP::hph*$^+$*::loxP*	This study
N3378	*mat a his-3*; *chap -3xHA::loxP::hph*$^+$*::loxP*	This study
N3393	*mat a his-3*; *hpo-3xFLAG::loxP::hph*$^+$*::loxP*; *chap -3xHA::loxP::hph*$^+$*::loxP*	This study
N3431	*mat A his-3*; *hpo-gfp::loxP::hph*$^+$*::loxP*; *dim-5 leu-2 pan-1*	(Honda & Selker, 2008)
N3435	*mat A his-3*; Δ*hda-1::hph*$^+$	This study
N3610	*mat a*; Δ*hda-1::hph*$^+$	FGSC #12003
N3612	*mat a*; Δ*chap::hph*$^+$	FGSC #12802
N3613	*mat A*; Δ*chap::hph*$^+$	FGSC #12803
N3615	*mat A his-3* Δ*cdp-2::hph*$^+$	(Honda et al., 2012)
N3642	*mat a*; Δ*chap::hph*$^+$; *pan-2::hph*$^+$*::tk*$^+$	This study
N3643	*mat A*; Δ*chap::hph*$^+$; *pan-2::hph*$^+$*::tk*$^+$	This study
N3649	*mat A his-3*; *hpo-gfp::loxP::hph*$^+$*::loxP*; Δ*chap::hph*$^+$	This study
N3650	*mat A*; *hpo-gfp::loxP::hph*$^+$*::loxP*; Δ*chap::hph*$^+$	This study
N3680	*mat a* Δ*cdp-2::hph*$^+$; Δ*hda-1::hph*$^+$	This study
N3698	*mat a*; Δ*chap::hph*$^+$ Δ*hda-1::hph*$^+$	This study
N3704	*mat a his-3*; *hpo-3xFLAG::loxP::hph*$^+$*::loxP*; *hda-1-3xHA::loxP::hph*$^+$*::loxP*	This study
N3705	*mat a his-3*; *hpo-3xFLAG::loxP::hph*$^+$*::loxP*; *hda-1-3xHA::loxP::hph*$^+$*::loxP*	This study
N3714	*mat a his-3* Δ*cdp-2::hph*$^+$; Δ*chap::hph*$^+$	This study
N3717	*mat a his-3*; *hpo-3xFLAG::loxP::hph*$^+$*::loxP*; *chap-3xHA::loxP::hph*$^+$*::loxP* Δ*hda-1::hph*$^+$	This study
N3718	*mat A his-3*; *hpo-3xFLAG::loxP::hph*$^+$*::loxP*; *chap-3xHA::loxP::hph*$^+$*::loxP* Δ*hda-1::hph*$^+$	This study
N3719	*mat A his-3*$^+$*::P*$_{cdp-2}$*::cdp-2-3xFLAG* Δ*cdp-2::hph*$^+$; *chap-3xHA::loxP::hph*$^+$*::loxP* Δ*hda-1::hph*$^+$	This study
N3720	*mat A his-3*; *hpo-3xFLAG::loxP::hph*$^+$*::loxP*; *hda-1-3xHA::loxP::hph*$^+$*::loxP* Δ*chap::hph*$^+$	This study
N3728	*mat A his-3* Δ*cdp-2::hph*$^+$; *chap-3xFLAG::loxP::hph*$^+$*::loxP* *hda-1-3xHA::loxP::hph*$^+$*::loxP*	This study
N3729	*mat A his-3* Δ*cdp-2::hph*$^+$; *chap-3xFLAG::loxP::hph*$^+$*::loxP*	This study

	hda-1-3xHA::loxP::hph$^+$::loxP	
N3730	*mat A his-3*; *chap-3xFLAG::loxP::hph$^+$::loxP* ; *hda-1-3xHA::loxP::hph$^+$::loxP*	This study
N3733	*mat A his-3* Δ*cdp-2::hph$^+$*; *hpo-3xFLAG::loxP::hph$^+$::loxP*; *hda-1-3xHA::loxP::hph$^+$::loxP*	This study
N3734	*mat A his-3* Δ*cdp-2::hph$^+$*; *hpo-3xFLAG::loxP::hph$^+$::loxP*; *hda-1-3xHA::loxP::hph$^+$::loxP*	This study
N3735	*mat A his-3*; *hpo-3xFLAG::loxP::hph$^+$::loxP*; *hda-1-3xHA::loxP::hph$^+$::loxP*; *dim-5 leu-2 pan-1*	This study
N3736	*mat a his-3*; *hpo-3xFLAG::loxP::hph$^+$::loxP*; *hda-1-3xHA::loxP::hph$^+$::loxP*; *dim-5 leu-2 pan-1*	This study
N3752	*mat A*	FGSC #2489
N3753	*mat a*	FGSC #4200
N3757	*mat A his-3*; *hpo-gfp::loxP::hph$^+$::loxP*; Δ*hda-1::hph$^+$*	This study
N3758	*mat a*; *hpo-gfp::loxP::hph$^+$::loxP*; Δ*hda-1::hph$^+$*	This study
N3759	*mat a his-3* Δ*cdp-2::hph$^+$*; *hpo-gfp::loxP::hph$^+$::loxP*	(Honda et al., 2012)
N3760	*mat A* Δ*cdp-2::hph$^+$*; *hpo-gfp::loxP::hph$^+$::loxP*	(Honda et al., 2012)
N3766	*mat A* Δ*cdp-2::hph$^+$*	(Honda et al., 2012)
N3767	*mat a his-3* Δ*cdp-2::hph$^+$*	(Honda et al., 2012)
N3772	*mat a his-3*; *chap-3xFLAG::loxP::hph$^+$::loxP* *hda-1-3xHA::loxP::hph$^+$::loxP*	This study
N3779	*mat a his-3*; *hpo-3xFLAG::loxP::hph$^+$::loxP*; *hda-1-3xHA::loxP::hph$^+$::loxP* Δ*chap::hph$^+$*	This study
N3790	*mat a his-3$^+$::P$_{ccg-1}$::cdp-2-gfp* Δ*cdp-2::hph$^+$*	(Honda et al., 2012)
N3791	*mat A his-3$^+$::P$_{ccg-1}$::cdp-2-gfp* Δ*cdp-2::hph$^+$*	(Honda et al., 2012)
N3792	*mat a his-3$^+$::P$_{ccg-1}$::cdp-2-gfp* Δ*cdp-2::hph$^+$*; Δ*hda-1::hph$^+$*	This study
N3793	*mat A his-3$^+$::P$_{ccg-1}$::cdp-2-gfp* Δ*cdp-2::hph$^+$*; Δ*hda-1::hph$^+$*	This study
N3794	*mat a his-3$^+$::P$_{ccg-1}$::cdp-2-gfp* Δ*cdp-2::hph$^+$*; Δ*chap::hph$^+$*	This study
N3800	*mat A his-3*; *hpo-3xFLAG::loxP::hph$^+$::loxP*; *chap-3xHA::loxP::hph$^+$::loxP*; *dim-5 leu-2 pan-1*	This study
N3802	*mat a his-3$^+$::P$_{cdp-2}$::cdp-2-3xFLAG* Δ*cdp-2::hph$^+$*; *hda-1-3xHA::loxP::hph$^+$::loxP* Δ*chap::hph$^+$*	This study
N3803	*mat A his-3$^+$::P$_{cdp-2}$::cdp-2-3xFLAG* Δ*cdp-2::hph$^+$*; *chap-3xHA::loxP::hph$^+$::loxP*	This study
N3804	*mat a his-3* Δ*cdp-2::hph$^+$*; *hpo-3xFLAG::loxP::hph$^+$::loxP*; *chap-3xHA::loxP::hph$^+$::loxP*	This study
N3805	*mat A his-3*; *hpo-3xFLAG::loxP::hph$^+$::loxP*; *chap-3xHA::loxP::hph$^+$::loxP*	This study
N3806	*mat A his-3*; *chap-3xFLAG::loxP::hph$^+$::loxP* *hda-1-3xHA::loxP::hph$^+$::loxP*; *dim-5 leu-2 pan-1*	This study
N3807	*mat a his-3*; *chap-3xFLAG::loxP::hph$^+$::loxP* *hda-1-3xHA::loxP::hph$^+$::loxP*; *dim-5 leu-2 pan-1*	This study
N3808	*mat A his-3$^+$::P$_{cdp-2}$::cdp-2-3xFLAG* Δ*cdp-2::hph$^+$*; *hda-1-3xHA::loxP::hph$^+$::loxP*	This study
N3809	*mat a his-3$^+$::P$_{cdp-2}$::cdp-2-3xFLAG* Δ*cdp-2::hph$^+$*; *hda-1-3xHA::loxP::hph$^+$::loxP*	This study
N3818	*mat a*; Δ*chap::hph$^+$*; *pan-2$^+$::P$_{chap}$::chap-3xHA*	This study
N3819	*mat A*; Δ*chap::hph$^+$*; *pan-2$^+$::P$_{chap}$::chap-3xHA*	This study
N3820	*mat a*; Δ*chap::hph$^+$*; *pan-2$^+$::P$_{chap}$::chap^{ATh1}-3xHA*	This study
N3821	*mat A*; Δ*chap::hph$^+$*; *pan-2$^+$::P$_{chap}$::chap^{ATh1}-3xHA*	This study
N3822	*mat A*; Δ*chap::hph$^+$*; *pan-2$^+$::P$_{chap}$::chap^{ATh2}-3xHA*	This study
N3823	*mat a*; Δ*chap::hph$^+$*; *pan-2$^+$::P$_{chap}$::chap^{ATh2}-3xHA*	This study
N3824	*mat A*; Δ*chap::hph$^+$*; *pan-2$^+$::P$_{chap}$::chap^{Zf2}-3xHA*	This study
N3825	*mat a*; Δ*chap::hph$^+$*; *pan-2$^+$::P$_{chap}$::chap^{Zf2}-3xHA*	This study
N3826	*mat A*; Δ*chap::hph$^+$*; *pan-2$^+$::P$_{chap}$::chap$^{Zf1\&2}$-3xHA*	This study
N3827	*mat a*; Δ*chap::hph$^+$*; *pan-2$^+$::P$_{chap}$::chap$^{Zf1\&2}$-3xHA*	This study

N3835	*mat a his-3^{+}::P$_{cdp-2}$::cdp-2-3xFLAG Dcdp-2::hph^{+}; hpo-GFP::hph^{+}; dim-5 leu-2 pan-1*	This study
N3836	*mat a his-3^{+}::P$_{cdp-2}$::cdp-2-3xFLAG Dcdp-2::hph^{+}; hpo-GFP::hph^{+}*	This study
N3837	*mat A his-3^{+}::P$_{cdp-2}$::cdp-2-3xFLAG Dcdp-2::hph^{+}; hpo-GFP::hph^{+}*	This study
N3838	*mat a his-3^{+}::P$_{cdp-2}$::cdp-2-3xFLAG Δcdp-2::hph^{+}; hpo-gfp::loxP::hph^{+}::loxP; Δhda-1::hph^{+}*	This study
N3839	*mat a his-3^{+}::P$_{cdp-2}$::cdp-2-3xFLAG Δcdp-2::hph^{+}; hpo-gfp::loxP::hph^{+}::loxP; Δchap::hph^{+}*	This study
N3841	*mat A his-3; chap-3xFLAG::loxP::hph^{+}::loxP hda-1-3xHA::loxP::hph^{+}::loxP; hpo^{RIP2}*	This study
N3842	*mat A his-3^{+}::P$_{cdp-2}$::cdp-2-3xFLAG Δcdp-2::hph^{+}; chap-3xHA::loxP::hph^{+}::loxP; dim-5 leu-2 pan-1*	This study
N3843	*mat A his-3^{+}::P$_{cdp-2}$::cdp-2-3xFLAG Δcdp-2::hph^{+}; chap-3xHA::loxP::hph^{+}::loxP; hpo^{RIP2}*	This study
N3844	*mat a his-3^{+}::P$_{cdp-2}$::cdp-2-3xFLAG Δcdp-2::hph^{+}; chap-3xHA::loxP::hph^{+}::loxP; hpo^{RIP2}*	This study
N3845	*mat a; Δchap::hph^{+}; pan-2^{+}::P$_{chap}$::chap$^{ATh1\&2}$-3xHA*	This study
N3846	*mat a; Δchap::hph^{+}; pan-2^{+}::P$_{chap}$::chap^{Zf1}-3xHA*	This study
N3852	*mat A his-3^{+}::P$_{cdp-2}$::cdp-2-3xFLAG Δcdp-2::hph^{+}; hda-1-3xHA::loxP::hph^{+}::loxP; dim-5 leu-2 pan-1*	This study
N3853	*mat a his-3^{+}::P$_{cdp-2}$::cdp-2-3xFLAG Δcdp-2::hph^{+}; hda-1-3xHA::loxP::hph^{+}::loxP; hpo^{RIP2}*	This study
N3911	*his-3^{+}::P$_{ccg-1}$::cdp-2-gfp Δcdp-2::hph^{+}; trp-2; dim-5::bar*	(Honda et al., 2012)
N3913	*his-3^{+}::P$_{ccg-1}$::cdp-2-gfp Δcdp-2::hph^{+}; trp-2; hpo^{RIP2} trp-2*	(Honda et al., 2012)
N3986	*mat a his-3; Δchap::hph^{+}; pan-2^{+}::P$_{chap}$::chap$^{ATh1\&2}$-3xHA; hpo-3xFLAG::loxP::hph^{+}::loxP*	This study
N3992	*mat A Δcdp-2::hph^{+} his-3^{+}::P$_{cdp-2}$::cdp-2^{W446G}-3xFLAG*	This study
N3993	*mat a Δcdp-2::hph^{+} his-3^{+}::P$_{cdp-2}$::cdp-2^{W446G}-3xFLAG*	This study
N3995	*mat A his-3^{+}::P$_{hda-1}$::hda-1-dam; Δhda-1::hph^{+}*	This study
N3996	*mat a his-3^{+}::P$_{hda-1}$::hda-1-dam; Δhda-1::hph^{+}*	This study
N3997	*mat A his-3^{+}::P$_{hda-1}$::hda-1-3xFLAG; Δhda-1::hph^{+}*	This study
N3998	*mat A his-3^{+}::P$_{hda-1}$::hda-1^{D263N}-3xFLAG; Δhda-1::hph^{+}*	This study
N3999	*mat a his-3^{+}::P$_{hda-1}$::hda-1^{D263N}-3xFLAG; Δhda-1::hph^{+}*	This study
N4000	*mat A his-3^{+}::P$_{hda-1}$::hda-1^{D263N}-3xFLAG; Δhda-1::hph^{+} chap-3xHA::loxP::hph^{+}::loxP*	This study
N4001	*mat a his-3^{+}::P$_{hda-1}$::hda-1^{D263N}-3xFLAG; Δhda-1::hph^{+} chap-3xHA::loxP::hph^{+}::loxP*	This study
N4002	*mat A his-3^{+}::P$_{hda-1}$::hda-1^{D263N}-3xFLAG; Δhda-1::hph^{+} hpo-gfp::loxP::hph^{+}::loxP*	This study
N4006	*mat A Δcdp-2::hph^{+}his-3^{+}::P$_{cdp-2}$::cdp-2-3xFLAG*	This study
N4007	*mat a Δcdp-2::hph^{+}his-3^{+}::P$_{cdp-2}$::cdp-2-3xFLAG*	This study
N4011	*mat A his-3^{+}::P$_{cdp-2}$::cdp-2-dam Δcdp-2::hph^{+}*	This study
N4013	*mat a his-3^{+}::P$_{cdp-2}$::cdp-2-dam Δcdp-2::hph^{+}; hpo^{RIP2}*	This study
N4014	*mat A his-3^{+}::P$_{cdp-2}$::cdp-2-dam Δcdp-2::hph^{+}; hpo^{RIP2}*	This study
N4023	*mat A Δcdp-2::hph^{+} his-3^{+}::P$_{hda-1}$::hda-1-dam; Δhda-1::hph^{+}*	This study
N4026	*mat A his-3^{+}::P$_{cdp-2}$::cdp-2^{W446G}-dam Δcdp-2::hph^{+}*	This study
N4043	*mat A his-3^{+}::P$_{hda-1}$::hda-1-3xFLAG; Δhda-1::hph^{+} hpo-gfp::loxP::hph^{+}::loxP*	This study
N4045	*mat A his-3^{+}::P$_{chap}$::chap-dam; Δchap::hph^{+}*	This study
N4082	*mat A his-3^{+}::P$_{hda-1}$::hda-1-dam; Δhda-1::hph^{+} Δchap::hph^{+}*	This study
N4083	*mat a his-3^{+}::P$_{cdp-2}$::cdp-2-dam Δcdp-2::hph^{+}; Δhda-1::hph^{+}*	This study
N4084	*mat A his-3^{+}::P$_{cdp-2}$::cdp-2-dam Δcdp-2::hph^{+}; Δhda-1::hph^{+}*	This study
N4085	*mat A his-3^{+}::P$_{cdp-2}$::cdp-2-dam Δcdp-2::hph^{+}; Δchap::hph^{+}*	This study
N4088	*mat A Δcdp-2::hph^{+} his-3^{+}::P$_{cdp-2}$::cdp-2$^{\Delta CD}$-3xFLAG*	This study
N4089	*mat A Δcdp-2::hph^{+} his-3^{+}::P$_{cdp-2}$::cdp-2$^{1-419}$-3xFLAG*	This study
N4090	*mat a Δcdp-2::hph^{+} his-3^{+}::P$_{cdp-2}$::cdp-2$^{1-419}$-3xFLAG*	This study

N4687	*mat A his-3^{+}::P$_{chap}$::chap-dam Δcdp-2::hph^{+}; Δchap::hph^{+}*	This study
N4690	*mat A his-3^{+}::P$_{chap}$::chap-dam; Δhda-1::hph^{+} Δchap::hph^{+}*	This study
N4695	*mat a; Δhda-1::hph^{+}; Δdim-2::hph^{+}*	This study
N4699	*his-3^{+}::P$_{hda-1}$::hda-1-3xFLAG; Δhda-1::hph^{+} chap-3xHA::loxP::hph^{+}::loxP*	This study
N4890	*mat A his-3; cenVIR::bar trp-2*	This study
N4891	*mat A his-3; cenVIR::bar trp-2 hpo^{RIP2}*	This study
N4909	*mat a his-3; cenVIR::bar trp-2*	(Honda et al., 2012)
N4915	*mat A Δcdp-2::hph^{+}; cenVIR::bar trp-2*	This study
N4916	*mat a Δcdp-2::hph^{+}; cenVIR::bar trp-2*	This study
N4922	*mat a, Δhpo::hph^{+}*	FGSC #14522
N5015	*mat a his-3^{+}::P$_{ccg-1}$::h2a-GFP; Δhda-1::hph^{+}*	This study
N5017	*mat a his-3^{+}::P$_{ccg-1}$::h2a-GFP Δcdp-2::hph^{+}; ΔSad-2::hph^{+}*	This study
N5024	*mat a his-3^{+}::P$_{ccg-1}$::h2a-GFP; Δchap::hph^{+}*	This study
N5026	*mat a his-3^{+}::P$_{ccg-1}$::h2a-GFP*	This study
N5430	*mat a, Δhpo::hph^{+}*	This study
N5580	*mat a Δhpo::hph^{+}; his-3*	This study
N5868	*his-3^{+}::hpo^{WT}, cenVIR::bar trp-2*	This study
N5869	*his-3^{+}::hpo^{ΔCD}, cenVIR::bar trp-2*	This study
N5870	*his-3^{+}::hpo^{ΔCD}, cenVIR::bar trp-2*	This study
N5871	*his-3^{+}::hpo^{W98G}, cenVIR::bar trp-2*	This study
N5872	*his-3^{+}::hpo^{W98G}, cenVIR::bar trp-2*	This study
N6166	*mat a his-3^{+}::LexA Operator; hpo-LexADBD::hph^{+}*	This study
N6390	*mat a his-3^{+}::LexA Operator; hpo^{ΔCD}-LexADBD::hph^{+}*	This study
N6391	*mat a his-3^{+}::LexA Operator; hpo^{ΔCD}-LexADBD::hph^{+}; Δchap::hph^{+}*	This study
N6392	*mat a his-3^{+}::LexA Operator; chap::hph^{+}*	This study
N6393	*mat a his-3^{+}::LexA Operator; cdp-2^{ΔCD}-LexADBD::nat-1^{+}*	This study
N6394	*mat a his-3^{+}::LexA Operator; cdp-2^{ΔCD}-LexADBD::nat-1^{+}; hpo^{ΔCD}-LexADBD::hph^{+}*	This study
#775	*mat A; Δhda-1::bar^{+}*	This study
#888	*mat A Δcdp-2::hph^{+} his-3^{+}::P$_{cdp-2}$-cdp-2-3xFLAG; cenVIR::bar; trp-2*	This study
#889	*mat A Δcdp-2::hph^{+} his-3^{+}::P$_{cdp-2}$-cdp-2-3xFLAG; cenVIR::bar; trp-2*	This study
#890	*mat A Δcdp-2::hph^{+} his-3^{+}::P$_{cdp-2}$-cdp-2^{W446G}-3xFLAG; cenVIR::bar; trp-2*	This study
#891	*mat A Δcdp-2::hph^{+} his-3^{+}::P$_{cdp-2}$-cdp-2^{W446G}-3xFLAG; cenVIR::bar; trp-2*	This study
#892	*mat A Δcdp-2::hph^{+} his-3^{+}::P$_{cdp-2}$-cdp-2^{ΔCD}-3xFLAG; cenVIR::bar; trp-2*	This study
#893	*mat A Δcdp-2::hph^{+} his-3^{+}::P$_{cdp-2}$-cdp-2^{ΔCD}-3xFLAG; cenVIR::bar; trp-2*	This study
#894	*mat a Δcdp-2::hph^{+} his-3^{+}::P$_{cdp-2}$-cdp-2$^{1-419aa}$-3xFLAG; cenVIR::bar; trp-2*	This study
#895	*mat a Δcdp-2::hph^{+} his-3^{+}::P$_{cdp-2}$-cdp-2$^{1-419aa}$-3xFLAG; cenVIR::bar; trp-2*	This study
#903	*mat a; Δchap::hph^{+}*	This study
#949	*mat A Δcdp-2::hph^{+}*	This study
#3440	*mat A Δcdp-2::hph^{+} his-3^{+}::P$_{cdp-2}$-cdp-2$^{IE/AA}$-3xFLAG; hpo-GFP::hph^{+}::loxP*	This study
#3441	*mat a Δcdp-2::hph^{+} his-3^{+}::P$_{cdp-2}$-cdp-2$^{IE/AA}$-3xFLAG; hpo-GFP::hph^{+}::loxP*	This study
#3443	*mat A Δcdp-2::hph^{+} his-3^{+}::P$_{cdp-2}$-cdp-2^{ΔPPITL}-3xFLAG; hpo-GFP::hph^{+}::loxP*	This study
#3444	*mat A Δcdp-2::hph^{+} his-3^{+}::P$_{cdp-2}$-cdp-2^{ΔPPITL}-3xFLAG; hpo-GFP::hph^{+}::loxP*	This study
#3445	*mat A Δcdp-2::hph^{+} his-3^{+}::P$_{cdp-2}$-cdp-2$^{IE/AA}$-3xFLAG; hda-1-3xHA::hph^{+}::loxP*	This study
#3446	*mat A Δcdp-2::hph^{+} his-3^{+}::P$_{cdp-2}$-cdp-2$^{IE/AA}$-3xFLAG; hda-1-3xHA::hph^{+}::loxP*	This study
#3447	*mat A Δcdp-2::hph^{+} his-3^{+}::P$_{cdp-2}$-cdp-2^{ΔPPITL}-3xFLAG; hda-1-3xHA::hph^{+}::loxP*	This study
#3448	*mat a Δcdp-2::hph^{+} his-3^{+}::P$_{cdp-2}$-cdp-2^{DPPITL}-3xFLAG; hda-1-3xHA::hph^{+}::loxP*	This study

Chapter IV

Strain	Genotype	Reference
N150	*mat A*	FGSC#2489
N1853	*mat A; Δdim-2::hph*$^{+}$	this study
N1909	*mat a his-3*$^{+}$*::pqa::dim-2*^{C926A}*; Δdim-2::hph*$^{+}$	(Kouzminova & Selker, 2001)
N2930	*mat A his-3;* Δ*mus-52::bar*$^{+}$	(Honda & Selker, 2008)
N3012	*mat a his-3;* Δ*mus-52::bar*$^{+}$	this study
N3435	*mat A his-3; Δhda-1::hph*$^{+}$	(Honda et al., 2016)
N3752	*mat A*	FGSC#2489
N3753	*mat a*	FGSC#4200
N3944	*mat A; Δdim-5::bar*$^{+}$	(Lewis, Adhvaryu, Honda, Shiver, Knip, Sack, et al., 2010b)
N3998	*mat A his-3*$^{+}$*::phda-1::hda-1*^{D263N}*-3XFLAG; Δhda-1::hph*$^{+}$	(Honda et al., 2016)
N4863	*mat A Sad-1 his-3; Δdim-5::hph*$^{+}$	this study
		this study
N5643	*mat a his-3*$^{+}$*::LexAO (heterokaryon);* Δ*mus-52::bar*$^{+}$	this study
N5644	*mat a his-3*$^{+}$*::LexAO; dim-5-LexA DBD::hph*$^{+}$*;* Δ*mus-52::bar*$^{+}$	
N5647	*mat ? his-3*$^{+}$*::LexAO; dim-9-LexA DBD::hph*$^{+}$*;* Δ*mus-52::bar*$^{+}$	this study
N5649	*mat A his-3*$^{+}$*::LexAO;* Δ*mus-52::bar*$^{+}$	this study
N6166	*mat a his-3*$^{+}$*::LexA Operator*; *hpo-LexADBD::hph*$^{+}$*;* Δ*mus-52::bar*$^{+}$	(Honda et al., 2016)
N6390	*mat ? his-3*$^{+}$*::LexA Operator*; *hpo*$^{\Delta CD}$*-LexADBD::hph*$^{+}$*;* Δ*mus-52::bar*$^{+}$*?*	(Honda et al., 2016)
N6610	*mat a his-3*$^{+}$*::LexAO::nat-1*$^{+}$*;* Δ*mus-52::bar*$^{+}$	this study
N6611	*mat a his-3*$^{+}$*::LexAO::nat-1*$^{+}$*; hpo-LexA DBD::hph*$^{+}$*;* Δ*mus-52::bar*$^{+}$	this study
N6612	*mat ? his-3*$^{+}$*::LexAO::nat-1*$^{+}$*; dim-5-LexA DBD::hph*$^{+}$*;* Δ*mus-52::bar*$^{+}$	this study
N6613	*mat ? his-3*$^{+}$*::LexAO; Δdim-7::nat-1*$^{+}$*; dim-5-LexA DBD::hph*$^{+}$*;* Δ*mus-52::bar*$^{+}$*?*	this study
N6614	*mat ? his-3*$^{+}$*::LexAO; Δddb1::hph*$^{+}$*; dim-5-LexA DBD::hph*$^{+}$*;* Δ*mus-52::bar*$^{+}$*?*	this study
N6615	*mat ? his-3*$^{+}$*::LexAO; Δdim-9::hph*$^{+}$ *dim-5-LexA DBD::hph*$^{+}$*;* Δ*mus-52::bar*$^{+}$*?*	this study
N6616	*mat ? his-3*$^{+}$*::LexAO; dim-5-LexA DBD::hph*$^{+}$*; cul4*^{RIP1} Δ*mus-52::bar*$^{+}$*?*	this study
N6619	*mat ? his-3*$^{+}$*::LexAO; Δdim-5::hph*$^{+}$*; hpo-LexA DBD::hph*$^{+}$*;* Δ*mus-52::bar*$^{+}$*?*	this study
N6620	*mat ? his-3*$^{+}$*::LexAO; Δdmm-1::hph*$^{+}$*; hpo-LexA DBD::hph*$^{+}$*;* Δ*mus-52::bar*$^{+}$*?*	this study
N6621	*mat ? his-3*$^{+}$*::LexAO; Δmi-2::hph*$^{+}$*; hpo-LexA DBD::hph*$^{+}$*;* Δ*mus-52::bar*$^{+}$*?*	this study
N6622	*mat ? his-3*$^{+}$*::LexAO; Δhda-1::hph*$^{+}$*; hpo-LexA DBD::hph*$^{+}$*;* Δ*mus-52::bar*$^{+}$*?*	this study
N6623	*mat ? his-3*$^{+}$*::LexAO; Δdim-2::hph*$^{+}$*; hpo-LexA DBD::hph*$^{+}$*;* Δ*mus-52::bar*$^{+}$*?*	this study
N6624	*mat ? his-3*$^{+}$*::LexAO; dim-2*^{C926A}*-3xFLAG::hph*$^{+}$*; hpo-LexA DBD::hph*$^{+}$*;* Δ*mus-52::bar*$^{+}$	this study
N6625	*mat ? his-3*$^{+}$*::LexAO; hda-1*^{D263N}*-3xFLAG::hph*$^{+}$*; hpo-LexA DBD::hph*$^{+}$*;* Δ*mus-52::bar*$^{+}$	this study
N6626	*mat ? his-3*$^{+}$*::LexAO Δcdp-2::hph*$^{+}$*; hpo-LexA DBD::hph*$^{+}$*;* Δ*mus-52::bar*$^{+}$*?*	this study
N6627	*mat ? his-3*$^{+}$*::LexAO; Δchap::hph*$^{+}$*; hpo-LexA DBD::hph*$^{+}$*;* Δ*mus-52::bar*$^{+}$*?*	this study
N6628	*mat a his-3*$^{+}$*::LexAO; hda-1-LexA DBD::hph*$^{+}$*;* Δ*mus-52::bar*$^{+}$*?*	this study
N6629	*mat ? his-3*$^{+}$*::LexAO; hda-1*^{D263N}*-LexA DBD::hph*$^{+}$*;* Δ*mus-52::bar*$^{+}$*?*	this study
N6630	*mat ? his-3*$^{+}$*::LexAO::nat-1*$^{+}$*; Δdim-2::hph*$^{+}$*; hpo-LexA DBD::hph*$^{+}$*;* Δ*mus-52::bar*$^{+}$*?*	this study
N6631	*mat ? his-3*$^{+}$*::LexAO::nat-1*$^{+}$*; Δdim-5::hph*$^{+}$*; hpo-LexA DBD::hph*$^{+}$*;* Δ*mus-52::bar*$^{+}$*?*	this study
N6632	*mat ? his-3*$^{+}$*::LexAO::nat-1*$^{+}$*; Δhda-1::hph*$^{+}$*; hpo-LexA DBD::hph*$^{+}$*;* Δ*mus-52::bar*$^{+}$*?*	this study
N6633	*mat ? his-3*$^{+}$*::LexAO::nat-1*$^{+}$*; Δchap::hph*$^{+}$*; hpo-LexA DBD::hph*$^{+}$*;* Δ*mus-52::bar*$^{+}$*?*	this study
N6635	*mat ? his-3*$^{+}$*::LexAO; hpo*^{Y244E}*-LexA DBD::hph*$^{+}$*;* Δ*mus-52::bar*$^{+}$*?*	this study
N6636	*mat ? his-3*$^{+}$*::LexAO; chap*$^{ATH1/2}$*::bar*$^{+}$*::nat*$^{+}$*; hpo-LexA DBD::hph*$^{+}$	this study

N6637	*mat ?; Δdim-5::bar$^+$; Δhda-1::hph$^+$*	this study
N6638	*mat ?; Δtrp-2::pdim-5::dim-5-3XFLAG::nat-1$^+$; Δdim-5::bar$^+$*	this study
N6639	*mat ?; Δtrp-2::pdim-5::dim-5-3XFLAG::nat-1$^+$; Δdim-5::bar$^+$; Δhda-1::hph$^+$*	this study
N6640	*mat A his-3; Δtrp-2::LexAO::nat-1$^+$; Δmus-52::bar$^+$*	this study
N6641	*mat ? his-3; dim-5-LexA DBD::hph$^+$; Δtrp-2::LexAO::nat-1$^+$; Δmus-52::bar$^+$*	this study
N6642	*mat ? his-3; hpo-LexA DBD::hph$^+$ Δtrp-2::LexAO::nat-1$^+$; Δmus-52::bar$^+$*	this study
N6643	*mat ? his-3; hda-1-LexA DBD::hph$^+$; Δtrp-2::LexAO::nat-1$^+$; Δmus-52::bar$^+$*	this study
N6646	*mat ? his-3; dim-9-LexA DBD::hph$^+$; Δtrp-2::LexAO::nat-1$^+$; Δmus-52::bar$^+$*	this study
N6647	*mat a his-3$^+$::LexAO::nat-1$^+$; Δmus-52::bar$^+$*	this study
N6648	*mat ? his-3$^+$::LexAO::nat-1$^+$; hpo-LexA DBD::hph$^+$; Δmus-52::bar$^+$*	this study
N6649	*mat ? his-3$^+$::LexAO::nat-1; dim-5-LexA DBD::hph$^+$; Δmus-52::bar$^+$*	this study
N6650	*mat ? his-3$^+$::LexAO; Δhda-1::hph$^+$; Δmus-52::bar$^+$?*	this study
N6651	*mat ? his-3$^+$::LexAO; Δhda-1::hph$^+$; dim-5-LexA DBD::hph$^+$; Δmus-52::bar$^+$?*	this study
N6652	*mat ? his-3$^+$::LexAO; dim-2-DAM::hph$^+$; Δmus-52::bar$^+$?*	this study
N6653	*mat ? his-3$^+$::LexAO; Δhda-1::hph$^+$; dim-2-DAM::hph$^+$; Δmus-52::bar$^+$?*	this study
N6654	*mat ? his-3$^+$::LexAO; dim-5-LexA DBD::hph$^+$; dim-2-DAM::hph$^+$; Δmus-52::bar$^+$?*	this study
N6655	*mat ? his-3$^+$::LexAO; dim-5-LexA DBD::hph$^+$; Δhda-1::hph$^+$; dim-2-DAM::hph$^+$; Δmus-52::bar$^+$?*	this study
N6656	*mat ? his-3$^+$::LexAO; dim-2-DAM::hph$^+$; Δmus-52::bar$^+$?*	this study
N6657	*mat ? his-3$^+$::LexAO; Δhda-1::hph$^+$; dim-2-DAM::hph$^+$; Δmus-52::bar$^+$?*	this study
N6658	*mat ? his-3$^+$::LexAO; hpo-LexA DBD::hph$^+$; dim-2-DAM::hph$^+$; Δmus-52::bar$^+$?*	this study
N6659	*mat ? his-3$^+$::LexAO; hpo-LexA DBD::hph$^+$; Δhda-1::hph$^+$; dim-2-DAM::hph$^+$; Δmus-52::bar$^+$?*	this study
N6662	*mat ? his-3$^+$::LexAO cdp-2-LexA DBD::hph$^+$; Δmus-52::bar$^+$?*	this study
N6663	*mat ? his-3$^+$::LexAO; chap-LexA DBD::hph$^+$; Δmus-52::bar$^+$?*	this study
N6691	*mat ? his-3$^+$::LexAO; dim-2-3xFLAG::hph$^+$; hpo-LexA DBD::hph$^+$; Δmus-52::bar$^+$?*	this study
N6692	*mat ? his-3$^+$::LexAO; hda-1-3xFLAG::hph$^+$; hpo-LexA DBD::hph$^+$; Δmus-52::bar$^+$?*	this study
N6865	*mat ? his-3$^+$::LexAO; cul4-LexA DBD::hph$^+$ Δmus-52::bar$^+$*	this study
N6866	*mat ? his-3; Δtrp-2::LexAO::nat-1$^+$; cul4-LexA DBD::hph$^+$ Δmus-52::bar$^+$*	this study
N6867	*mat ? his-3$^+$::LexAO; ddb1-LexA DBD::hph$^+$; Δmus-52::bar$^+$*	this study
N6868	*mat ? his-3 $^+$; Δtrp-2::LexAO::nat-1$^+$; ddb1-LexA DBD::hph Δmus-52::bar$^+$*	this study
N6869	*mat ? his-3$^+$::LexAO; dim-2-DAM::hph$^+$; Δdim-5::hph$^+$; Δmus-52::bar$^+$?*	this study
N6870	*mat ? his-3$^+$::LexAO; dim-2-DAM::hph$^+$; Δdim-5::hph$^+$; hpo-LexA DBD::hph$^+$; Δmus-52::bar$^+$?*	this study
N6871	*mat ? his-3$^+$::LexAO; dim-2-DAM::hph$^+$; hpo-LexA DBD::hph$^+$; Δmus-52::bar$^+$?*	this study
N6921	*mat ? his-3$^+$::LexAO; dim-2-LexA DBD::hph$^+$; Δmus-52::bar$^+$*	this study
N6922	*mat ?; dim-2-LexA DBD::hph$^+$; Δtrp-2::LexAO::nat-1$^+$; Δmus-52::bar$^+$*	this study
N6924	*mat ? his-3$^+$::LexAO; dim-7-LexA DBD::hph$^+$; Δmus-52::bar$^+$*	this study
N6925	*mat ?; dim-7-LexA DBD::hph$^+$; Δtrp-2::LexAO::nat-1$^+$; Δmus-52::bar$^+$*	this study
GT82-25	*mat A his-3; chap$^{ATH1/2(missense)}$::nat-1$^+$; Δmus-52::bar$^+$*	this study
GC330-2	*mat a his-3$^+$::LexAO; chap$^{ATH1/2(missense)}$::nat-1$^+$; hpo-LexA DBD::hph$^+$; Δmus-52::bar$^+$*	this study
GC330-3	*mat a his-3$^+$::LexAO; chap$^{ATH1/2(missense)}$::nat-1$^+$; hpo-LexA DBD::hph$^+$; Δmus-52::bar$^+$*	this study
GC330-6	*mat a his-3$^+$::LexAO; chap$^{ATH1/2(missense)}$::nat-1$^+$; hpo-LexA DBD::hph$^+$; Δmus-52::bar$^+$*	this study
GC342-4	*mat a his-3$^+$::LexAO; chap$^{ATH1/2(missense)}$::nat-1$^+$; hpo-LexA DBD::hph$^+$*	this study

APPENDIX D

PRIMER TABLES

Chapter II

Primer	Sequence
1652	CCGTCGACAGAAGATGATATTGAAGGAGC
1653	AATTAACCCTCACTAAAGGGAACAAAAGC
1654	AGCTGACATCGACACCAACG
1664	ATTCAGACCCCATTAGCCGTCCACGCC
2193	CGCTTAAGAGCGCTGACATAGCGATGATGCTT
2194	GCTCTAGAGCCATTCGTTAGAATCACAATACA
2201	GCGCGTCCTCAACAAACACCC
2286	GTGCGCATCATGGCCAGCCGGAAGAAG
2287	CTTCTTCCGGCTGGCCATGATGCGCAC
3417	GTGCGCATCATGCGCAGCCGGAAGAAG
3418	CTTCTTCCGGCTGCGCATGATGCGCAC
2338	ATAAGAATGCGGCCGCGCCTGATCGCTGATGGGA
2686	CGGAATTCAAGTTCTTGACTCGCGTT
2271	CTCCTTCCTAAGGCCACCGGCAAGACT
2272	AGTCTTGCCGGTGGCCTTAGGAAGGAG
2318	GTAACGCCAGGGTTTTCCCAGTCACGACGGGATCCGCCTGATCGCTGATGGGA
2319	GTGGATGCACGTCTGCCCTGGAGATTGTTGGAGCTCTAAGACTCGGAAGTCGCG
2320	TGGTGGTTGTTGACCGTGATACAAACTCCTAGCTAGCCTGTATAAAGTAACGATA
2321	TGAGCGGATAACAATTTCACACAGGAAACAGCGAATTCGTACCTAGTGGAGTGAAC
1497	GCCGAGCTCCAACAATCTCCAGGGCAGACG
1498	GCCGCTAGCTAGGAGTTTGTATCACGGTCA
2852	GTAACGCCAGGGTTTTCCCAGTCACGACGAAAGGTCAGGGGCGTTGA
2853	ACCGGGATCCACTTAACGTTACTGAAATCTGTTTCTTAGTACTTTTG
2854	GCTCCTTCAATATCATCTTCTGTCGACGGACATCTACCGGTACCGGA
2855	GCGGATAACAATTTCACACAGGAAACAGCGCTTCATTGCTTCATTGC
hph-FP	CCGTCGACAGAAGATGATATTGAAGGAGC
hph-RP	AGCTGACATCGACACCAACG
JGP1	CGATGCGAGATCTATGGCCACGGGCAAAACACCA
JGP3	CGATGCGTCTAGAGAACTTGGGATCGGTGAAGGA
JGP52	CGATGCGACTAGTAACGGCCGCCAGTGTGCTGGA
JGP54	CGATGCGGGGCCCCTAGAACTTGGGATCGGTGAA
JGP158	AGCAAGGCGGCGATAAGGGGT
JGP159	TTCTGTCGACTTCAACTGTCTTTTTGAATCTCTCGTTCG
JGP160	GACAGTTGAAGTCGACAGAAGATGATATTGAAGG
JGP161	TACCGCGGAACTACTCTATTCCTTTGCCCTCGG
JGP162	AATAGAGTAGTTCCGCGGTACTTGCTAGGG
JGP163	GTGGGTCCTAGAAGGGAACTAGCT

Chapter III

Primer	Sequence
Dam vector	
#3058	5'-CCTTAATTAAGGGCGGAGGCGGCGGAGGCGGCGGAGGCATGAAGAAAAA TCGCGCTTT-3'
#3059	5'-GGAATTCATTTTTTCGCGGGTGAAACG-3
his-3 targeting constructs of *hda-1*	
hda-1 promoter	
#2091	5'-AAGGAAAAAAGCGGCCGCCGGTTTGGTGTTGC-3'
#3086	5'-GGACTAGTTCTAGACTTGAAATGGTCCGTCCAGA-3'
hda-1 ORF	
#3062	5'-GGACTAGTATGGTCGACAACGACAATG-3'
#2093	5'-CCTTAATTAACGCGTCCTCCACCATCTCATC-3'
3' his-3 + hda-1 promoter	
#3131	5'-ATCCAATGCGGATGGATTCG-3'
#3126	5'-CATCACGATATCATTGTCGTTGTCGACCATCTTGAAATGGTCCGTCCAGA -3'
Tag + 5' Δ his-3	
#3125	5'-AAACTGGGGGATGAGATGGTGGAGGACGCGTTAATTAAGGGCGGAGGCG G-3'
#3128	5'-CGATTTAGGTGACACTATAG-3'
his-3 targeting vectors	
chap-dam	
#2090	5'-AAGGAAAAAAGCGGCCGCCGCCCAGGAAGATACAAGG-3'
#2092	5'-CCTTAATTAAATCCTGGTACAACCCCCTCC-3'
pan-2 targeting vectors	
chap-3xHA	
#2090	5'-AAGGAAAAAAGCGGCCGCCGCCCAGGAAGATACAAGG-3'
#2497	5'-CCGCTCGAGTCAGCACTGAGCAGCGTAATC-3'
Binding assay	
Peak33-1 (221 bp)	
#3019	5'-CGACGGAACAAATTACTACTATACACAAC-3'
#3020	5'-GGTTTTCGTATAGTAAGTTACCCGCTTC-3'
Peak33-2 (230 bp)	
#2483	5'-TGGTTCCAGCCTCATCATCC-3'
#2484	5'-AGAGTAGGCTCGGAAGTTGG-3'
Yeast two-hybrid assay	
hda-1$^{1-744}$	
#3007	5'-GGAATTCGTCGACAACGACAATGATATC-3'
#3008	5'-CGGGATCCTCACGCGTCCTCCACCATCTC-3'
hda-1$^{1-474}$	
#3007	5'-GGAATTCGTCGACAACGACAATGATATC-3'
#3010	5'-CGGGATCCTAATGTAACCTTTGGCCACCTTG-3'

hda-1$^{422\text{-}744}$

#3009	5’-GGAATTCGGCGAACCACCCCCAAAGATG-3’
#3008	5’-CGGGATCCTCACGCGTCCTCCACCATCTC-3’

hda-1$^{1\text{-}379}$

#3007	5’-GGAATTCGTCGACAACGACAATGATATC-3’
#3134	5’-CCGGGATCCTAAGCTGGCGATACAAAGCAAG-3’

hda-1$^{87\text{-}474}$

#3132	5’-CGGAATTCGACTTTGGTCCAAATCCCCA-3’
#3010	5’-CGGGATCCTAATGTAACCTTTGGCCACCTTG-3’

hda-1$^{183\text{-}474}$

#3067	5’-CGGAATTCTCCCTGTACGTCGGCAGTA-3’
#3010	5’-CGGGATCCTAATGTAACCTTTGGCCACCTTG-3’

hda-1$^{422\text{-}666}$

#3009	5’-GGAATTCGGCGAACCACCCCCAAAGATG-3’
#3135	5’-CCGGGATCCTAATCCGTGTCGACGTCCGATT-3’

hda-1$^{422\text{-}600}$

#3009	5’-GGAATTCGGCGAACCACCCCCAAAGATG-3’
#3084	5’-CCGGGATCCTACTCCTGGATCTGTGCTTGTTG-3’

hda-1$^{478\text{-}744}$

#3133	5’-CGGAATTCCGGAACGCAAGTGAAGCCCG-3’
#3008	5’-CGGGATCCTCACGCGTCCTCCACCATCTC-3’

hda-1$^{550\text{-}744}$

#3083	5’-CGGAATTCGAGGACACGGAGTCATTGGC-3’
#3008	5’-CGGGATCCTCACGCGTCCTCCACCATCTC-3’

cdp-2$^{1\text{-}90}$

#3156	5’-CCCGGATCCATGGCCGGCAAGCCTGTCAGC-3’
#3137	5’-GCCGTCGACTAGTCGAGGACTTCGTCGCATG-3’

cdp-2$^{1\text{-}29}$

#3156	5’-CCCGGATCCATGGCCGGCAAGCCTGTCAGC-3’
#3169	5’-GCCGTCGACTAACCCGAGCCACGGGTGTACT-3’

cdp-2$^{24\text{-}54}$

#3156	5’-CCCGGATCCATGGCCGGCAAGCCTGTCAGC-3’
#3186	5’-GAAGATCTAGTACTTTTTGATGGAAGGGA-3’

chap$^{1\text{-}552}$

#3011	5’-GGAATTCCCCTACGACCCGGACCTCTAC-3’
#3012	5’-CCATCGATCTCGAGTCAATCCTGGTACAACCCCC-3’

chap$^{1\text{-}274}$

#3011	5’-GGAATTCCCCTACGACCCGGACCTCTAC-3’
#3069	5’-CCGGGATCCTCAGAGGAAGCGGATGTACCT-3’

chap$^{253\text{-}552}$

#3070	5’-CGGAATTCAAGAAGCCCCATGAGTTGC-3’

#3012	5’-CCATCGATCTCGAGTCAATCCTGGTACAACCCCC-3’

Mutagenesis

chap$^{ATh1(R210A)}$

#2433	5’-ACAAAGAAACGAGGGGCGCCGTTCGGGTGGAG-3’
#2434	5’-CTCCACCCGAACGGCGCCCCTCGTTTCTTTGT-3’

chap$^{ATh2(R250A)}$

#2435	5’-GTCAAGCGCAGAGGCGCGCCACCCAAGAAGCCC-3’
#2436	5’-GGGCTTCTTGGGTGGCGCGCCTCTGCGCTTGAC-3’

chap$^{Zf1(C280A)}$

#2437	5’-TGCGAATGGGAGGGAGCTCCGGCCGAGCTGCAC-3’
#2438	5’-GTGCAGCTCGGCCGGAGCTCCCTCCCATTCGCA-3’

chap$^{Z2f(C327A)}$

#2439	5’-TTGCAAATGGGCTTCTGCGCACAGCAAGCGTCTC-3’
#2440	5’-GAGACGCTTGCTGTGCGCAGAAGCCCATTTGCAA-3’

hda-1^{D263N}

#3054	5’-TTTGCCGCAAGATACTTATTCTCAATTGGGACGTTCACCATGGCAA-3’
#3055	5’-TTGCCATGGTGAACGTCCCAATTGAGAATAAGTATCTTGCGGCAAA-3’

cdp-2$^{I114A,\ E15A}$

#3187	5’- GCGGCCGTCCCAAGACGACTGCAGCAATACCTCTCCCTTCCATCAA-3’
#3188	5’- TTGATGGAAGGGAGAGGTATTGCTGCAGTCGTCTTGGGACGGCCGC-3’

cdp-2^{W446G}

#3056	5’-TTCACAAGTATCTGGTTCTCGGGGAAGGCAACTGGCCCCCT-3’
#3057	5’-AGGGGGCCAGTTGCCTTCCCCGAGAACCAGATACTTGTGAA-3’

cdp-2$^{\Delta PPITL}$

#3138	5’-GTGGCTCGGGTCCACCGCCGGCGCCGCCTCGAGATTCGAC-3’
#3139	5’-GTCGAATCTCGAGGCGGCGCCGGCGGTGGACCCGAGCCAC-3’

cdp-2$^{\Delta CD(444-459aa)}$

#3171	5’-TCAAGGTTCACAAGTATCTGCCTGAGGACAACATTGATGA-3’
#3172	5’-TCATCAATGTTGTCCTCAGGCAGATACTTGTGAACCTTGA-3’

HP1^{W98G}

#3081	5’- AGCCACTCTTCCTCGTGAAGGGGGAGGGTTACGAGAAAAAG-3’
#3082	5’- CTTTTTCTCGTAACCCTCCCCCTTCACGAGGAAGAGTGGCT-3’

HP1$^{\Delta CD}$ primers

#4525	5’-GCTCTAGAAAAATGCCGTACGATCCATCGGCTCTC-3’
JGP123	5’-GCCGCCTCCGCCGCCTCCGCCGCCTTGCGAGACGCTGCCCTCGCGATC-3’
JGP62	5’-GGCGGCGGAGGCGGCGGAGGCGGC-3’
JGP63	5’-TGATATCGAATTCAGGTTGTCTTCTTAATACGACTCACTATAGGGCGA-3’
JGP60	5’-GAAGACAACCTGAATTCGATATCA-3’
JGP61	5’-CTTGGTACCGAGCTCGGATCC-3’
JGP124	5’-GGATCCGAGCTCGGTACCAAGAAGACCGAGGTAGCACTTCTCGAA-3’
JGP125	5’-AGAGAGCCGCAAGGCTCAGGGACT-3’
#5246	5’-GGCATGTCTAGATGCCGTACGATCCATCGGCTC-3’
#5247	5’-CGAAAATCTTCTCTCGACCGTCCTCCTCCTCCTCGTCACCTTCCTCG-3’
#5248	5’-TGACGAGGAGGAGGAGGACGGTCGAGAGAAGATTTTCGAAGCTTCCG-3’
#5249	5’-GCCTCCGCCTCCGCCGCCTCCGCCC-3’

CDP-2$^{\Delta CD}$ primers

#3064	5’-GCTCTAGAAAAATGCCGTACGATCCATCGGCTCTC-3’
JGP281	5’-CAGGTTGTCTTCCCAACTTGCTCACCTTGGGAATGTCTTCTGGTACTG-3’
JGP282	5’-GAGCTCGGTACCAAGCTTGATGGAGGAAGATGCTCAGGCCTATG-3’
#3145	5’-TAGACATAGTACGCCCGTCG-3’

In-Fusion mutagenesis

cdp-2$^{I14A, E15A}$

SH4442	5’-CGACTGCAGCAATACCTCTCCCTTCCATCA-3’
SH4443	5’-GTATTGCTGCAGTCGTCTTGGGACGGCCGCT-3’

cdp-2$^{\Delta PPITL}$

SH4444	5’-CACCGCCGGCGCCGCCTCGAGATTCGAC-3’
SH4445	5’-GCGGCGCCGGCGGTGGACCCGAGCCAC-3’

cdp-2 replacement (NotI and AfeI sites)

SH4441	5’-ACCGCGGTGGCGGCCGCAAAGGTGTTCCAGTCCAG-3’
SH4447	5’-GCGGGTGCGTCAAGCGCTGG-3’

Chapter IV

Primer	Sequence
his-3 targeting *LexAO*	
#3757	5’- CTATCGATATCTATCGATAGGTACCTCG -3’
#3758	5’- TTCAGCGGATCTCGAGCG -3
#5514	5’- CGATGCGgaattcaagcttgatatctatcgatag -3’
#5515	5’- acttcgaatagggcgaattgg -3
his-3 targeting *LexAO::nat-1* reporter	
#6240	5’- tgctatacgaagttattccaactgatattgaaggagcatttttgg -3’
#6239	5’- ttggtaccgagctctcaggggcagggcatgctca -3
#5532	5’- CTTCTGCTTATGGACAAGCAACTG -3’
#5533	5’- tcgaattcaggttgtcttcccaacGATCGAAACGTGGATGTCACAATG -3
#5534	5’- gagctcggtaccaagcttgatTGTGCTTCCCCCGTTCATGTA -3
#5535	5’- GCTTTGGCAAGCAGTACTCTG -3
trp-2 targeting *LexAO::nat-1*	
#4878	5’- gatcgaccgcggCTAAACTGTATAGTGTCCGG -3’
#5541	5’- ctatcgatagatatcaagcttGAATTCCTGAACAACTGAACTGTAACG -3’
#5542	5’- gagctcggtaccaagcttgatGACTGGCTAAAGCGAACCGGCC -3’
#4865	5’- gatcgagatatcGGTCTGGATCTCGGAGGCG -3’
LexADBD tagging at native loci	
hph + LexADBD	
#3755	5’- AGGCGCGCCTCCAAAAAAGAAGAGAAAGG -3’
#3756	5’- GCTCTAGATTAGGGTTCACCGGCAGCCA -3’
#5506	5’- gaagacaacctgaattcgatatca -3’
#5507	5’- cttggtaccgagctcggatcc -3’
#5508	5’- ggcggcggaggcggcggaggcggc -3’
#5509	5’- tgatatcgaattcaggttgtcttcttaatacgactcactatagggcga -3’
DIM-5	
#5516	5’- ACAAAAGTCGAGGCCAGCTTGAAT -3’
#5517	5’- gccgcctccgccgcctccgccgccCCACAGATAGCCTCTGCACTTGGC -3’
#5518	5’- ggatccgagctcggtaccaagTGGGGGAAGATGTTAACTCACAAA -3’
#5519	5’- GGGGGGAAGCTCTGTCGTTACCTA -3’
HP1	
#5520	5’- TCACACCAGCTCATAAAAATGCCG -3’
#5521	5’- gccgcctccgccgcctccgccgccTTGCGAGACGCTGCCCTCGCGATC -3’
#5522	5’- ggatccgagctcggtaccaagAAGACCGAGGTAGCACTTCTCGAA -3’
#5523	5’- AGAGAGCCGCAAGGCTCAGGGACT -3’
DIM-2	
#5510	5’- GGCCTGGAACAACGGGAACGGGGT -3’
#5511	5’- gccgcctccgccgcctccgccgccCAACTTGACAATCGTCATGCCGTT -3’
#5512	5’- ggatccgagctcggtaccaagTGCGACGAGGTAACGCCATGTCCG -3’
#5513	5’- ATAAATCCGTGATGCATCCGTTGC -3’
DIM-7	
#5524	5’- GGCTCATCGTTCTGTTGGGAGAAG -3’
#5525	5’- gccgcctccgccgcctccgccgccAATCAACAACCGACGTTTGATCGG -3’
#5526	5’- ggatccgagctcggtaccaagGTCGACAAAATAAATGGCCTTCCT -3’
#5527	5’- GGAACACTTCCCGAGATGATCCAC -3’

DIM-9

#5528 5’- TGTCATGCCCATCAGCTTCGGTTC -3’

#5529 5’- gccgcctccgccgcctccgccgccGAATTCATCAATGTCGCTTCCATT -3’

#5530 5’- ggatccgagctcggtaccaagTTATTTTAAGAGTTCTATGTAATCAGCGATCA -3’

#5531 5’- CGGGGACATGGTTGCCCTCTCTGT -3’

DDB1

#4757 5’- ACGTCTCTGGTCGAGTACGTCCCGGC -3’

#5686 5’- gccgcctccgccgcctccgccgccGTGCATCCTCCGTAGCTCCT -3’

#5687 5’- ggatccgagctcggtaccaagCCAACGGTTAGACACTTAACGTGC -3’

#5678 5’- TAGTTCTTGGGTGTTCGTGGGTG -3’

CUL4

#5675 5’- CATGGGTCGCAGTGCTAGCCG -3’

#5684 5’- gccgcctccgccgcctccgccgccCGCAAGATAGACATAATTCCCACCCT -3’

#5685 5’- ggatccgagctcggtaccaagATGTTGAGCTTGTGGGTAGGTAGG -3’

#5676 5’- TGAAGGGGGTTAAGAATAGGT -3’

HDA-1

#3007 5’- GGAATTCGTCGACAACGACAATGATATC -3’

#5536 5’- gccgcctccgccgcctccgccgccCGCGTCCTCCACCATCTCATC -3’

#5537 5’- ggatccgagctcggtaccaagAAGACGGGCCTTGGTCCC -3’

#5679 5’- CGGTGGTGGTGATGCTTGAAG -3’

CDP-2

#3064 5’- CCCGGATCCGAGATCCCCAGGTTTGAT -3’

#5551 5’- gccgcctccgccgcctccgccgccCCTTGGGAATGTCTTCTGGTACTG -3’

#5552 5’- ggatccgagctcggtaccaagGAGGAAGATGCTCAGGCCTATG -3’

#3145 5’- TAGACATAGTACGCCCGTCG -3’

CHAP

#3070 5’- CGGAATTCAAGAAGCCCCATGAGTTGC -3’

#5553 5’- gccgcctccgccgcctccgccgccATCCTGGTACAACCCCCTCC -3’

#5554 5’- ggatccgagctcggtaccaagGTTTAAGCGGGAGGGCGAAG -3’

#5540 5’- TATCCAGCGCTACCAAGCGTC -3’

CHAP AT-Hook Mutagenesis

#3063 5’- GGACTAGTATGCCCTACGACCCGGACC -3’

#5538 5’- caggttgtcttcccaacttgcTCAATCCTGGTACAACCCCCTCC -3’

#5539 5’- gagctcggtaccaagcttgatgGTTTAAGCGGGAGGGCGAAG -3’

#5540 5’- TATCCAGCGCTACCAAGCGTC -3’

#5680 5’- GCTTTCGTTGACGTGGGCT -3’

#5681 5’- CACAAGAGCCCAAGACTTGC -3’

#5656 5’- GCGTCGTTCTGGGCTCATatcgatgcttgggtagaataggta -3’

#5682 5’- ggttgtcttcccaacttgcccTCAATCCTGGTACAACCCCCTCC -3’

#5683 5’- GCCCGTCACCGAGATCTGATgttgggaagacaacctgaattcga -3’

#1658 5’- AGAAACCCACGTCATGCCAGT -3’

#1659 5’- ATCGTCAACCACTACATCGAG -3’

Generation of *hda-1*^{D263N}*-3XFLAG* and *dim-2*^{C926A}*-3XFLAG*

#3007 5’- GGAATTCGTCGACAACGACAATGATATC -3’

#2077 5’- CCTCCGCCTCCGCCTCCGCCGCCTCCGCCCGCGTCCTCCACCATCTCATC -3’

#2078 5’- TGCTATACGAAGTTATGGATCCGAGCTCGAAACAAGACGGGCCTTGGTC -3’

#2079 5’- ACCGCGGTGGCGGCCGCTCTAGAACTAGTGGTTCCGGCAAGGATAGAGG -3’
#4447 5’- gatcgaGGATCCccGGGAGCGTGAAGCCTAAAGC -3’
#2013 5’- CCTCCGCCTCCGCCTCCGCCGCCTCCGCCCAACTTGACAATCGTCATGC -3’
#1989 5’- TGCTATACGAAGTTATGGATCCGAGCTCGTGCGACGAGGTAACGCCATG -3’
#1990 5’- ACCGCGGTGGCGGCCGCTCTAGAACTAGTACAAGACCGGCAACCATCTG -3’

dim-5 expression from the *trp-2* locus
#4878 5’- gatcgaccgcggCTAAACTGTATAGTGTCCGG -3’
#5555 5’- catacagccttaccagcccactgCTGAACAACTGAACTGTAACG -3’
#5677 5’- CAGTGGGCTGGTAAGGCTGTATG -3’
#1993 5’- CCTCCGCCTCCGCCTCCGCCGCCTCCGCCCCACAGATAGCCTCTGCACTTG -3’
#4883 5’- aaccccatccgccggtacgcg -3’
#4884 5’- tccttcaccaccgacaccgtcttcc -3’
#5542 5’- gagctcggtaccaagcttgatGACTGGCTAAAGCGAACCGGCC -3’
#4865 5’- gatcgagatatcGGTCTGGATCTCGGAGGCG -3’

ChIP
Peak 33
#3019 5’- CGACGGAACAAATTACTACTATACACAAC -3’
#3020 5’- GGTTTTCGTATAGTAAGTTACCCGCTTC -3’

LexA #2
#4776 5’- AACAGCTGAGGGAGCCAATG -3’
#4777 5’- GTTTCAGGGGTTTCGTTCGC -3’

Actin
#3209 5’- AATGGGTCGGGTATGTGCAA -3’
#3210 5’- CTTCTGGCCCATACCGATCAT -3’

Southern blot
LexAO*
#5514 5’- CGATGCGgaattcaagcttgatatctatcgatag -3’
#5515 5’- acttcgaatagggcgaattgg -3’
*Note: Amplified product was digested with AvaI prior to probe synthesis.

8:A6
#1877 5’- TGGTTGGTCGATTGTGGTGG -3’
#1878 5’- TTTTGAGGATCCGCCATCCG -3’

8:G3
#1864 5’- AAACGCGTTACGGCTCTTGC -3’
#1869 5’- GTCCGGGTAACTTGATGTGG -3’

8:F10
#1900 5’- TATCTCTTAAGCGGCGGTCG -3’
#1901 5’- GACCGGTATTAGCTACTCTCTATAG -3’

nat-1
#6270 5’- atggccaccctcgacgacacg -3’
#6269 5’- tcaggggcagggcatgctcatg -3’

pan-1	
#3181	5’- CGATAAGCTTGATATCGAATTCAGGTTGTCCGGCCATCTCAGTCTGATCC -3’
#3182	5’- TCGCATACGCCAACCCATGC -3’
CenVIIM	
#2543	5’- TTGGATTCCCTATAGAAGAGAGG -3’
#2544	5’- AATAGCCCTAGAGGCTAGCC -3’

REFERENCES CITED

Aagaard, L., Laible, G., Selenko, P., Schmid, M., Dorn, R., Schotta, G., et al. (1999). Functional mammalian homologues of the Drosophila PEV-modifier Su(var)3-9 encode centromere-associated proteins which complex with the heterochromatin component M31. *Embo*, *18*(7), 1923–1938. http://doi.org/10.1093/emboj/18.7.1923

Adhvaryu, K. K., & Selker, E. U. (2008). Protein phosphatase PP1 is required for normal DNA methylation in Neurospora. *Genes & Development*, *22*(24), 3391–3396. http://doi.org/10.1101/gad.1738008

Adhvaryu, K. K., Berge, E., Tamaru, H., Freitag, M., & Selker, E. U. (2011). Substitutions in the amino-terminal tail of Neurospora histone H3 have varied effects on DNA methylation. *PLoS Genetics*, *7*(12), e1002423. http://doi.org/10.1371/journal.pgen.1002423

Adhvaryu, K. K., Gessaman, J. D., Honda, S., Lewis, Z. A., Grisafi, P. L., & Selker, E. U. (2014). The Cullin-4 complex DCDC does not require E3 ubiquitin ligase elements to control heterochromatin in Neurospora. *Eukaryotic Cell*, EC.00212–14. http://doi.org/10.1128/EC.00212-14

Afgan, E., Baker, D., van den Beek, M., Blankenberg, D., Bouvier, D., Čech, M., et al. (2016). The Galaxy platform for accessible, reproducible and collaborative biomedical analyses: 2016 update. *Nucleic Acids Research*, *44*(W1), W3–W10. http://doi.org/10.1093/nar/gkw343

Anderson, D. C., Green, G. R., Smith, K., & Selker, E. U. (2010). Extensive and varied modifications in histone H2B of wild-type and histone deacetylase 1 mutant *Neurospora crassa. Biochemistry*, *49*(25), 5244–5257. http://doi.org/10.1021/bi100391w

Aravind, L., & Landsman, D. (1998). AT-hook motifs identified in a wide variety of DNA-binding proteins. *Nucleic Acids Research*, *26*(19), 4413–4421.

Avalos, J., Geever, R. F., & Case, M. E. (1989). Bialaphos resistance as a dominant selectable marker in *Neurospora crassa*. *Current Genetics*, *16*(5-6), 369–372.

Bennett, E. J., Rush, J., Gygi, S. P., & Harper, J. W. (2010). Dynamics of cullin-RING ubiquitin ligase network revealed by systematic quantitative proteomics. *Cell*, *143*(6), 951–965. http://doi.org/10.1016/j.cell.2010.11.017

Bjerling, P., Silverstein, R. A., Thon, G., Caudy, A., Grewal, S., & Ekwall, K. (2002). Functional divergence between histone deacetylases in fission yeast by distinct cellular localization and in vivo specificity. *Molecular and Cellular Biology*, *22*(7), 2170–2181. http://doi.org/10.1128/MCB.22.7.2170-2181.2002

Blankenberg, D., Gordon, A., Kuster, Von, G., Coraor, N., Taylor, J., Nekrutenko, A., Galaxy Team. (2010). Manipulation of FASTQ data with Galaxy. *Bioinformatics*,

26(14), 1783–1785. http://doi.org/10.1093/bioinformatics/btq281

Boh, B. K., Smith, P. G., & Hagen, T. (2011). Neddylation-induced conformational control regulates cullin RING ligase activity in vivo. *Journal of Molecular Biology*, *409*(2), 136–145. http://doi.org/10.1016/j.jmb.2011.03.023

Bonasio, R., Tu, S., & Reinberg, D. (2010). Molecular signals of epigenetic states. *Science*, *330*(6004), 612–616. http://doi.org/10.1126/science.1191078

Braun, S., Garcia, J. F., Rowley, M., Rougemaille, M., Shankar, S., & Madhani, H. D. (2011). The Cul4-Ddb1(Cdt)² ubiquitin ligase inhibits invasion of a boundary-associated antisilencing factor into heterochromatin. *Cell*, *144*(1), 41–54. http://doi.org/10.1016/j.cell.2010.11.051

Bühler, M., & Gasser, S. M. (2009). Silent chromatin at the middle and ends: lessons from yeasts. *Embo*, *28*(15), 2149–2161. http://doi.org/10.1038/emboj.2009.185

Callebaut, I., Courvalin, J. C., & Mornon, J. P. (1999). The BAH (bromo-adjacent homology) domain: a link between DNA methylation, replication and transcriptional regulation. *FEBS Letters*, *446*(1), 189–193.

Cambareri, E. B., Jensen, B. C., Schabtach, E., & Selker, E. U. (1989). Repeat-induced G-C to A-T mutations in Neurospora. *Science*, *244*(4912), 1571–1575.

Cedar, H., & Bergman, Y. (2009). Linking DNA methylation and histone modification: patterns and paradigms. *Nature Reviews. Genetics*, *10*(5), 295–304. http://doi.org/10.1038/nrg2540

Chan, S. W.-L., Henderson, I. R., & Jacobsen, S. E. (2005). Gardening the genome: DNA methylation in Arabidopsis thaliana. *Nature Reviews. Genetics*, *6*(5), 351–360. http://doi.org/10.1038/nrg1601

Chin, H. G., Patnaik, D., Estève, P.-O., Jacobsen, S. E., & Pradhan, S. (2006). Catalytic properties and kinetic mechanism of human recombinant Lys-9 histone H3 methyltransferase SUV39H1: participation of the chromodomain in enzymatic catalysis. *Biochemistry*, *45*(10), 3272–3284. http://doi.org/10.1021/bi051997r

Choo, Y. Y., Boh, B. K., Lou, J. J. W., Eng, J., Leck, Y. C., Anders, B., et al. (2011). Characterization of the role of COP9 signalosome in regulating cullin E3 ubiquitin ligase activity. *Molecular Biology of the Cell*, *22*(24), 4706–4715. http://doi.org/10.1091/mbc.E11-03-0251

Davis, R. H. (2000a). *Neurospora: Contributions of a Model Organism*. Oxford, UK: Oxford Univ Press.

Davis, R. H. (2000b). *Neurospora: Contributions of a Model Organism*. Oxford University Press.

Dodge, J. E., Kang, Y.-K., Beppu, H., Lei, H., & Li, E. (2004). Histone H3-K9 methyltransferase ESET is essential for early development. *Molecular and Cellular Biology*, *24*(6), 2478–2486. http://doi.org/10.1128/MCB.24.6.2478-2486.2004

Du, J., Johnson, L. M., Jacobsen, S. E., & Patel, D. J. (2015). DNA methylation pathways and their crosstalk with histone methylation. *Nature Reviews Molecular Cell Biology*, *16*(9), 519–532. http://doi.org/10.1038/nrm4043

Duda, D. M., Borg, L. A., Scott, D. C., Hunt, H. W., Hammel, M., & Schulman, B. A. (2008). Structural Insights into NEDD8 Activation of Cullin-RING Ligases: Conformational Control of Conjugation. *Cell*, *134*(6), 995–1006. http://doi.org/10.1016/j.cell.2008.07.022

Ebbole, D. J., & Sachs, M. S. (1990). A rapid and simple method for isolation of *Neurospora crassa* homokaryons using microconidia. *Fungal Genet Newsl*, (37).

Ekwall, K. (2005). Genome-wide analysis of HDAC function. *Trends in Genetics : TIG*, *21*(11), 608–615. http://doi.org/10.1016/j.tig.2005.08.009

Elgin, S. C. R., & Reuter, G. (2013). Position-effect variegation, heterochromatin formation, and gene silencing in Drosophila. *Cold Spring Harbor Perspectives in Biology*, *5*(8), a017780–a017780. http://doi.org/10.1101/cshperspect.a017780

Feinberg, A. P. (2007). Phenotypic plasticity and the epigenetics of human disease. *Nature*, *447*(7143), 433–440. http://doi.org/10.1038/nature05919

Fischle, W., Tseng, B. S., Dormann, H. L., Ueberheide, B. M., Garcia, B. A., Shabanowitz, J., et al. (2005). Regulation of HP1-chromatin binding by histone H3 methylation and phosphorylation. *Nature*, *438*(7071), 1116–1122. http://doi.org/10.1038/nature04219

Freitag, M., Hickey, P. C., Khlafallah, T. K., Read, N. D., & Selker, E. U. (2004a). HP1 is essential for DNA methylation in Neurospora. *Molecular Cell*, *13*(3), 427–434.

Freitag, M., Lee, D. W., Kothe, G. O., Pratt, R. J., Aramayo, R., & Selker, E. U. (2004b). DNA methylation is independent of RNA interference in Neurospora. *Science*, *304*(5679), 1939–1939. http://doi.org/10.1126/science.1099709

Galagan, J. E., Calvo, S. E., Borkovich, K. A., Selker, E. U., Read, N. D., Jaffe, D., et al. (2003). The genome sequence of the filamentous fungus *Neurospora crassa*. *Nature*, *422*(6934), 859–868. http://doi.org/10.1038/nature01554

Galazka, J. M., Klocko, A. D., Uesake, M., Honda, S., Selker, E. U., & Freitag, M. (2016). Neurospora chromosomes are organized by blocs of importin alpha-dependent heterochromatin that are largely independent of H3K9me3. *Genome Research*, gr.203182.115. http://doi.org/10.1101/gr.203182.115

Glozak, M. A., Sengupta, N., Zhang, X., & Seto, E. (2005). Acetylation and deacetylation

of non-histone proteins. *Gene*, *363*, 15–23. http://doi.org/10.1016/j.gene.2005.09.010

Goldstein, A. L., & McCusker, J. H. (1999). Three new dominant drug resistance cassettes for gene disruption in *Saccharomyces cerevisiae*. *Yeast (Chichester, England)*, *15*(14), 1541–1553. http://doi.org/10.1002/(SICI)1097-0061(199910)15:14<1541::AID-YEA476>3.0.CO;2-K

Grewal, S. I. S., & Jia, S. (2007). Heterochromatin revisited. *Nature Reviews. Genetics*, *8*(1), 35–46. http://doi.org/10.1038/nrg2008

Guerrero-Santoro, J., Kapetanaki, M. G., Hsieh, C. L., Gorbachinsky, I., Levine, A. S., & Rapić-Otrin, V. (2008). The cullin 4B-based UV-damaged DNA-binding protein ligase binds to UV-damaged chromatin and ubiquitinates histone H2A. *Cancer Research*, *68*(13), 5014–5022. http://doi.org/10.1158/0008-5472.CAN-07-6162

Haldar, S., Saini, A., Nanda, J. S., Saini, S., & Singh, J. (2011). Role of Swi6/HP1 self-association-mediated recruitment of Clr4/Suv39 in establishment and maintenance of heterochromatin in fission yeast. *The Journal of Biological Chemistry*, *286*(11), 9308–9320. http://doi.org/10.1074/jbc.M110.143198

Hathaway, N. A., Bell, O., Hodges, C., Miller, E. L., Neel, D. S., & Crabtree, G. R. (2012). Dynamics and Memory of Heterochromatin in Living Cells. *Cell*, *149*(7), 1447–1460. http://doi.org/10.1016/j.cell.2012.03.052

Hays, S. M., Swanson, J., & Selker, E. U. (2002). Identification and characterization of the genes encoding the core histones and histone variants of *Neurospora crassa*. *Genetics*, *160*(3), 961–973.

He, Qun, Cheng, P., He, Q., & Liu, Y. (2005). The COP9 signalosome regulates the Neurospora circadian clock by controlling the stability of the SCFFWD-1 complex. *Genes & Development*, *19*(13), 1518–1531. http://doi.org/10.1101/gad.1322205

Heard, E., & Disteche, C. M. (2006). Dosage compensation in mammals: fine-tuning the expression of the X chromosome. *Genes & Development*, *20*(14), 1848–1867. http://doi.org/10.1101/gad.1422906

Heckman, K. L., & Pease, L. R. (2007). Gene splicing and mutagenesis by PCR-driven overlap extension. *Nature Protocols*, *2*(4), 924–932. http://doi.org/10.1038/nprot.2007.132

Heitz, E. (1928). Das heterochromatin der moose. *I Jahrb Wiss Botanik*, (69), 762–818.

Henikoff, S. (2000). Heterochromatin function in complex genomes. *Biochimica Et Biophysica Acta*, *1470*(1), O1–8.

Hershko, A., & Ciechanover, A. (1998). The ubiquitin system. *Annual Review of Biochemistry*, *67*(1), 425–479. http://doi.org/10.1146/annurev.biochem.67.1.425

Higa, L. A., Wu, M., Ye, T., Kobayashi, R., Sun, H., & Zhang, H. (2006). CUL4–DDB1 ubiquitin ligase interacts with multiple WD40-repeat proteins and regulates histone methylation. *Nature Cell Biology*, *8*(11), 1277–1283. http://doi.org/10.1038/ncb1490

Hines, K. A., Cryderman, D. E., Flannery, K. M., Yang, H., Vitalini, M. W., Hazelrigg, T., et al. (2009). Domains of heterochromatin protein 1 required for *Drosophila melanogaster* heterochromatin spreading. *Genetics*, *182*(4), 967–977. http://doi.org/10.1534/genetics.109.105338

Hohl, M., Wagner, M., Reil, J.-C., Müller, S.-A., Tauchnitz, M., Zimmer, A. M., et al. (2013). HDAC4 controls histone methylation in response to elevated cardiac load. *The Journal of Clinical Investigation*, *123*(3), 1359–1370. http://doi.org/10.1172/JCI61084

Holliday, R., & Pugh, J. E. (1975). DNA modification mechanisms and gene activity during development. *Science*, *187*(4173), 226–232.

Honda, S., & Selker, E. U. (2008). Direct interaction between DNA methyltransferase DIM-2 and HP1 is required for DNA methylation in *Neurospora crassa*. *Molecular and Cellular Biology*, *28*(19), 6044–6055. http://doi.org/10.1128/MCB.00823-08

Honda, S., & Selker, E. U. (2009). Tools for fungal proteomics: multifunctional Neurospora vectors for gene replacement, protein expression and protein purification. *Genetics*, *182*(1), 11–23. http://doi.org/10.1534/genetics.108.098707

Honda, S., Bicocca, V. T., Gessaman, J. D., Rountree, M. R., Yokoyama, A., Yu, E. Y., et al. (2016). Dual chromatin recognition by the histone deacetylase complex HCHC is required for proper DNA methylation in *Neurospora crassa*. *Proceedings of the National Academy of Sciences*, *113*(41), E6135–E6144. http://doi.org/10.1073/pnas.1614279113

Honda, S., Lewis, Z. A., Huarte, M., Cho, L. Y., David, L. L., Shi, Y., & Selker, E. U. (2010). The DMM complex prevents spreading of DNA methylation from transposons to nearby genes in *Neurospora crassa*. *Genes & Development*, *24*(5), 443–454. http://doi.org/10.1101/gad.1893210

Honda, S., Lewis, Z. A., Shimada, K., Fischle, W., Sack, R., & Selker, E. U. (2012). Heterochromatin protein 1 forms distinct complexes to direct histone deacetylation and DNA methylation. *Nature Structural & Molecular Biology*, *19*(5), 471–7– S1. http://doi.org/10.1038/nsmb.2274

Hong, E.-J. E., Villén, J., Gerace, E. L., Gygi, S. P., & Moazed, D. (2005). A cullin E3 ubiquitin ligase complex associates with Rik1 and the Clr4 histone H3-K9 methyltransferase and is required for RNAi-mediated heterochromatin formation. *RNA Biology*, *2*(3), 106–111.

Horn, P. J., Bastie, J.-N., & Peterson, C. L. (2005). A Rik1-associated, cullin-dependent E3 ubiquitin ligase is essential for heterochromatin formation. *Genes &*

Development, *19*(14), 1705–1714. http://doi.org/10.1101/gad.1328005

Hoshino, A., & Fujii, H. (2009). Insertional chromatin immunoprecipitation: a method for isolating specific genomic regions. *Journal of Bioscience and Bioengineering*, *108*(5), 446–449. http://doi.org/10.1016/j.jbiosc.2009.05.005

Hotton, S. K., & Callis, J. (2008). Regulation of cullin RING ligases. *Annual Review of Plant Biology*, *59*(1), 467–489. http://doi.org/10.1146/annurev.arplant.58.032806.104011

Inoue, H. (2011). Exploring the processes of DNA repair and homologous integration in Neurospora. *Mutation Research*, *728*(1-2), 1–11. http://doi.org/10.1016/j.mrrev.2011.06.003

Jackson, S., & Xiong, Y. (2009). CRL4s: the CUL4-RING E3 ubiquitin ligases. *Trends in Biochemical Sciences*, *34*(11), 562–570. http://doi.org/10.1016/j.tibs.2009.07.002

James, P., Halladay, J., & Craig, E. A. (1996). Genomic libraries and a host strain designed for highly efficient two-hybrid selection in yeast. *Genetics*, *144*(4), 1425–1436.

Jamieson, K., Rountree, M. R., Lewis, Z. A., Stajich, J. E., & Selker, E. U. (2013). Regional control of histone H3 lysine 27 methylation in Neurospora. *Proceedings of the National Academy of Sciences*, *110*(15), 6027–6032. http://doi.org/10.1073/pnas.1303750110

Jamieson, K., Wiles, E. T., McNaught, K. J., Sidoli, S., Leggett, N., Shao, Y., et al. (2015). Loss of HP1 causes depletion of H3K27me3 from facultative heterochromatin and gain of H3K27me2 at constitutive heterochromatin. *Genome Research*, gr.194555.115. http://doi.org/10.1101/gr.194555.115

Jeltsch, A., & Jurkowska, R. Z. (2016). Allosteric control of mammalian DNA methyltransferases - a new regulatory paradigm. *Nucleic Acids Research*, gkw723. http://doi.org/10.1093/nar/gkw723

Jia, S., Kobayashi, R., & Grewal, S. I. S. (2005). Ubiquitin ligase component Cul4 associates with Clr4 histone methyltransferase to assemble heterochromatin. *Nature Cell Biology*, *7*(10), 1007–1013. http://doi.org/10.1038/ncb1300

Jolma, A., Kivioja, T., Toivonen, J., Cheng, L., Wei, G., Enge, M., et al. (2010). Multiplexed massively parallel SELEX for characterization of human transcription factor binding specificities. *Genome Research*, *20*(6), 861–873. http://doi.org/10.1101/gr.100552.109

Kagansky, A., Folco, H. D., Almeida, R., Pidoux, A. L., Boukaba, A., Simmer, F., et al. (2009). Synthetic heterochromatin bypasses RNAi and centromeric repeats to establish functional centromeres. *Science*, *324*(5935), 1716–1719. http://doi.org/10.1126/science.1172026

Kapetanaki, M. G., Guerrero-Santoro, J., Bisi, D. C., Hsieh, C. L., Rapić-Otrin, V., & Levine, A. S. (2006). The DDB1-CUL4ADDB2 ubiquitin ligase is deficient in xeroderma pigmentosum group E and targets histone H2A at UV-damaged DNA sites. *Proceedings of the National Academy of Sciences of the United States of America*, *103*(8), 2588–2593. http://doi.org/10.1073/pnas.0511160103

Kawabata, T., Kato, A., Suzuki, K., & Inoue, H. (2007). Neurosprora crassa RAD5 homologue, mus-41, inactivation results in higher sensitivity to mutagens but has little effect on PCNA-ubiquitylation in response to UV-irradiation. *Current Genetics*, *52*(3-4), 125–135. http://doi.org/10.1007/s00294-007-0146-x

Keller, C., Adaixo, R., Stunnenberg, R., Woolcock, K. J., Hiller, S., & Bühler, M. (2012). HP1(Swi6) mediates the recognition and destruction of heterochromatic RNA transcripts. *Molecular Cell*, *47*(2), 215–227. http://doi.org/10.1016/j.molcel.2012.05.009

Klocko, A. D., Rountree, M. R., Grisafi, P. L., Hays, S. M., Adhvaryu, K. K., & Selker, E. U. (2015). Neurospora Importin α Is Required for Normal Heterochromatic Formation and DNA Methylation. *PLoS Genetics*, *11*(3), e1005083. http://doi.org/10.1371/journal.pgen.1005083

Komander, D., & Rape, M. (2012). The ubiquitin code. *Annual Review of Biochemistry*, *81*(1), 203–229. http://doi.org/10.1146/annurev-biochem-060310-170328

Kouzminova, E., & Selker, E. U. (2001). *dim-2* encodes a DNA methyltransferase responsible for all known cytosine methylation in Neurospora. *Embo*, *20*(15), 4309–4323. http://doi.org/10.1093/emboj/20.15.4309

Kuscu, C., Zaratiegui, M., Kim, H. S., Wah, D. A., Martienssen, R. A., Schalch, T., & Joshua-Tor, L. (2014). CRL4-like Clr4 complex in *Schizosaccharomyces pombe* depends on an exposed surface of Dos1 for heterochromatin silencing. *Proceedings of the National Academy of Sciences*, *111*(5), 1795–1800. http://doi.org/10.1073/pnas.1313096111

Langmead, B., & Salzberg, S. L. (2012). Fast gapped-read alignment with Bowtie 2. *Nature Methods*, *9*(4), 357–359. http://doi.org/10.1038/nmeth.1923

Lee, J., & Zhou, P. (2007). DCAFs, the missing link of the CUL4-DDB1 ubiquitin ligase. *Molecular Cell*, *26*(6), 775–780. http://doi.org/10.1016/j.molcel.2007.06.001

Lewis, Z. A., Adhvaryu, K. K., Honda, S., Shiver, A. L., & Selker, E. U. (2010a). Identification of DIM-7, a protein required to target the DIM-5 H3 methyltransferase to chromatin. *Proceedings of the National Academy of Sciences*, *107*(18), 8310–8315. http://doi.org/10.1073/pnas.1000328107

Lewis, Z. A., Adhvaryu, K. K., Honda, S., Shiver, A. L., Knip, M., Sack, R., & Selker, E. U. (2010b). DNA methylation and normal chromosome behavior in Neurospora depend on five components of a histone methyltransferase complex, DCDC. *PLoS*

Genetics, *6*(11), e1001196. http://doi.org/10.1371/journal.pgen.1001196

Lewis, Z. A., Honda, S., Khlafallah, T. K., Jeffress, J. K., Freitag, M., Mohn, F., et al. (2009). Relics of repeat-induced point mutation direct heterochromatin formation in *Neurospora crassa*. *Genome Research*, *19*(3), 427–437. http://doi.org/10.1101/gr.086231.108

Li, Y., Danzer, J. R., Alvarez, P., Belmont, A. S., & Wallrath, L. L. (2003). Effects of tethering HP1 to euchromatic regions of the Drosophila genome. *Development*, *130*(9), 1817–1824.

Lichius, A., & Read, N. D. (2010). A versatile set of Lifeact-RFP expression plasmids for live-cell imaging of F-actin in filamentous fungi. *Fungal Genetics Reports*, *57*, 8–14.

Liu, J., & Nussinov, R. (2011). Flexible cullins in cullin-RING E3 ligases allosterically regulate ubiquitination. *The Journal of Biological Chemistry*, *286*(47), 40934–40942. http://doi.org/10.1074/jbc.M111.277236

Margolin, B. S., Freitag, M., & Selker, E. U. (1997). Improved plasmids for gene targeting at the his-3 locus of *Neurospora crassa* by electroporation. *Fungal Genet Newsl*, (44), 34–36.

Matsui, T., Leung, D., Miyashita, H., Maksakova, I. A., Miyachi, H., Kimura, H., et al. (2010). Proviral silencing in embryonic stem cells requires the histone methyltransferase ESET. *Nature*, *464*(7290), 927–931. http://doi.org/10.1038/nature08858

Melcher, M., Schmid, M., Aagaard, L., Selenko, P., Laible, G., & Jenuwein, T. (2000). Structure-function analysis of SUV39H1 reveals a dominant role in heterochromatin organization, chromosome segregation, and mitotic progression. *Molecular and Cellular Biology*, *20*(10), 3728–3741.

Merlet, J., Burger, J., Gomes, J.-E., & Pintard, L. (2009). Regulation of cullin-RING E3 ubiquitin-ligases by neddylation and dimerization. *Cellular and Molecular Life Sciences : CMLS*, *66*(11-12), 1924–1938. http://doi.org/10.1007/s00018-009-8712-7

Miao, V. P., Freitag, M., & Selker, E. U. (2000). Short TpA-rich segments of the zeta-eta region induce DNA methylation in *Neurospora crassa*. *Journal of Molecular Biology*, *300*(2), 249–273. http://doi.org/10.1006/jmbi.2000.3864

Motamedi, M. R., Hong, E.-J. E., Li, X., Gerber, S., Denison, C., Gygi, S., & Moazed, D. (2008). HP1 proteins form distinct complexes and mediate heterochromatic gene silencing by nonoverlapping mechanisms. *Molecular Cell*, *32*(6), 778–790. http://doi.org/10.1016/j.molcel.2008.10.026

Muchardt, C., Guilleme, M., Seeler, J.-S., Trouche, D., Dejean, A., & Yaniv, M. (2002). Coordinated methyl and RNA binding is required for heterochromatin localization of mammalian HP1alpha. *EMBO Reports*, *3*(10), 975–981. http://doi.org/10.1093/embo-

reports/kvf194

Nakayama, J., Rice, J. C., Strahl, B. D., Allis, C. D., & Grewal, S. I. (2001). Role of histone H3 lysine 9 methylation in epigenetic control of heterochromatin assembly. *Science*, *292*(5514), 110–113. http://doi.org/10.1126/science.1060118

Nielsen, P. R., Nietlispach, D., Mott, H. R., Callaghan, J., Bannister, A., Kouzarides, T., et al. (2002). Structure of the HP1 chromodomain bound to histone H3 methylated at lysine 9. *Nature*, *416*(6876), 103–107. http://doi.org/10.1038/nature722

Oakley, C. E., Weil, C. F., Kretz, P. L., & Oakley, B. R. (1987). Cloning of the riboB locus of Aspergillus nidulans. *Gene*, *53*(2-3), 293–298.

Okano, M., Bell, D. W., Haber, D. A., & Li, E. (1999). DNA methyltransferases Dnmt3a and Dnmt3b are essential for de novo methylation and mammalian development. *Cell*, *99*(3), 247–257.

Pall, M. L. (1993). The use of Ignite (Basta; glufosinate; phosphinothricin) to select transformants of *bar*-containing plasmids in *Neurospora crassa*. *Fungal Genet Newsl*, *40*, 58.

Peng, J. C., & Karpen, G. H. (2008). Epigenetic regulation of heterochromatic DNA stability. *Current Opinion in Genetics & Development*, *18*(2), 204–211. http://doi.org/10.1016/j.gde.2008.01.021

Peters, A. H., O'Carroll, D., Scherthan, H., Mechtler, K., Sauer, S., Schöfer, C., et al. (2001). Loss of the Suv39h histone methyltransferases impairs mammalian heterochromatin and genome stability. *Cell*, *107*(3), 323–337.

Petroski, M. D., & Deshaies, R. J. (2005). Function and regulation of cullin-RING ubiquitin ligases. *Nature Reviews Molecular Cell Biology*, *6*(1), 9–20. http://doi.org/10.1038/nrm1547

Pickart, C. M. (2001). Mechanisms underlying ubiquitination. *Annual Review of Biochemistry*, *70*(1), 503–533. http://doi.org/10.1146/annurev.biochem.70.1.503

Pierce, N. W., Lee, J. E., Liu, X., Sweredoski, M. J., Graham, R. L. J., Larimore, E. A., et al. (2013). Cand1 promotes assembly of new SCF complexes through dynamic exchange of F box proteins. *Cell*, *153*(1), 206–215. http://doi.org/10.1016/j.cell.2013.02.024

Ragunathan, K., Jih, G., & Moazed, D. (2014). Epigenetic inheritance uncoupled from sequence-specific recruitment. *Science*, 1–13. http://doi.org/10.1126/science.1258699

Reik, W., & Walter, J. (2001). Genomic imprinting: parental influence on the genome. *Nature Reviews. Genetics*, *2*(1), 21–32. http://doi.org/10.1038/35047554

Reik, W., Dean, W., & Walter, J. (2001). Epigenetic reprogramming in mammalian

development. *Science*, *293*(5532), 1089–1093. http://doi.org/10.1126/science.1063443

Riggs, A. D. (1975). X inactivation, differentiation, and DNA methylation. *Cytogenetics and Cell Genetics*, *14*(1), 9–25.

Robertson, K. D. (2005). DNA methylation and human disease. *Nature Reviews. Genetics*, *6*(8), 597–610. http://doi.org/10.1038/nrg1655

Robinson, J. T., Thorvaldsdóttir, H., Winckler, W., Guttman, M., Lander, E. S., Getz, G., & Mesirov, J. P. (2011). Integrative genomics viewer. *Nature Biotechnology*, *29*(1), 24–26. http://doi.org/10.1038/nbt.1754

Ronemus, M. J., Galbiati, M., Ticknor, C., Chen, J., & Dellaporta, S. L. (1996). Demethylation-induced developmental pleiotropy in Arabidopsis. *Science*, *273*(5275), 654–657.

Rountree, M. R., & Selker, E. U. (2009). Genome Defense: The Neurospora Paradigm. In A. C. Ferguson-Smith, J. M. Greally, & R. A. Martienssen (Eds.), *Epigenomics* (pp. 321–341). Dordrecht, The Netherlands.

Rountree, M. R., & Selker, E. U. (2010). DNA methylation and the formation of heterochromatin in *Neurospora crassa*. *Heredity*, *105*(1), 38–44. http://doi.org/10.1038/hdy.2010.44

Saksouk, N., Barth, T. K., Ziegler-Birling, C., Olova, N., Nowak, A., Rey, E., et al. (2014). Redundant Mechanisms to Form Silent Chromatin at Pericentromeric Regions Rely on BEND3 and DNA Methylation. *Molecular Cell*, *56*(4), 580–594. http://doi.org/10.1016/j.molcel.2014.10.001

Saksouk, N., Simboeck, E., & Déjardin, J. (2015). Constitutive heterochromatin formation and transcription in mammals. *Epigenetics & Chromatin*, *8*(1), 3. http://doi.org/10.1186/1756-8935-8-3

Saze, H., Shiraishi, A., Miura, A., & Kakutani, T. (2008). Control of genic DNA methylation by a jmjC domain-containing protein in Arabidopsis thaliana. *Science*, *319*(5862), 462–465. http://doi.org/10.1126/science.1150987

Schotta, G., Ebert, A., Krauss, V., Fischer, A., Hoffmann, J., Rea, S., et al. (2002). Central role of Drosophila SU(VAR)3-9 in histone H3-K9 methylation and heterochromatic gene silencing. *Embo*, *21*(5), 1121–1131. http://doi.org/10.1093/emboj/21.5.1121

Selker, E. U. (1990). Premeiotic instability of repeated sequences in *Neurospora crassa*. *Annual Review of Genetics*, *24*(1), 579–613. http://doi.org/10.1146/annurev.ge.24.120190.003051

Selker, E. U. (1998). Trichostatin A causes selective loss of DNA methylation in

Neurospora. *Proceedings of the National Academy of Sciences of the United States of America*, *95*(16), 9430–9435.

Selker, E. U., & Stevens, J. N. (1987). Signal for DNA methylation associated with tandem duplication in *Neurospora crassa*. *Molecular and Cellular Biology*, *7*(3), 1032–1038.

Selker, E. U., Tountas, N. A., Cross, S. H., Margolin, B. S., Murphy, J. G., Bird, A. P., & Freitag, M. (2003). The methylated component of the *Neurospora crassa* genome. *Nature*, *422*(6934), 893–897. http://doi.org/10.1038/nature01564

Seum, C., Delattre, M., Spierer, A., & Spierer, P. (2001). Ectopic HP1 promotes chromosome loops and variegated silencing in Drosophila. *Embo*, *20*(4), 812–818. http://doi.org/10.1093/emboj/20.4.812

Sharma, S., Kelly, T. K., & Jones, P. A. (2010). Epigenetics in cancer. *Carcinogenesis*, *31*(1), 27–36. http://doi.org/10.1093/carcin/bgp220

Sinha, K. K., Gross, J. D., & Narlikar, G. J. (2017). Distortion of histone octamer core promotes nucleosome mobilization by a chromatin remodeler. *Science*, *355*(6322), eaaa3761. http://doi.org/10.1126/science.aaa3761

Slotkin, R. K., & Martienssen, R. (2007). Transposable elements and the epigenetic regulation of the genome. *Nature Reviews. Genetics*, *8*(4), 272–285. http://doi.org/10.1038/nrg2072

Smallwood, A., Estève, P.-O., Pradhan, S., & Carey, M. (2007). Functional cooperation between HP1 and DNMT1 mediates gene silencing. *Genes & Development*, *21*(10), 1169–1178. http://doi.org/10.1101/gad.1536807

Smith, K. M., Dobosy, J. R., Reifsnyder, J. E., Rountree, M. R., Anderson, D. C., Green, G. R., & Selker, E. U. (2010). H2B- and H3-specific histone deacetylases are required for DNA methylation in *Neurospora crassa*. *Genetics*, *186*(4), 1207–1216. http://doi.org/10.1534/genetics.110.123315

Song, Q., Decato, B., Hong, E. E., Zhou, M., Fang, F., Qu, J., et al. (2013). A reference methylome database and analysis pipeline to facilitate integrative and comparative epigenomics. *PloS One*, *8*(12), e81148. http://doi.org/10.1371/journal.pone.0081148

Sugiyama, T., Cam, H. P., Sugiyama, R., Noma, K.-I., Zofall, M., Kobayashi, R., & Grewal, S. I. S. (2007). SHREC, an effector complex for heterochromatic transcriptional silencing. *Cell*, *128*(3), 491–504. http://doi.org/10.1016/j.cell.2006.12.035

Swerdlow, P. S., Schuster, T., & Finley, D. (1990). A conserved sequence in histone H2A which is a ubiquitination site in higher eucaryotes is not required for growth in Saccharomyces cerevisiae. *Molecular and Cellular Biology*, *10*(9), 4905–4911.

Tachibana, M., Sugimoto, K., Nozaki, M., Ueda, J., Ohta, T., Ohki, M., et al. (2002). G9a histone methyltransferase plays a dominant role in euchromatic histone H3 lysine 9 methylation and is essential for early embryogenesis. *Genes & Development*, *16*(14), 1779–1791. http://doi.org/10.1101/gad.989402

Tamaru, H., & Selker, E. U. (2001). A histone H3 methyltransferase controls DNA methylation in *Neurospora crassa*. *Nature*, *414*(6861), 277–283. http://doi.org/10.1038/35104508

Tamaru, H., & Selker, E. U. (2003). Synthesis of signals for *de novo* DNA methylation in *Neurospora crassa*. *Molecular and Cellular Biology*, *23*(7), 2379–2394.

Tamaru, H., Zhang, X., McMillen, D., Singh, P. B., Nakayama, J.-I., Grewal, S. I., et al. (2003). Trimethylated lysine 9 of histone H3 is a mark for DNA methylation in *Neurospora crassa*. *Nature Genetics*, *34*(1), 75–79. http://doi.org/10.1038/ng1143

Thiru, A., Nietlispach, D., Mott, H. R., Okuwaki, M., Lyon, D., Nielsen, P. R., et al. (2004). Structural basis of HP1/PXVXL motif peptide interactions and HP1 localisation to heterochromatin. *Embo*, *23*(3), 489–499. http://doi.org/10.1038/sj.emboj.7600088

Thliveris, A. T., & Mount, D. W. (1992). Genetic identification of the DNA binding domain of *Escherichia coli* LexA protein. *Proceedings of the National Academy of Sciences of the United States of America*, *89*(10), 4500–4504.

Ulrich, H. D., & Walden, H. (2010). Ubiquitin signalling in DNA replication and repair. *Nature Reviews Molecular Cell Biology*, *11*(7), 479–489. http://doi.org/10.1038/nrm2921

Vogel, M. J., Peric-Hupkes, D., & van Steensel, B. (2007). Detection of *in vivo* protein-DNA interactions using DamID in mammalian cells. *Nature Protocols*, *2*(6), 1467–1478. http://doi.org/10.1038/nprot.2007.148

Wang, D., Kon, N., Lasso, G., Jiang, L., Leng, W., Zhu, W.-G., et al. (2016). Acetylation-regulated interaction between p53 and SET reveals a widespread regulatory mode. *Nature*, *538*(7623), 118–122. http://doi.org/10.1038/nature19759

Wang, J., Hu, Q., Chen, H., Zhou, Z., Li, W., Wang, Y., et al. (2010). Role of individual subunits of the *Neurospora crassa* CSN complex in regulation of deneddylation and stability of cullin proteins. *PLoS Genetics*, *6*(12), e1001232. http://doi.org/10.1371/journal.pgen.1001232

Weber, M., & Schübeler, D. (2007). Genomic patterns of DNA methylation: targets and function of an epigenetic mark. *Current Opinion in Cell Biology*, *19*(3), 273–280. http://doi.org/10.1016/j.ceb.2007.04.011

Wu, J.-T., Chan, Y.-R., & Chien, C.-T. (2006). Protection of cullin-RING E3 ligases by CSN-UBP12. *Trends in Cell Biology*, *16*(7), 362–369.

http://doi.org/10.1016/j.tcb.2006.05.001

Wu, S., Zhu, W., Nhan, T., Toth, J. I., Petroski, M. D., & Wolf, D. A. (2013). CAND1 controls in vivo dynamics of the cullin 1-RING ubiquitin ligase repertoire. *Nature Communications*, *4*, 1642. http://doi.org/10.1038/ncomms2636

Xu, H., Wang, J., Hu, Q., Quan, Y., Chen, H., Cao, Y., et al. (2010). DCAF26, an adaptor protein of Cul4-based E3, is essential for DNA methylation in *Neurospora crassa*. *PLoS Genetics*, *6*(9), e1001132. http://doi.org/10.1371/journal.pgen.1001132

Yamada, T., Fischle, W., Sugiyama, T., Allis, C. D., & Grewal, S. I. S. (2005). The nucleation and maintenance of heterochromatin by a histone deacetylase in fission yeast. *Molecular Cell*, *20*(2), 173–185. http://doi.org/10.1016/j.molcel.2005.10.002

Yang, Y., Liu, R., Qiu, R., Zheng, Y., Huang, W., Hu, H., et al. (2015). CRL4B promotes tumorigenesis by coordinating with SUV39H1/HP1/DNMT3A in DNA methylation-based epigenetic silencing. *Oncogene*, *34*(1), 104–118. http://doi.org/10.1038/onc.2013.522

Zeng, L., & Zhou, M. M. (2002). Bromodomain: an acetyl-lysine binding domain. *FEBS Letters*, *513*(1), 124–128.

Zhang, K., Mosch, K., Fischle, W., & Grewal, S. I. S. (2008). Roles of the Clr4 methyltransferase complex in nucleation, spreading and maintenance of heterochromatin. *Nature Structural & Molecular Biology*, *15*(4), 381–388. http://doi.org/10.1038/nsmb.1406

Zhao, Y., Shen, Y., Yang, S., Wang, J., Hu, Q., Wang, Y., & He, Q. (2010). Ubiquitin ligase components Cullin4 and DDB1 are essential for DNA methylation in *Neurospora crassa*. *The Journal of Biological Chemistry*, *285*(7), 4355–4365. http://doi.org/10.1074/jbc.M109.034710

Zhou, W., Wang, X., & Rosenfeld, M. G. (2009). Histone H2A ubiquitination in transcriptional regulation and DNA damage repair. *The International Journal of Biochemistry & Cell Biology*, *41*(1), 12–15. http://doi.org/10.1016/j.biocel.2008.09.016

Zhu, Q., Pao, G. M., Huynh, A. M., Suh, H., Tonnu, N., Nederlof, P. M., et al. (2011). BRCA1 tumour suppression occurs via heterochromatin-mediated silencing. *Nature*, *477*(7363), 179–184. http://doi.org/10.1038/nature10371

Zimmerman, E. S., Schulman, B. A., & Zheng, N. (2010). Structural assembly of cullin-RING ubiquitin ligase complexes. *Current Opinion in Structural Biology*, *20*(6), 714–721. http://doi.org/10.1016/j.sbi.2010.08.010